AN INVESTIGATION INTO THE REGULATION OF *PEROXIDASIN* GENE EXPRESSION BY THE SNAI1 TRANSCRIPTION FACTOR AND ITS INVOLVEMENT IN EPITHELIAL-TO-MESENCHYMAL TRANSITION IN HUMAN CERVICAL CARCINOMA CELL LINES

Boitumelo Nonhlanhla Moleya

Supervisor: Dr Demetra Mavri-Damelin

A thesis submitted to the Faculty of Science, University of the Witwatersrand, in fulfillment of the requirements for the degree of Doctor of Philosophy.

Johannesburg, 2018

Declaration

I, Boitumelo Nonhlanhla Moleya (0301783J), am a student registered for the degree of Doctor of Philosophy in the academic year 2018.

I hereby declare the following:

I am aware that plagiarism (the use of someone else's work without their permission and/or without acknowledging the original source) is wrong.
I confirm that the work submitted for assessment for the above degree is my own unaided work except where explicitly indicated otherwise and acknowledged.
I have not submitted this work before for any other degree or examination at this or any other University.
The information used in the thesis has not been obtained by me while employed by, or working under the aegis of, any person or organisation other than the University.
I have followed the required conventions in referencing the thoughts and ideas of others.
I understand that the University of the Witwatersrand may take disciplinary action against me if there is a belief that this is not my own unaided work or that I have failed to acknowledge the source of the ideas or words in my writing.

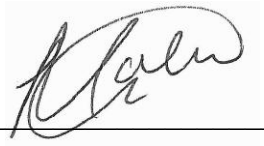

_____ 24th August 2018

Boitumelo Nonhlanhla Moleya

Abstract

Peroxidasin (PXDN) is a unique member of the peroxidase - cyclooxygenase superfamily and differs from its counterparts in that in addition to an enzymatic peroxidase domain, PXDN has protein-binding domains characteristic of proteins found in the extracellular matrix. PXDN is integral to basement membrane consolidation and catalyses sulfilimine bonds in collagen IV and covalent cross-linking of dityrosine. PXDN also has microbicidal activity in plasma through the generation of hypochlorous acid and may also catalyse peroxidative reactions intracellularly. Additionally, PXDN is involved in processes where epithelial-to-mesenchymal transition (EMT) takes place, namely fibrosis, development and cancer. In cancer, PXDN has been found to be aberrantly expressed in a colorectal cancer cell line undergoing p53-dependent apoptosis, in malignant primary glial and metastatic brain tumours; and was identified as a candidate tumour suppressor gene silenced by DNA methylation in patients diagnosed with acute myeloid leukemias. PXDN has also been implicated in tumour invasion of choriocarcinoma and melanoma cells. Considering PXDN expression can be modified by transforming growth factor β1 (TGF-β1), a major signaling molecule involved in the initiation of EMT, in this study we aimed to investigate the role of PXDN in TGF-β1-induced EMT in human cervical cancer cells. This included i) identifying whether Snai1, the main transcription factor involved in EMT, regulates the expression of *PXDN*; and ii) whether PXDN contributes to the various aspects of EMT in cervical carcinoma cell lines.

During TGF-β1-induced EMT, PXDN expression decreased in HeLa and SiHa cells, with concomitant increases in Snai1 and vimentin, and decrease in E-cadherin, as quantified by western blotting and visualised by immunofluorescence microscopy. We showed that TGF-β1 induced Snai1 binding to the *PXDN* promoter, as assessed by chromatin immunoprecipitation-PCR, and significantly repressed luciferase reporter gene expression, as did Snai1 over- expression. We also found that knocking down PXDN expression decreases proliferation, attachment and invasion of HeLa and SiHa cells and increases the migration rate of HeLa cells but decreases that of SiHa cells.

In summary, our findings show that Snai1 mediates repression of *PXDN* and consolidates a role for this ECM-modifier during EMT, in particular during proliferation, attachment and migration of the cervical carcinoma cells, HeLa and SiHa.

Research Outputs

Original publication:

Sitole, B.N., and Mavri-Damelin, D., 2018. Peroxidasin is regulated by the epithelial-mesenchymal transition master transcription factor Snai1. *Gene* 646, 195–202.

Conferences:

Hanmer, K.L., Moleya, B.N. and Mavri-Damelin, D. Peroxidasin is involved in mediating cell attachment, migration and invasion in cervical carcinoma cells under oxidative stress. Molecular Biosciences Research Thrust (MBRT) Postgraduate Day, University of the Witwatersrand, Johannesburg, 2017. Poster presentation.

Moleya, B.N. and Mavri-Damelin, D. Investigating the role of PXDN in EMT and regulation of *PXDN* gene expression by Snai1. Molecular Biosciences Research Thrust (MBRT) Postgraduate Day, University of the Witwatersrand, Johannesburg, 2015. Poster presentation.

McGowan, K.L., Moleya, B.N., Mavri-Damelin, D. and Nikitina, N. Identifying the gene expression patterns of *peroxidasin* and *peroxidasin-like* during embryonic development using the chick model organism. University of the Witwatersrand's 6th Cross Faculty Graduate Symposium, Johannesburg, 2014. Poster presentation.

Moleya, B.N. and Mavri-Damelin, D. Peroxidasin expression in human carcinoma cells: a target for cancer therapy. 15th Biennial Conference of the South African Society of Human Genetics (SASHG), Johannesburg, 2013. Poster presentation.

Moleya, B.N. and Mavri-Damelin, D. Peroxidasin expression in human carcinoma cells: a target for cancer therapy. SASHG Young Researchers Forum, Johannesburg, 2013. Poster presentation.

Dedication

For my parents, whose love flows in my veins

Acknowledgements

Do not go where the path may lead, go instead where there is no path and leave a trail.
-Ralph Waldo Emerson

This project was one of the most challenging adventures I have ever been on and I would like to thank the following people whose love and support was a blessing on this journey.

First and foremost I would like to thank God, who blew life into me and makes me new every day. Thank You.

I would like to thank my supervisor, Dr Demetra Mavri-Damelin, for conceptualising this project. Dr Mavri-Damelin has always given more than what is expected from a supervisor, and her support, encouragement and guidance lead me to achieve more than I thought possible in these past years in the Functional Genetics Research Laboratory. I count myself lucky to have been under her guidance for the duration of this project. Words cannot express my gratitude.

I acknowledge Prof Robin B. Veale as my advisor and for the use of his tissue culture facility. I am grateful to Elsabe Scott and Sabeeha Mahomed for assistance with cell culture. I would like to thank Pamela Sharp for training me in the use of the Zeiss LSM 780 confocal microscope at the NRF-funded Life Sciences Imaging Facility, and Dr Deran Reddy for assistance with the use of the Olympus BX63 microscope at the Microscopy and Microanalysis Unit. I thank Dr Clement Penny for provision of HEK293 cells. I thank Dr Leonard Damelin for his assistance on certain aspects of this project.

I am grateful to the funding bodies that supported me, and this work, financially, through the provision of bursaries and awards. This work was funded by Innovation bursaries from the National Research Foundation and Postgraduate Merit Awards from the University of the Witwatersrand.

To the DNA Divas, Dr Rupal Jivan, Dr Charissa Mynhardt, Malehlohonolo Radebe and Kerry Leigh Hanmer. I thank them sincerely for their love, support and encouragement over the past years. They made tough days in the lab bearable and I will always cherish the memories we shared together. A special mention to my partner in all things PXDN; I would not have reached this point without the love, support and friendship of Kerry Leigh Hanmer. I am eternally grateful to her for her assistance with experiments, but

most importantly for being there every step of the way with a word of encouragement, an ear to hear me cry and complain and a joke to make me smile again. I am grateful for the friend I have gained on this journey.

Last, but most definitely not least, a huge thank you to my family. Each of them in their own way contributed to where I am today. My Mama-bear, Dr Nono Simelela, who every day sets an example that makes me strive to be better than what I was the day before. She made this achievement possible, thank you Mama. My angel on Earth, Gogo Annah Simelela, whose prayers have surely turned into miracles in my life. My mothers, Vuvu Mabudusha, Dorah Sitole and Mary Moleya, whose love and prayers support me each day. My fathers, James Tshetlo Moleya, John Moleya, Seragi Mabudusha and Archibald Sitole, whose love and pride in me are palpable and make me want to achieve even more. My sisters, Rudzani Moleya, Thato Mabudusha, Phumzile Sitole, Ayanda Sitole and Unathi Mabudusha whose magic has rubbed off on me in the most profound way, they are grace and power personified and I know they will change the world! My brothers, Thabang Moleya, Neo Kabe, Motheo Mabudusha and Bulelani Mabudusha ,who shower me with more love than I know what to do with, and who give me the confidence that I can do anything! I would also like to thank my friends, for their love, prayers and encouragement. And lastly, to the amazing men in my life: my babies who are my heart and who bring so much joy to my life. They are the reason I pursue my dreams and they make each day better with their unconditional love. And to my husband, Sibusiso Sitole, whose love is my sustenance; you ignite my bones and every moment with you is love and happiness made manifest, thank you.

"Be strong and courageous. Do not be terrified, do not be discouraged; for the Lord your God will be with you wherever you go."
- Joshua 1:9

Contents

List of Figures

List of Tables

Abbreviations

AML	Acute myeloid leukemia
ApoE	Apolipoprotein E
APS	Ammonium persulfate
ARCaP	Androgen refractory cancer of the prostate
ASD	Anterior segment dysgenesis
Bcl-xL	B-cell lymphoma-extra large
BLAST	Basic local alignment search tool
BLBC	Basal-like breast cancer
BM	Basement membrane
BSA	Bovine albumin serum
ChIP	Chromatin immunoprecipitation
CTL	Cytolytic T lymphocyte
DAC	5-aza-2′-deoxycytidine
DAPI	4',6-diamidino-2-phenylindole
DEPC	Diethyl pyrocarbonate
DIC	Differential interference contrast
DMEM	Dulbecco's Modified Eagle's Medium
DMSO	Dimethyl sulfoxide
dPXN	*Drosophila melanogaster* peroxidasin
DT	Dityrosine
E-cadherin	Epithelial-cadherin
ECM	Extracellular matrix
EDTA	Ethylenediaminetetraacetic acid
ELISA	Enzyme-linked immunosorbent assay
EMT	Epithelial-to-mesenchymal transition
ENU	N-ethyl-N-nitrosourea
EPO	Eosinophil peroxidase
ER	Endoplasmic reticulum

EtBr	Ethidium bromide
FBS	Fetal bovine serum
FITC	Fluorescein isothiocyanate
GAPDH	Glyceraldehyde 3-phosphate dehydrogenase
GEM	Glioma endothelial marker
GF	Growth factor
H_2O_2	Hydrogen peroxide
HDAC	Histone deacetylase
HEK	Human embryonic kidney
HiFi	High Fidelity
HO-1	Heme oxygenase-1
HOBR	Hypobromous acid
HOCl	Hypochlorous acid
HOX	Hypohalous acids
HRP	Horseradish peroxidase
IDT	Integrated DNA Technologies
IF	Immunofluorescence
Ig	Immunoglobulin
IP	Immunoprecipitated
IR	Ischemia-reperfusion
JNK	c-Jun N-terminal kinase
LB	Lysogeny broth
LDL	Low-density lipoprotein
LLR	Leucine-rich repeats
LPO	Lactoperoxidase
MAPK	Mitogen-activated protein kinase
MDCK	Madin-Darby canine kidney
MET	Mesenchymal-to-epithelial transition
MG50	Melanoma gene 50
MMP	Matrix metalloproteinase

MPO	Myeloperoxidase
MTT	3-(4,5-dimethylthiazol-2-yl)-2,5 diphenyltetrazolium bromide
NADPH	Nicotinamideadenine dinucleotide phosphate
NC	Non-collagenous
Nox	Nicotinamideadenine dinucleotide phosphate oxidase
NSCLC	Non-small cell lung carcinoma
Ox-LDL	Oxidized low-density lipoprotein
PBS	Phosphate buffered saline
PCR	Polymerase chain reaction
PMSF	Phenylmethanesulfonyl fluoride
PRG	p53 responsive gene
PRG2	p53 response gene 2
PVDF	Polyvinylidene fluoride
PXDN	Peroxidasin
PXN-1	*Caenorhabditis elegans* peroxidasin 1
PXN-2	*Caenorhabditis elegans* peroxidasin 2
ROS	Reactive oxygen species
RT	Room temperature
SAHA	Suberoyl anilide bishydroxamide
SD	Standard deviation
SDS	Sodium dodecyl sulfate
SDS-PAGE	SDS polyacrylamide gel electrophoresis
SNAG	Snai1/Gfi
SNP	Single nucleotide polymorphism
SOB	Super optimal broth
TAE	Tris-acetate-EDTA
TBS	Tris buffered saline
TBS/T	Tris buffered saline/Tween®20
TCA	Trichloroacetic acid
TEMED	Tetramethyl-ethylenediamine

TGF-β	Transforming growth factor-β
TGF-β1	Transforming growth factor β1
TGFBI	Transforming growth factor-β–induced
TGFβR	TGF-β receptor
TMB	Tetramethylbenzidine
TPO	Thyroid peroxidase
TR	Texas Red
UV	Ultraviolet
VPO1	Vascular peroxidase 1
VWC	von Willebrand factor, type C
Xtpxn	*Xenopus tropicalis* peroxidasin

Chapter 1: Introduction

Cancer cells have a fundamental property, deregulated growth and proliferation. The potential to metastasise allows tumours to grow and spread uncontrollably, wreaking havoc on the body and often resulting in death (Klug *et al*., 2009). An important aspect of cancer therapy research focuses on identifying novel treatment methods by targeting a wide range of molecular elements of cancer initiation and progression, including pathways and the genes and proteins involved in them. It is such research that first led to the identification of a novel gene, *peroxidasin* (*PXDN*), aberrantly expressed in cancer cells (Hutchins *et al*., 1991).

1.1. Peroxidasin

1.1.1. A unique heme-peroxidase

PXDN was first identified in *Drosophila melanogaster* (Nelson *et al*., 1994) as an extracellular matrix (ECM)-associated peroxidase secreted only by head mesoderm-derived hemocytes. In *Drosophila melanogaster*, hemocytes produce numerous ECM components, one being collagen IV. These cells are the equivalent of vertebrate white blood cells (hemocytes phagocytose apoptotic cells) and interstitial cells (Fessler and Fessler, 1989). *Drosophila melanogaster* PXDN (dPXN) was found to play a role in several important biological processes such as: the removal and destruction of cells undergoing apoptosis; consolidation of the ECM by catalysing the covalent cross-linking of dityrosine (DT), which stabilises collagen; and host defense (Nelson *et al*., 1994). dPXN is a homotrimeric peroxidase with motifs commonly found in ECM-associated proteins, with a peroxidase domain homologous to two human peroxidases, namely myeloperoxidase (MPO) and eosinophil peroxidase (EPO) (Nelson *et al*., 1994).

In humans, the *PXDN* gene has been mapped to chromosome 2, location 2p25.3 on the reverse strand (Weiler *et al*., 1994). Functional characterisation of PXDN has been carried out in various organisms in which homologues of the *dPXN* gene have been

identified, including *Xenopus tropicalis* (Tindall *et al.*, 2005), *Mus musculus* (Homma *et al.*, 2009) and *Caenorhabditis elegans* (Gotenstein *et al.*, 2010).

PXDN is the most recent addition to the mammalian family of peroxidases, which include MPO, EPO, lactoperoxidase (LPO) and thyroid peroxidase (TPO) (O'Brien, 2000; Cheng *et al.*, 2008). However, PXDN differs from its counterparts in that the PXDN protein has both an enzymatic peroxidase domain and protein-binding domains, namely leucine-rich repeats and C2-type immunoglobulin domains localised to the N-terminus, and a von Willebrand factor type C (VWC) domain at the C-terminus of the protein. All of the latter are characteristic of proteins found in the ECM (Fig. 1.1). These domains suggest the potential for protein-protein interactions, suggesting that PXDN may interact with and influence other ECM-associated proteins (Cheng *et al.*, 2008; Lázár *et al.*, 2015).

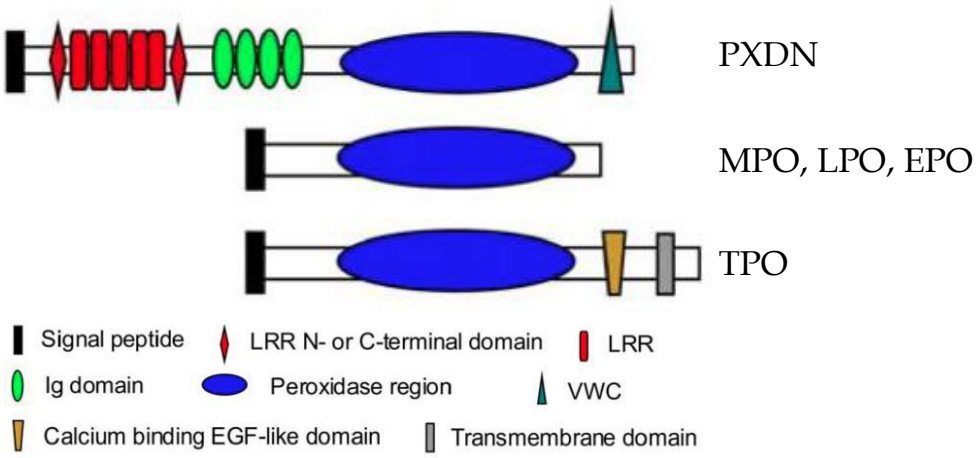

Figure 1.1: Conserved domain architecture of PXDN, MPO, LPO, EPO and TPO.
All conserved domains of other heme-containing peroxidases (such as the peroxidase region and signal peptide) are also observed in PXDN. Abbreviations: LLR (leucine-rich repeats), Ig (immunoglobulin C2), VWC (von Willebrand factor type C) (adapted from Cheng *et al.*, 2008).

1.1.2. Peroxidasin expression

In humans, *PXDN* mRNA expression occurs in several tissues including heart, skeletal muscle, colon, spleen, kidney, liver, small intestine and placenta (Horikoshi *et al.*, 1999; Cheng *et al.*, 2008; Péterfi *et al.*, 2009). Incongruous with its mRNA expression pattern, PXDN protein expression has been found to be highly localised to vascular tissue and secreted by vascular endothelial cells (Cheng *et al.*, 2008). However, in pathological states the pattern of PXDN expression is altered. For example, PXDN shows increased expression in transforming growth factor β (TGF-β)-induced differentiating myofibroblasts and is incorporated into the ECM of fibrotic kidney tissue (Péterfi *et al.*, 2009); and PXDN is also upregulated by oxidized low-density lipoprotein (ox-LDL) and subsequently contributes to the development of atherosclerosis (Bai *et al.*, 2011). Dysregulation of PXDN has also been observed in a variety of cancers (Castronovo *et al.*, 2006; Desmond *et al.*, 2007; Péterfi *et al.*, 2009; Liu *et al.*, 2010; Tauber *et al.*, 2010; Jayachandran *et al.*, 2016), which is discussed further in this chapter. Over the years as additional studies on PXDN have emerged in various disease contexts, several synonyms have been used to refer to PXDN, namely melanoma gene 50 (*MG50*) (Hutchins *et al.*, 1991), p53 response gene 2 (*PRG2*) (Horikoshi *et al.*, 1999) and recently, vascular peroxidase 1 (*VPO1*) (Cheng *et al.*, 2008; Bai *et al.*, 2011). Presently, VPO1 is the most used synonym when referring to PXDN.

1.1.3. Peroxidasin oligomerisation

Mammalian PXDN protein exists in both a monomeric (Cheng *et al.*, 2011) and trimeric form, and the peroxidase activity of PXDN is not required for supramolecular assembly of the protein into its trimeric form (Lázár *et al.*, 2015). Intermolecular disulfide bridge formation has been identified as the primary mechanism of oligomerisation with two cysteines (C736 and C1315) responsible for the formation of the PXDN trimer (Lázár *et al.*, 2015). The way in which PXDN oligomerisation occurs is likely to be the same in all organisms since the two cysteines responsible for oligomerisation are conserved across many species. When these cysteines were mutated simultaneously, PXDN was found

only in its monomeric form. When C1315 was mutated into serine, PXDN was found mostly in its dimeric form, suggesting that in the absence of C1315 the remaining cysteines can still form sufficient intermolecular disulfide bridges required for the formation of dimers (Lázár *et al.*, 2015).

Peroxidase assays revealed that monomeric PXDN (C736S, C1315S) is as equally active as the wild-type protein. Exclusion of the VWC domain did not affect enzymatic activity, but loss of the N-terminal LRR and the Ig domains abolished PXDN peroxidase activity. It was found that the monomeric form of PXDN (C736S, C1315S) is not able to fully effect the function of PXDN to cross-link collagen IV, suggesting that optimal coupling of NC1 (non-collagenous) domains requires the trimeric form of the protein (Lázár *et al.*, 2015).

1.1.4. Peroxidasin function

Until recently, the function of human PXDN has been unknown. However, research shows that human PXDN functions similarly to dPXN, in that it plays a role in consolidation of collagen IV in the ECM, host immunity and induction of apoptosis via the production of reactive oxygen species (ROS) (Bai *et al.*, 2011; Bhave *et al.*, 2012; Li *et al.*, 2012a). PXDN is a member of the peroxidase - cyclooxygenase superfamily (animal, heme-containing peroxidase family) that function by enzymatic oxidation of substrates in the presence of hydrogen peroxide (H_2O_2) (a non-radical ROS), via the donation of electrons which bind to and hydrolyse substrates (Zamocky *et al.*, 2008; Cheng *et al.*, 2011). In the human body, H_2O_2 is a byproduct of oxidative metabolism and is broken down into water and oxygen by peroxidases. Animal peroxidases have been found to play a role in many processes including the metabolism of xenobiotics and defense against pathogens (O'Brien, 2000; Zamocky *et al.*, 2008). Heme-containing peroxidases can generate hypohalous acids (HOX), and though conventionally HOX have the capacity to damage cells by oxidising proteins, lipids and DNA, they may also act as intermediaries in other reactions such as in the formation of an intramolecular sulfilimine bond to convert methionine into dehydromethionine (Wells, 2002; Bhave *et*

al., 2012). In the case of PXDN, substrates include chloride, bromide and thiocynate (Li *et al.*, 2012b).

1.1.4.1. Peroxidasin in host immunity

As a peroxidase, PXDN was hypothesised to play a role in host immunity (Péterfi *et al.*, 2009). However, the presence of ECM-type protein domains in PXDN suggested an additional role for PXDN as an ECM modifier. PXDN's role in immunity has been recently identified. Li *et al.* (2012a) found that PXDN has microbicidal activity in plasma through the generation of bactericidal hypochlorous acid (HOCl). Previously, it was thought that MPO alone was responsible for the sterility of plasma. However, since PXDN is actively secreted into circulating plasma, at concentrations four times that of MPO (Cheng *et al.*, 2011), while MPO is 'leaked' (not actively secreted) by phagocytes into the circulatory system, PXDN may be the primary peroxidase responsible for killing bacteria in plasma. In this context, PXDN was found to utilise Nox2-generated (nicotinamideadenine dinucleotide phosphate oxidase 2) H_2O_2 (dismutated from superoxide), to oxidise chloride in order to produce HOCl, which is powerfully bactericidal.

1.1.4.2. Peroxidasin in ox-LDL-induced apoptosis

One study that supports H_2O_2-induced PXDN expression looked at the role of PXDN in mediating ox-LDL-induced endothelial cell apoptosis (Fig. 1.2) (Bai *et al.*, 2011). Oxidation of low-density lipoproteins (LDLs) has been shown to induce apoptosis due to the toxicity and negative effects of ox-LDL. Ox-LDL is more readily taken up by macrophages, causing the formation of foam cells that initiate and contribute to the formation of atherosclerotic plaques in blood vessels. Ox-LDL also promotes lipid accumulation, proinflammatory responses and apoptotic cell death (with apoptotic cells present in atherosclerotic lesions) (Norata *et al.*, 2002) and contribute to endothelial dysfunction, destabilisation of atherosclerotic plaques and thrombosis (Xu *et al.*, 2009).

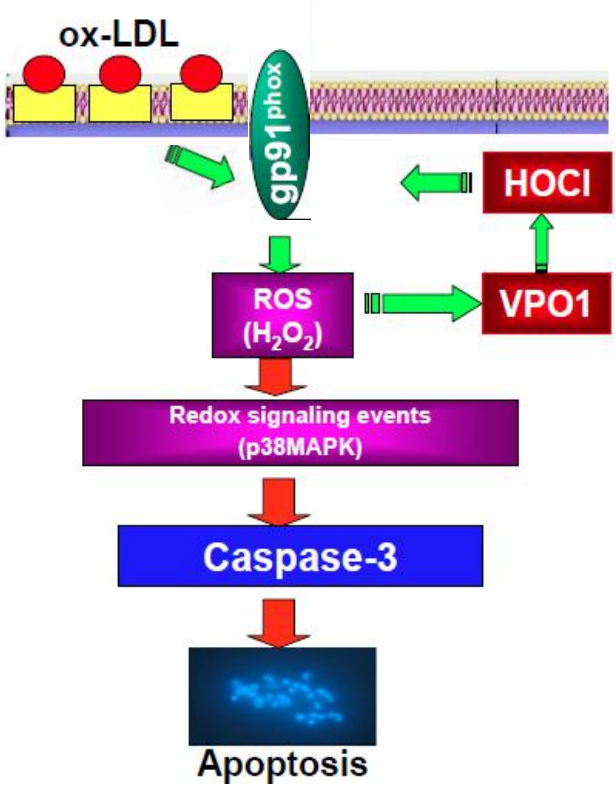

Figure 1.2: The ox-LDL-induced endothelial cell apoptosis pathway with the proposed role of PXDN (referred to as VPO1) indicated in the pathway. Ox-LDL increases the expression of the NADPH oxidase subunit gp91phox leading to the increase of intracellular ROS production, increased VPO1 expression and increased HOCl production. A positive feedback loop exists between VPO1/HOCl and the NADPH oxidase/ROS pathway, this activates the p38 MAPK/caspase-3-dependent signaling pathway to mediate apoptosis (adapted from Bai *et al.*, 2011).

Bai *et al.* (2011) found that PXDN expression was upregulated by ox-LDL in a time and concentration-dependent manner, and along with increased PXDN expression, ox-LDL-induced endothelial cell apoptosis resulted in increased intracellular ROS and HOCl generation, upregulated expression of nicotinamideadenine dinucleotide phosphate (NADPH) oxidase $gp91^{phox}$ subunit, and phosphorylation of p38 mitogen-activated protein kinase (MAPK) (Fig. 1.2). This demonstrated that PXDN plays an important role

in ox-LDL-induced endothelial cell apoptosis and showed that there is a positive feedback loop between PXDN/HOCl and the known dogma that the NADPH oxidase/ROS/p38 MAPK/caspase-3 pathway is involved in ox-LDL-induced endothelial cell apoptosis (Nihei *et al.*, 2005; Bai *et al.*, 2009). These effects were inhibited when PXDN and NADPH oxidase were silenced. Inhibiting p38 MAPK or caspase-3 resulted in inhibition of ox-LDL-induced endothelial cell apoptosis and intracellular ROS or HOCl generation, while the NADPH oxidase gp91^{phox} subunit and PXDN expression remained unaffected. This data shows that with elevation of intracellular ROS and HOCl, PXDN induces endothelial cell apoptosis; furthermore, the positive feedback loop between PXDN and NADPH oxidase gp91^{phox} subunit activates the p38 MAPK/caspase-3-dependent signaling pathway.

1.1.4.3. Peroxidasin and oxidative stress

PXDN has also been found to play a significant role in increased oxidative stress in the myocardium following ischemia-reperfusion (IR) (Zhang *et al.*, 2012). Although reperfusion may be used in an attempt to restore coronary flow following myocardial ischemia, reperfusion may cause more injury to the heart (Kaminski *et al.*, 2002). Cellular reperfusion injury occurs as a result of increased ROS production, which may lead to necrosis or apoptosis (Zweier and Talukder, 2006). Zhang *et al.* (2012) found that following IR, Nox2 was upregulated in response to ischemia, with production of the associated superoxide anions, which spontaneously dismutate to H_2O_2 (Ma, Zhang and Peng, 2013). PXDN then catalyses the formation of HOCl from H_2O_2 and chloride anions, which promotes cell death in IR. This study confirmed that increased Nox2 activity resulted in increased H_2O_2 production, which induced PXDN protein expression via c-Jun N-terminal kinase (JNK)/p38 MAPK-dependent signaling pathways. An additional oxidative function of PXDN has been identified where Yang *et al.* (2013) found that PXDN also plays a role in the oxidation of apolipoprotein E (ApoE), contributing to the development of atherosclerosis. ApoE is an important component of lipoproteins responsible for transporting lipids in the blood and facilitating lipid transport through cell membranes. Oxidation of ApoE causes

structural changes that impair its ability to clear plasma lipids resulting in lipid deposition in vessel walls and the development of atherosclerosis. PXDN was shown to co-localise with ApoE at atherosclerotic lesions, where PXDN oxidises ApoE, in the presence of Nox-generated H_2O_2 (Yang *et al.*, 2013).

1.1.4.4. Peroxidasin as a mediator of dityrosine cross-linking

PXDN also has the ability to modify proteins by mediating DT cross-linking of ECM and basement membrane (BM) proteins (Cheng *et al.*, 2011). The DT cross-link is formed through a carbon-carbon bond between two proximal tyrosines, and can occur either intramolecularly (between two tyrosine residues in the same molecule) or intermolecularly (between two molecules) (Balasubramanian and Kanwar, 2002). DT is one of the specific biomarkers of protein oxidation and has been implicated in many disease states (Kato *et al.,* 2000; Souza *et al.,* 2000) including atherosclerosis (Leeuwenburgh *et al.,* 1997). Cheng *et al*. (2011) described PXDN as a glycosylated monomeric protein (170 kDa) circulating in human plasma and secreted by vascular endothelial cells. Since PXDN expression and secretion were found to be upregulated by proinflammatory factors such as tumour necrosis factor–α, it was hypothesised that PXDN was a contributor to inflammatory pathology in the vascular system via the catalysis of DT formation. Cheng *et al.* (2011) found two isoforms of endogenous VPO1 in endothelial cells and normal human plasma, as two different sized proteins recognised by the same VPO1 antibody. The reason for the presence of the two isoforms was not identified. It could be due to either differential glycosylation, alternative N-terminal start sites for translation, or the isoforms may be the two described by Horikoshi *et al.* (1999), the full PXDN protein and the isoform lacking a secretory signal.

1.1.4.5. Peroxidasin stabilises collagen IV in the ECM

As previously mentioned, PXDN protein has domains characteristic of ECM-associated proteins. Bhave *et al.* (2012) identified a role for PXDN in the formation of sulfilimine bonds in collagen IV. Type IV collagen and laminin are the major components of the BM, which is a specialised form of ECM (Ioachim *et al.*, 2002). Collagen IV is the only

member of the 28-member collagen superfamily that occurs only in the BM (Khoshnoodi, Pedchenko and Hudson, 2008), where it promotes cell adhesion and motility via interactions with cell surface receptors such as integrins (Miles *et al.*, 1994). During malignant cancer progression, production and assembly of BM is disrupted suggesting that collagen IV α5/α6 chains might protect against rapid cancer progression (Haraguchi, 2009).

The triple helical protomer is the building block that self assembles into collagen IV networks by oligomerisation (Fig. 1.3). Two protomers associate with each other at their C-terminal trimeric NC1 domains to form a hexameric structure (Vanacore, 2009). As shown in Fig. 1.3, the covalent cross-link formed by the sulfilimine bond occurs between apposed hydroxylysine (Hyl211) and methionine (Met93) residues (Bhave *et al.*, 2012). Through the generation of hypobromous acid (HOBr), PXDN assists in the formation of an intermolecular sulfilimine bond across two collagen IV protomers.

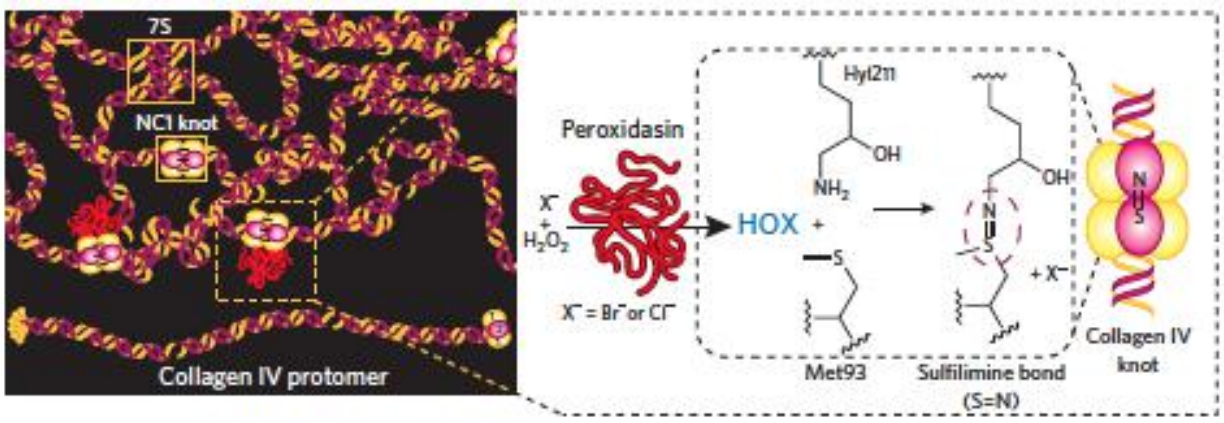

Figure 1.3: PXDN and the NC1 sulfilimine bond. On the left, in the box indicated by a dashed yellow line, PXDN (red conglomerate) sits on an NC1 dimer and introduces sulfilimine cross-links. On the right, the H_2O_2-dependent oxidation of substrates by PXDN generates the respective HOX that cross-links Met93 to Hyl211 to form a sulfilimine bond (taken from Weiss, 2012).

Lázár *et al.* (2015) highlighted the significant role of PXDN cross-linking to stablise collagen IV by comparing the formation of NC1 dimers between wild type and knockout PXDN mouse embryonic fibroblasts. Knockout cells failed to form cross-linked NC1 domains and no compensatory pathways for sulfilimine-mediated collagen IV cross-linking were found. Additionally, it was found that cellular localisation of PXDN was dependent on the quaternary structure of PXDN protein. Subsequent protein sequence alignments of PXDN with other mammalian heme-peroxidases identified cysteine residues in PXDN (previously mentioned in section 1.1.3.), involved in intramolecular disulfide bridge formation, which stabilises the protein structure. As previously mentioned, it was also found that C736 and C1315 play an important role in the oligomerisation of PXDN. Wild-type PXDN and the PXDN mutants all showed the characteristic appearance in the endoplasmic reticulum (ER), but only wild-type PXDN and the mutants that were able to form trimmers could be detected extracellularly on the plasma membrane. Monomeric PXDN mutant however, although able to be secreted from cells, did not localise to the plasma membrane, indicating that trimer formation of PXDN is a prerequisite for extracellular localisation, but not for secretion (Lázár *et al.*, 2015). Since collagen IV cross-linking occurs outside the cell, Lázár *et al.* (2015) suggested that cross-linking may occur on the cell surface where PXDN was found to be localised. Alternatively, PXDN on the cell surface may play a role in adhesion to other components of the BM through LLRs, Ig and VWC motifs that are found in other adhesion proteins (Lázár *et al.*, 2015). Bhave *et al.* (2012) showed that loss of PXDN function results in decreased collagen IV in the BM as a result of the destabilising of collagen IV due to the lack of PXDN catalysed cross-links. Similarly, PXDN mutations in *Caenorhabditis elegans* and *Drosophila melanogaster* also resulted in defects in the BM (Nelson *et al.*, 1994; Gotenstein *et al.*, 2010).

Supporting the role of PXDN as an ECM protein, Péterfi *et al.* (2009) found that PXDN is expressed by human dermal fibroblasts, primary pulmonary, vascular endothelial and smooth muscle cells, and is intracellularly localised to the ER. The PXDN protein is also secreted to the extracellular space by myofibroblasts and incorporated into the ECM of

fibrotic kidney tissue, where it organises into a fibril-like network and is a feature of tissue fibrosis. It was proposed that this pathway of ECM modification is probably not mediated by the peroxidase activity of PXDN and that besides the secretion of well-known constituents of the ECM, PXDN secretion by myofibroblasts is a novel way of ECM modification and stabilisation via protein-protein interactions. Interestingly, PXDN expression was induced by TGF-β1; specifically, TGF-β1 stimulated primary fibroblasts to differentiate into myofibroblasts and increase both expression of PXDN protein and its secretion into the cell culture medium (Péterfi *et al.*, 2009).

1.1.5. Peroxidasin in other model organisms

In mice, PXDN was found to be involved in ECM consolidation and is essential for the functional integrity of the BM and cell adhesion during embryonic eye development (Yan *et al.*, 2014). Yan (2014) identified a nonsense mutation in the *PXDN* gene of ENU (N-ethyl-N-nitrosourea)-induced mutant mice. This mutation was thought to lead to a premature stop codon, causing the loss of the VWC domain, thereby affecting the peroxidase domain with subsequent loss of function of peroxidase enzyme activity. PXDN deficient mice also exhibited anterior segment dysgenesis and microphthalmia. These defects were found to be more severe in mice than in humans. The study also found that PXDN has multiple roles during eye development, affecting cell proliferation and differentiation and BM consolidation. As observed in *Drosophila melanogaster* and *Caenorhabditis elegans* animal models, Yan *et al.* (2014) found distinct changes in the ECM of the eyes of the mutant mice during embryonic development; namely the loss of the structural identity of the lens capsule and lens epithelium adhesion. Collagen IV expression was found to be decreased in the lens epithelium of embryo eyes and in the adult lens in the mutant mice and this was thought to be as a result of the failure to cross-link collagen IV by the mutant PXDN, destabilising the ocular BM (Yan *et al.*, 2014).

In *Xenopus tropicalis*, PXDN (Xtpxn) is expressed in several distinct tissues during early development, including the neural tube and the tail-forming region (Tindall *et al.*, 2005).

It was thought that Xtpxn might modify ECM components of the early pronephric primordium. Additionally, Xtpxn has also been proposed to be involved in detoxifying ROS in the functional pronephros, and the spatially restricted expression of Xtpxn in the early embryo may indicate a role for ROS species in cellular signaling processes during early development (Tindall *et al.*, 2005).

There are two highly related PXDNs identified in *Caenorhabditis elegans*, PXN-1 and PXN-2, with PXN-2 showing similarity to human PXDN (52% identity in the peroxidase domain). Gottenstein *et al.* (2010) found that PXN-2 plays a role in specific stages of embryonic morphogenesis and muscle-epidermal attachment. Postembryonically, PXN-2 is required for BM integrity and these roles rely on the peroxidase catalytic activity of PXN-2. Where PXN-2 is mutated, the ECM ultrastructure is disturbed, meaning PXN-2 may be important for BM consolidation. PXN-2 was also found to affect specific axon guidance choice points in the developing nervous system but was not necessary for maintenance of process positions. PXN-2 was also found to contribute to an inhibitory environment during axon regrowth because decreased PXN-2 function results in increased axonal regeneration after injury. *Caenorhabditis elegans* PXDNs also show antagonistic functions as PXN-2 mutant phenotypes are suppressed where there is loss of function in PXN-1 and aggravated by the overexpression of wild-type PXN-1. However, loss of function of PXN-1 does not cause obvious developmental defects (Gotenstein *et al.*, 2010).

1.1.6. Peroxidasin mutations

Khan *et al.* (2011) showed that homozygous mutations in *PXDN* cause a spectrum of ocular anterior segment dysgenesis (ASD) phenotypes. ASD is a group of heterogeneous disorders affecting many tissues involved in the formation of the eye including the iris, cornea and lens. ASD is caused by abnormal development of the anterior eye tissues and can result in mild to moderate congenital corneal opacity, cataracts and glaucoma with buphthalmos, severe opacification, and vascularisation of the cornea (Khan *et al.*, 2011; Yang *et al.*, 2016). Three families, all displaying various

ASD phenotypes, were found to have mutations in the *PXDN* gene (Khan *et al.*, 2011). The mutations included firstly a frameshift, and premature truncation of the protein, caused by a homozygous deletion of a C nucleotide in the coding sequence (p.Cys857AlafsX5). Secondly, a missense mutation in exon 17 changing a conserved arginine residue within the peroxidase domain to a cysteine (c.2638C>T [p.Arg880Cys]), possibly affecting the three-dimensional structure of the protein because of the position of the new cysteine being within range of interacting with one of the cysteines in the native disulfide bond. Lastly, a single nucleotide polymorphism (SNP) in exon 10 of *PXDN*, was predicted to be a pathogenic mutation since it causes premature protein truncation (c.1021C>T [p.Arg341X]). Khan *et al.* (2011) suggested that PXDN may be involved in providing adhesive support to the corneal epithelial layer and the lens epithelium since these are the structures in which PXDN is localised in embryonic and adult mice. However, PXDN may also be responsible, with other antioxidant enzymes, for metabolizing H_2O_2, superoxide anion, and hydroxyl free radicals generated through normal metabolism in response to cytokines or exposure to light and radiation. While glutathione peroxidase is the main intracellular antioxidant enzyme, PXDN may fulfill this role extracellularly (Khan *et al.*, 2011). Therefore the absence of PXDN in the abovementioned structures may cause the production of insoluble aggregates that lead to corneal clouding and cataractogenesis, with the aggregates forming as a result of a build-up of ROS intermediates that oxidise proteins and lipids. These ROS intermediates may also affect anterior segment structure development and differentiation (Khan *et al.*, 2011). In summation, this study showed that PXDN may have a dual role in development of structural support of the cornea and lens, and also functionally as an antioxidant protecting the lens, trabecular meshwork and cornea from oxidative damage.

Choi *et al.* (2015) reported a broader phenotype for *PXDN* mutations affecting the eye. Two PXDN mutations were identified in a family displaying ASD, sclerocornea, microphthalmia, hypotonia and developmental delays. One mutation was a maternally inherited nonsense mutation [c.1021C4T predicting p.(Arg341*)], and another was a

paternally inherited 23 bp deletion resulting in a frameshift and premature protein truncation [c.2375_2397del23, predicting p.(Leu792Hisfs*67)]. They also identified two additional PXDN mutations in a sporadic male with bilateral microphthalmia, cataracts and ASD. One of these mutations was a maternally inherited frameshift mutation [c.1192delT, predicting p.(Tyr398Thrfs*40)], while the second mutation was a paternally inherited missense substitution predicted to be deleterious [c.947A4C, predicting p.(Gln316Pro)] (Choi *et al.*, 2015).

Meyer *et al.* (2012) reported a novel 281 kb duplication on chromosome 2p25.3 in two male half-siblings with autism. The duplication was of the full *PXDN* gene and included partial duplication of *MYT1L*. Their mother was somatic mosaic but psychiatrically healthy, and harbored the duplication in her germline, and passed it on to her two sons. The duplication of *PXDN* was thought to be inconsequential and not the cause of the boys' condition. Duplication of part of the *MYT1L* gene may have contributed significantly since it is a gene expressed in the brain and linked with schizophrenia and depression (Meyer *et al.*, 2012).

1.1.7. Peroxidasin and cancer

In relation to cancer, *PXDN* was initially implicated as an apoptosis responsive gene. Horikoshi *et al.* (1999) identified six p53 responsive genes (PRGs), five of which are upregulated and one downregulated, in a colon cancer cell line undergoing p53-mediated apoptosis. One of the upregulated genes, *PRG2*, was identified as the human homologue of *dPXN* and was found to be expressed as two alternatively spliced mRNA variants. The longer, 7.5 kb mRNA was found highly expressed in the heart, spleen, intestines, ovary and placenta, while the shorter 4.5 kb mRNA (lacking the signal peptide) was expressed in testes and in a colon cancer cell line undergoing p53-mediated apoptosis (EB1). As with dPXN, PRG2 was found to have a secretory recognition sequence, suggesting that it can be secreted from the cell. Horikoshi *et al.* (1999) therefore hypothesised that induction of the *PRG2* mRNA (4.5 kb variant) may lead to: increased ROS production, which may be a trigger for p53-mediated apoptosis;

ECM consolidation by DT formation and host defense. P53 is a transcription factor and tumour suppressor that is activated in response to cell stress, such as DNA damage, and can effect gene regulation modifications that can lead to cell cycle arrest, apoptosis or alteration of glucose metabolism (Bensaad and Vousden, 2007). In the context of this study, proteins regulated by, and secreted in response to, p53 may alter the ECM and influence angiogenic signals in a localised region of a tissue (Harris and Levine, 2005). However, whilst an association between p53 and PXDN has been proposed, the relationship between the two has not been elucidated and p53 has not been shown to influence PXDN expression. Furthermore, as yet, the transcriptional regulators responsible for PXDN expression have not been identified.

Mitchell *et al.* (2000) sought to identify novel and rare genes that might encode melanoma tumour neoantigens. *MG50* (a synonym for *PXDN*) was one of the selected genes because of its distribution amongst tumour cells and normal cells. *MG50* was found to be one of the few melanoma-associated antigens that are not a melanocyte differentiation antigen or a mutated protein. It also encodes for at least six known human leukocyte antigen class I-restricted epitopes that are recognised by human cytolytic T lymphocytes (CTLs). The melanoma epitopes encoded by *MG50* are of importance since besides cancer vaccines, they could be used for *in vitro* immunisation of CTLs. In this study, Mitchell and colleagues attempted to sequence *MG50* by, amongst other methods, fragment homology to other sequences and polymerase chain reaction (PCR), to test the validity of the extensions. They were able to sequence 6.8 kb from the 3′ end but were unable to sequence 1.3 kb from the 5′ end. From their data, they constructed a hypothetical upstream extension of their original clone. They found that *MG50* had similarities with peroxidase precursors and 75% gene sequence identity with *PXDN*, though they suspected a closer relation between *MG50* and the IL-1 receptor intracellular binding protein (interleukin-1 receptor antagonist; IL-1Ra) because of their identical sequence in the 3′ region. Subsequently, Cheng *et al.* (2008) sequenced the entire *MG50* gene and found it 100% identical to *VPO1*.

PXDN expression has also been found to be upregulated in malignant primary glial and secondary metastatic brain tumours. These types of tumours induce a profound angiogenic response in the microvasculature of the brain, which then promotes tumour growth (Liu *et al.*, 2010). *PXDN* was one of 13 glioma endothelial marker (GEM) genes identified by Liu *et al.* (2010) found to show varying degrees of upregulated expression in gliomas compared to normal tissue. Many of these GEMs were ECM-associated genes, such as collagens. In this study, *PXDN* mRNA was also found to localise to microvascular endothelial cells and expressed in most of the brain tumour samples. In contrast, non-neoplastic temporal lobe specimens showed little or no *PXDN* mRNA expression, suggesting that PXDN may function in tumour angiogenesis in some cancers. However, this study did not look at protein expression levels.

More directly, Desmond *et al.* (2007) suggested a role for PXDN as a potential tumour suppressor. *PXDN* was identified as one of several genes possibly epigenetically silenced by methylation in acute myeloid leukemia (AML). The promoter region of *PXDN* was found to have CpG islands and *PXDN* expression was significantly diminished in all of the tested AML karyotypes. Desmond *et al.* (2007) also identified genes expressed in a normal cell line (CD34+) whose expression was upregulated in KG-1 cells (an AML cell line) following treatment of KG-1 cells with the demethylating agent 5-aza-2'-deoxycytidine (DAC), and the histone deacetylase inhibitor, suberoyl anilide bishydroxamide (SAHA). *PXDN* was found to be one of these epigenetically silenced genes. Since PXDN is expressed in cells of the cardiovascular system and is secreted into the bloodstream (Li *et al.*, 2012a), epigenetic silencing of *PXDN* expression in AML may indicate an anti-tumour function for PXDN in the vascular system. This function may be mediated by the microbicidal activity of PXDN in human plasma (Li *et al.*, 2012a) or its role in BM synthesis and stability since loss of integrity of the BM is associated with altered cancer progression and metastasis (Péterfi and Geiszt, 2014).

Tauber *et al.* (2010) found that PXDN plays a key role in heme oxygenase-1 (HO-1) dependent cell adhesion of neoplastic cells. Under normal conditions, HO-1 (a heat

shock protein) has anti-inflammatory, anti-apoptotic and anti-proliferative properties (Otterbein *et al.,* 2003). In cancer cells HO-1 has been implicated in, amongst others, invasion, metastasis and resistance to chemotherapeutic agents (Jozkowicz, Was and Dulak, 2007) by inducing the expression of anti-apoptotic protein B-cell lymphoma-extra large (Bcl-xL) and decreasing the expression of autophagic proteins Beclin-1 and LC3B-II (Banerjee *et al.*, 2012). Gene expression profiling identified a common gene set directly linked to HO-1 in 14 cancer types, and *PXDN* was one of the identified genes. Interestingly, of the 14 cancer types investigated, several have been linked to aberrant PXDN expression in other studies: breast (Young *et al.*, 2015), prostate (Barnett *et al.*, 2012), melanoma (Mitchell *et al.*, 2000; Jayachandran *et al.*, 2016), leukemia (Desmond *et al.*, 2007) and glioblastoma (Liu *et al.*, 2010). Of importance was the effect of HO-1 on the expression of genes directly or indirectly linked to cell adhesion and the integrity or remodeling of the ECM, and these genes included *TGF-β1* and *PXDN*. Functional studies using BeWo choriocarcinoma cells, a malignant placenta carcinoma cell line that expresses high levels of endogenous HO-1, showed that the adhesion-promoting effects of HO-1 were dependent on PXDN expression and that silencing of *PXDN* caused significantly decreased cell growth and invasion of the BeWo cells (Tauber *et al.*, 2010).

Recently, Jayachandran *et al.* (2016) identified that *PXDN* is a gene whose function is related to melanoma cell invasion. The study involved using a microarray screen to identify gene transcripts that were over-expressed in mesenchymal-like as compared to epithelial-like melanoma cells. *PXDN* was found to be consistently upregulated in mesenchymal-like melanoma cells (Jayachandran *et al.*, 2016). Two models were used to observe changes in the motile behaviour of the metastatic melanoma cell lines after PXDN expression was silenced. The first was a Transwell® invasion assay (*in vitro*), with reconstituted BM, which showed that when PXDN expression is silenced there is a significant reduction of invasion. The second model was the embryonic chicken transplantation model (*in vivo*), a powerful system for assessing the invasive behaviour and plasticity of melanoma cells (Busch, Krochmann and Drews, 2013; Jayachandran *et al.*, 2015). Here, melanoma cells are injected into the neural tube of chick embryos and

subsequently respond to cues in the embryonic microenvironment. The melanoma cells then mimic aspects of neural crest cell motility and undergo epithelial-to-mesenchymal transition (EMT) that allows them to exit from the neural tube, migrate and populate many areas in the embryo (Busch, Krochmann and Drews, 2013). PXDN siRNA-transfected melanoma cells injected into chick embryo neural tubes failed to migrate out of the neural tube (Jayachandran *et al.*, 2016), indicating that PXDN is required for migration of these cells.

BM architecture is critical for the maintenance of epithelial phenotype (Zeisberg *et al.*, 2001), more specifically, collagen IV chains may protect against rapid cancer progression (Ikeda *et al.*, 2006). With this in mind, and since PXDN functions to stabilise collagen IV in the BM (Bhave *et al.*, 2012), it is possible that aberrant PXDN expression may contribute to cancer progression. For example, since PXDN has been shown to be involved in adhesion and invasion of a malignant placenta carcinoma cell line (Tauber *et al.*, 2010), perhaps changes in PXDN expression in cancer cells may affect BM-related features of cancer progression such as EMT that results in metastasis.

1.2. Epithelial-to-mesenchymal transition

EMT is a biological process that causes a polarised epithelial cell, which normally interacts with BM via its basal surface, to undergo several biochemical changes that enable it to take on a mesenchymal cell phenotype (Kalluri and Weinberg, 2009). These changes include, but are not limited to, enhanced migratory capacity, increased invasive ability and resistance to apoptosis (Zavadil *et al.*, 2008). Under normal biological conditions, epithelial cells are tightly packed and mainly held together by three types of interactions: tight junctions (the area where the membranes of two adjacent cells meet), adheren junctions (cadherin based and connected to the actin cytoskeleton) and gap junctions (intercellular protein channels in cell membranes) (Kalluri and Weinberg, 2009). Furthermore, epithelial cells are polarised due to their distinctive apical and basal regions, the latter of which interacts with the BM. In contrast, mesenchymal cells are not polarised, not tightly packed together and have few cell-cell interactions (Radisky, 2005; Kalluri and Weinberg, 2009). At their leading edge, mesenchymal cells have filopodia extensions that interact with the ECM and these cells are also able to produce ECM-degrading matrix metalloproteinases (MMPs) (Ingber, 2002). During EMT (Fig. 1.4), epithelial cells lose their epithelial properties, such as polarity, cell-cell interactions, cell-ECM interactions and downregulation of proteins such as epithelial-cadherin (E-cadherin) (a cell adhesion molecule that is a significant marker of EMT). The epithelial cells then acquire mesenchymal properties, such as the ability to migrate, increased invasive potential and increased expression of proteins such as vimentin (intermediate filament protein), fibronectin and collagen precursors (Christiansen and Rajasekaran, 2006). As such, the EMT process involves several steps, including; activation of specific cell surface receptors, the activation of transcription factors, degradation of the ECM and BM, and migration of the transitioned cell to a secondary site (Christiansen and Rajasekaran, 2006).

A significant marker of EMT is the decrease of E-cadherin expression, which increases a cell's susceptibility to EMT inducing signals (Lee and Nelson, 2012). E-cadherin is a

transmembrane protein, mainly found in adherens junctions and BM, and is a central molecular marker expressed in epithelial cells (Christiansen and Rajasekaran, 2006). In embryogenesis, E-cadherin plays an important role in tissue organisation by forming intercellular adherent junctions and establishing cell polarisation (Poser and Bosserhoff, 2004). Eger *et al.* (2000) demonstrated that when E-cadherin (full length or β-catenin binding cytoplasmic portion) is ectopically expressed in cells undergoing EMT, cell proliferation is suppressed, and there is reorganisation of cell adhesion complexes. During EMT, β-catenin is translocated to the nucleus and induces loss of E-cadherin.

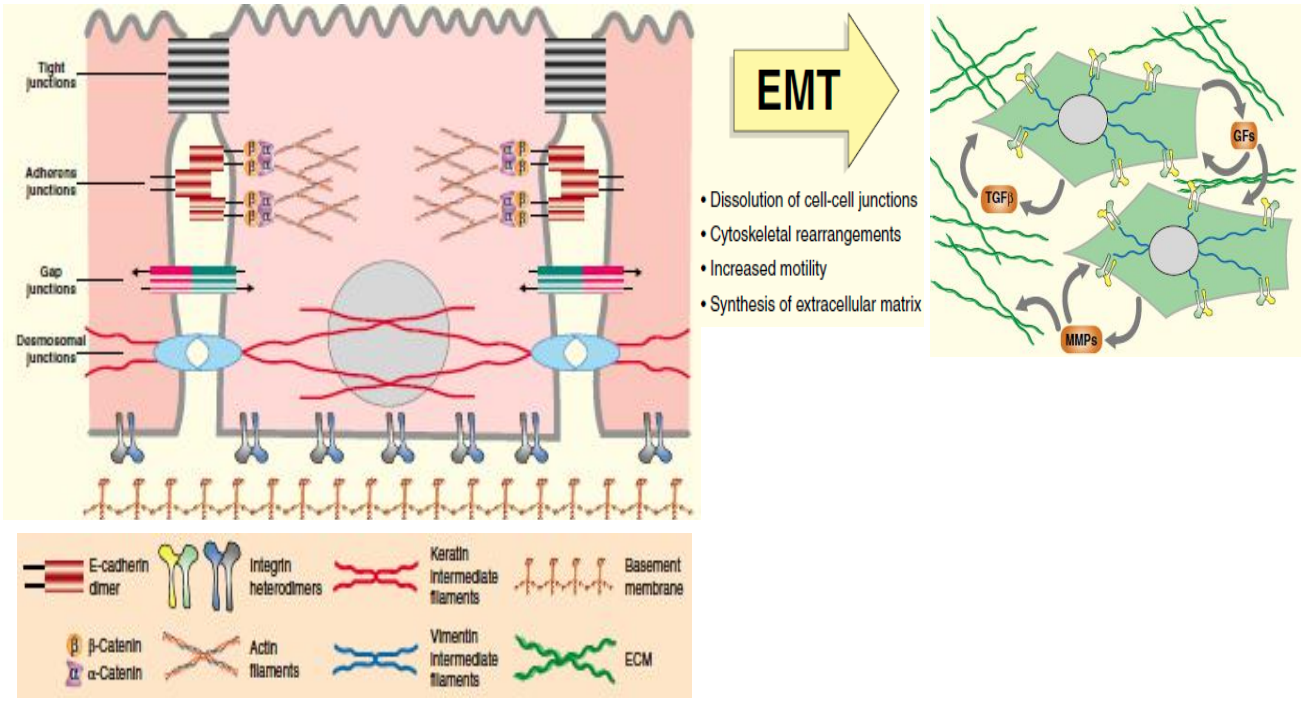

Figure 1.4: Features of EMT. During EMT, the cell-cell interactions (tight, adherens and gap junctions) characteristic of epithelial cells are lost and cells attain a mesenchymal phenotype (motile and invasive). EMT inducing factors include various growth factors (GFs) such as TGF-β, while MMPs are produced to digest and remodel the ECM (taken from Radisky, 2005).

EMT is transient and reversible and has been classified into three subtypes depending on the biological setting under which it occurs (Fig. 1.5). All EMT types produce different results and are thought to involve different pathways (Radisky, 2005). Type 1 EMT (Fig. 1.5A) is involved in early development (embryogenesis and development of organs) and generates mesenchymal cells that undergo mesenchymal to epithelial transition (MET) to form secondary epithelia. This EMT type is essential for the development of the mesoderm, endoderm and mobile neural crest cells and effects gastrulation, neural crest cell migration, and organ development (Kalluri and Weinberg, 2009; Zeisberg and Neilson, 2009). Type 2 EMT (Fig. 1.5B) is involved in fibrosis, wound healing and the regeneration of cells that are involved in tissue reconstruction following injury. Type 2 EMT responds to inflammatory signals, and may lead to fibrosis if the signals are not regulated (Radisky, 2005). Type 3 EMT (Fig. 1.5C) occurs in tumour cells and results in invasion and metastasis of cancer cells (Kalluri and Weinberg, 2009; Lee and Nelson, 2012) and as such, will be further discussed.

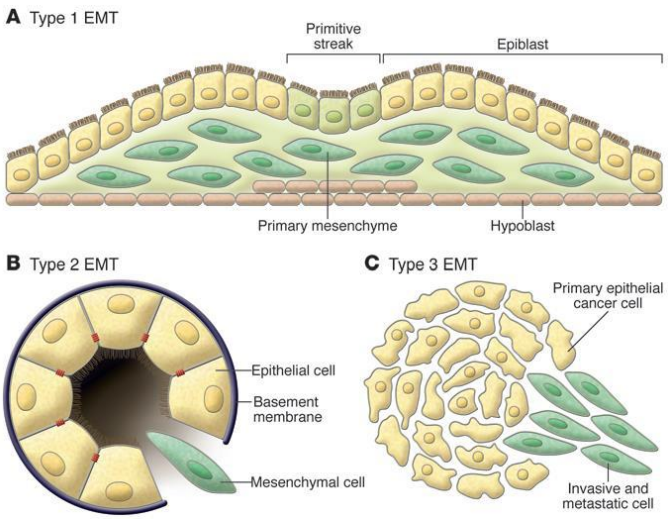

Figure 1.5: The three types of EMT. (A) Type 1 takes place in early development and results in formation of the mesoderm, endoderm, and mobile neural crest cells. (B) Type 2 EMT occurs in response to tissue damage and involves tissue regeneration that can lead to fibrosis. (C) Type 3 EMT is the primary mechanism through which cancer cells achieve an invasive phenotype leading to metastasis of carcinoma cells (taken from Kalluri and Weinberg, 2009).

1.2.1. Type 3 epithelial-to-mesenchymal transition

Carcinomas (cancers of epithelial origin) are the most prevalent forms of cancer (Christiansen and Rajasekaran, 2006). These cancers gain the ability to metastasise by activation of Type 3 EMT. In primary tumours, EMT usually occurs at the invasive front (tumour-stromal boundary) of the tumour, where these single migratory cells lose E-cadherin expression in order to exit the BM and enter the circulatory system (blood or lymphatic), or enter a secondary site and grow. At the primary tumour site the cells undergo EMT, while at the secondary site they undergo MET to revert to their epithelial phenotype (Kalluri and Weinberg, 2009; Thiery *et al.*, 2009). It has been suggested that the genetic changes that occur in cancer cells make them more susceptible to cellular signals from the cellular environment that initiate EMT. Several signaling molecules have been implicated in initiation of EMT; these include TGF-β, hepatocyte growth factor and epidermal growth factor. These signals may originate from mesenchymal

cells and act on epithelial cells, activating a number of transcription factors (Huber, Kraut and Beug, 2005).

1.2.2. TGF-β1 and epithelial-to-mesenchymal transition

The TGF-β family is made up of dimeric polypeptide growth factors that include, amongst at least 30 others, TGF-βs (five isoforms: TGF-β1-5), activins, bone morphogenetic proteins and other homodimers and heterodimers (Weiss and Attisano, 2013; Lamouille, Xu and Derynck, 2014). In general, the TGF-β family plays a role in growth inhibition, proliferation, differentiation, replication, invasion, metastasis, apoptosis, immune surveillance, and angiogenesis. The specific role of the TGF-β family is complex, cell-specific, as wells as context, concentration and exposure-time dependent (Jiang, Tang and Liang, 2011). It often appears to have conflicting roles since the TGF-β family is able to mediate stimulation or inhibition of growth; and apoptosis or differentiation (Jakowlew, 2006). Aberrant changes in the production of TGF-β have been linked to numerous disease states such as atherosclerosis and fibrotic disease of the kidney and other organs (Weiss and Attisano, 2013). Mutations in TGF-β genes, receptors, or intracellular signaling molecules related to TGF-β are also important in the pathogenesis of disease, predominantly cancer (Blobe, Schiemann and Lodish, 2000).

TGF-β1 is one of the five isoforms of TGF-β. Nearly every cell in the body produces TGFβ-1 and has receptors for this molecule (Blobe, Schiemann and Lodish, 2000). In normal cells, TGF-β1 regulates several cellular events such as proliferation, differentiation, migration, inflammation, apoptosis, immune responses and body organisation during embryonic development (Yi *et al.*, 2002). TGF-β1 can initiate and maintain EMT in several biological systems and pathophysiological contexts by activating major signaling pathways and transcriptional regulators integrated in extensive signaling networks (Zavadil and Böttinger, 2005). TGF-β1 can effect proliferation by inhibiting growth via a reversible G1 arrest and TGF-β1 stimulates fibroblasts and other cells to produce ECM proteins such as collagens and laminin (transcriptional and posttranslational regulation of expression), thereby regulating the

formation of stroma and deposition of ECM. Additionally, TGF-β1 down-regulates the expression of ECM-degrading proteases and induces expression of proteinase inhibitors (Hazelbag *et al.*, 2002).

In cancer, TGF-β1 is upregulated to a greater extent than any of the other isoforms, and has therefore been the focus for most of the cancer related studies to date (Bierie and Moses, 2006). TGF-β1 can increase the invasive and metastatic capacity of tumour cells by modifying the expression of many different integrins that alter cell adhesion and migration (Zhen, 2003). In culture, myofibroblasts have been shown to lead invasion of colon cancer cells on a collagen matrix, with TGF-β1 necessary for invasion by inducing N-cadherin expression at the tips of filopodia (Bierie and Moses, 2006).

TGF-β1 has been implicated in increased invasion and metastasis of cancer cells due to its effect on promoting EMT. TGF-β1 is the most well known growth factor involved in the regulation of EMT and induces EMT in wound healing, fibrosis, tissue morphogenesis at early embryonic development and cancer (Yi *et al.*, 2002; Lamouille, Xu and Derynck, 2014). SiHa cells undergo EMT when chronically stimulated by TGF-β1, resulting in increased invasion. After 24 hours of exposure, SiHa cells showed all characteristic features of EMT such as focal context formation at the ends of dense actin stress fibers and cell peripheral fibronectin matrix assembly; all features were found to be irreversible in these cells (Yi *et al.*, 2002). In carcinomas, increased expression and activation of TGF-β1 was found to promote an epithelial plasticity response, for example, squamous carcinomas respond to increased expression of TGF-β1 by conversion to invasive spindle cell carcinomas (Lamouille, Xu and Derynck, 2014). With regards to the proposed link between TGF-β1 and PXDN, perhaps TGF-β1 induction of PXDN expression and secretion could be a result of Nox4 induction by TGF-β1 (Péterfi *et al.*, 2009). The induction of Nox4 could subsequently lead to increased H_2O_2 production and thereby cause PXDN expression. Alternatively, TGF-β1 may induce PXDN expression as a means of remodeling the ECM in order to promote invasion of cancer cells. Since TGF-β1 induces EMT by up-regulating Snai1 transcription factor, the

master regulator of EMT (Wang *et al.*, 2013), it is possible that PXDN expression may be mediated by Snai1 in response to TGF-β1.

1.2.3. Snai1 transcription factor

Snai1 belongs to the mammalian family of Snail transcription factors that includes Snail (Snai1), Slug (Snai2), and Smuc (Snai3). They have a highly conserved carboxy-terminus containing 4 to 6 C_2H_2- (two conserved cysteines and histidines) type zinc fingers that bind to the E-box consensus sequence, CANNTG, a recognition site for transcription factors of the basic helix-loop-helix (Batlle *et al.*, 2000; Peinado, Olmeda and Cano, 2007). They also have an amino-terminal Snai1/Gfi (SNAG) domain required for localisation to the nucleus and for transcriptional repression (Lee and Nelson, 2012). The zinc fingers are structurally composed of two β-strands followed by an α-helix, the amino-terminal part of which binds to the major groove of the DNA. The C_2H_2 coordinate binding of a zinc ion (Nieto, 2002).

Expression of Snai1 protein is also involved in EMT, resulting in the acquisition of invasiveness during tumour progression (Poser, 2004). This aspect of Snai1 activity is associated with its ability to directly repress E-cadherin transcription via binding to the E-cadherin promoter (Cano *et al.*, 2000). Patients suffering from breast (Blanco *et al.*, 2002) or oral squamous cell carcinomas (Yokoyama *et al.*, 2001) show a negative correlation between Snai1 expression and a good prognosis.

1.2.4. Snai1 and epithelial-to-mesenchymal transition

Many signaling pathways cooperate in the initiation and progression of EMT and these often include activation of Snai1 expression (Lamouille, Xu and Derynck, 2014). Snai1 and Snai2 activate EMT during development, fibrosis and cancer. This is achieved by repressing epithelial genes such as E-cadherin (Lamouille, Xu and Derynck, 2014). E-cadherin maintains cell–cell adhesions that are required for the formation and maintenance of embryonic and adult epithelial tissue. Loss of E- cadherin is considered to be indicative of a poor clinical prognosis since *E-cadherin* is thought to be an

invasion-suppressor gene (Cano *et al.*, 2000). One of the independent ways in which the importance of Snai1 in initiating EMT in mammals was demonstrated was by observing Snai1 converting otherwise normal epithelial cells into mesenchymal cells through the direct repression of *E-cadherin* expression (Nieto, 2002). Since E-cadherin expression causes epithelial cells to become limited in their ability to move or migrate, E-cadherin downregulation correlates with dedifferentiation and metastasis (Hemavathy, Ashraf and Ip, 2000). After binding of Snai1 to the *E-cadherin* gene, other factors such as SIN3A, histone deacetylase (HDAC) 1, HDAC2, and components of the Poly-comb 2 complex are recruited to coordinate histone modifications such methylation and acetylation (Lamouille, Xu and Derynck, 2014). Where Snai1 is overexpressed, epithelial cells convert to a fibroblastic phenotype with concomitant loss of E-cadherin expression, and tumourigenic, invasive and migratory properties are acquired (Cano *et al.*, 2000), indicating that Snai1 overexpression may contribute to the development of cancer and metastasis. Furthermore, Snai1-mediated loss of E-cadherin is often observed in melanoma and is known to contribute to tumour progression. Poser *et al*. (2004) found that in a panel of different melanoma cell lines, E-cadherin expression was negatively regulated by upregulation of Snai1 and when human primary melanocytes were transfected with a Snai1 expression plasmid, E-cadherin expression was decreased 2.7-fold (Poser and Bosserhoff, 2004). Additionally, Snai1 and Snai2 regulate cell cycle progression and survival during EMT (Lee and Shen, 2012).

Snai1 may also act as a transcriptional activator of other genes required for the acquisition of the fibroblastic phenotype. This is because although Snai1 is able to inhibit expression of epithelial genes, it may positively affect the expression of genes involved in migration of cells (Cano *et al.*, 2000). Snai1 can contribute to EMT by inducing the expression of mesenchymal markers such as vimentin (Lee and Nelson, 2012). Snai1 has been shown to increase expression of the cytoskeletal protein, vimentin and induce the promoter activity of ZEB1, a transcriptional repressor implicated in EMT induction (De Craene *et al.*, 2005). Snai1 and ZEB1 were also found to induce MMP-2 expression in squamous cell carcinoma, positively affecting cells' ability to

invade since MMP-2 can degrade the BM (Yokoyama *et al*., 2003). Furthermore, fibrotic human kidney tissue has been shown to have increased levels of Snai1, along with deposition of collagen I and expression of vimentin (Boutet *et al*., 2006).

Snai1 is not found in well differentiated, non-invasive mouse and human carcinomas but is expressed in dedifferentiated and invasive areas of carcinomas and also in E-cadherin-deficient mice and human carcinoma cell lines and tumours (Cano *et al*., 2000). The mesodermal layer formed by Snai1-deficient animal embryos is composed of cells characteristic of epithelial cells. These cells are columnar with apical–basal polarity, microvilli and adherens junctions, indicating that they failed to undergo EMT (Nieto, 2002). In mouse embryos, for ingression of mesodermal cells at gastrulation to occur, E-cadherin needs to be downregulated. In Snai1-deficient embryos, mesodermal cells retain E-cadherin expression, showing that Snai1 acts as a repressor of E-cadherin expression (Nieto, 2002).

Haraguchi *et al*. (2008) found that collagen IV was reduced in Snai1-expressing Madin-Darby canine kidney (MDCK) cells. The ability of these cells to detach was significantly diminished when the cells were plated in collagen IV coated wells, showing that a reduction in collagen IV might be partially responsible for the increased detachment of MDCK/Snai1 cells.

1.3. Summary

In summary, PXDN was: a) found to be upregulated in a colorectal cancer cell line undergoing p53-dependent apoptosis (Horikoshi *et al.*, 1999), b) found to encode the interleukin 1 receptor antagonist and six epitopes recognised by human CTLs (Hutchins *et al.*, 1991; Mitchell *et al.*, 2000), c) identified as a candidate tumour suppressor gene silenced by methylation in patients diagnosed with AMLs (Desmond *et al.*, 2007), d) found to be upregulated in malignant primary glial and metastatic brain tumours (Liu *et al.*, 2010) and e) implicated in increased tumour invasion (Tauber *et al.*, 2010; Jayachandran *et al.*, 2016). Though these links have been made between cancer cells and aberrant PXDN expression, the question of whether or not the expression of PXDN in different carcinoma types puts the carcinoma cells at a survival advantage (in relation to proliferation and invasive potential) is still vague. Furthermore, as the regulatory mechanisms of PXDN expression become understood, this could allow PXDN and its associated factors, to become biomarkers for early diagnosis or targets for cancer therapy.

Therefore, in this study, we firstly propose that PXDN is involved in EMT in carcinoma cells by modifying the BM during tumour formation and progression. Secondly, we propose that the expression of *PXDN* is regulated by the EMT master transcription factor, Snai1. Lastly, we hypothesise that *PXDN* expression is upregulated in response to TGF-β1, as the cells undergo EMT, and that as Snai1 expression is upregulated, correspondingly, it binds to the *PXDN* promoter to regulate expression.

Aim

To investigate the regulation of *PXDN* gene expression by the Snai1 transcription factor, the major regulator of EMT, and to elucidate the role of PXDN in EMT in human cervical carcinoma cells.

Objectives

1. Determine if PXDN is a feature of TGF-β1-induced EMT in HeLa and SiHa cervical carcinoma cells.
   i. Observe, by differential interference contrast (DIC) microscopy, the EMT phenotype in response to TGF-β1 through changes in cell morphology.
   ii. Confirm, by western blot, EMT induction by TGF-β1 through EMT marker expression, namely Snai1, E-cadherin, and vimentin.
   iii. Investigate, by immunofluorescence (IF) microscopy, changes in PXDN expression and cellular localisation in response to TGF-β1 treatment.

2. Investigate whether the Snai1 transcription factor plays a role in regulating *PXDN* gene expression.
   i. Observe, by IF microscopy, the effect of Snai1 overexpression on PXDN and EMT marker expression and cellular localisation.
   ii. Identify whether TGF-β1 causes Snai1 to interact with the PXDN promoter through chromatin immunoprecipitation (ChIP).
   iii. Determine the effects of Snai1 overexpression on driving *PXDN* gene expression by luciferase reporter assay.

3. Elucidate the role of PXDN in EMT by functional studies, wherein *PXDN* expression is knocked down (silenced).
   i. Quantify, by enzyme-linked immunosorbent assay (ELISA), the level of PXDN knockdown after transfection with siRNA.
   ii. Investigate the proliferation of cells by 3-(4,5-dimethylthiazol-2-yl)-2,5

diphenyltetrazolium bromide (MTT) assay, after knockdown of *PXDN* expression.

iii. Observe the effect of *PXDN* knockdown on attachment characteristics of cells to tissue culture treated plates.

iv. Observe the effect of *PXDN* knockdown on the invasion ability of cells by invasion assay using reconstituted BM.

v. Observe the effect of *PXDN* knockdown on migration ability of cells by scratch assay.

Chapter 2: Materials And Methods

2.1. Reagents

Reagents were purchased from Sigma Aldrich (St Louis, Missouri, USA) unless otherwise stated.

2.2. Cell culture

The human cervical adenocarcinoma cell lines used in this study were HeLa and SiHa. The human embryonic kidney cell line, HEK293, was used for cloning and transfection purposes. HeLa cells were purchased from Cellonex (Johannesburg, South Africa), SiHa cells were purchased from ATCC (Manassas, Virginia, USA), and HEK293 cells were a kind gift from Dr. Clement Penny (Department of Internal Medicine, University of the Witwatersrand, Johannesburg).

Cells were cultured in Dulbecco's Modified Eagle's Medium (DMEM): Ham's F12 Nutrient Mixture (F12) (3:1 ratio), supplemented with 10 % Fetal Bovine Serum (FBS) (Lonza Group, Basil, Switzerland) and 100 U/ml penicillin/0.1 mg/ml streptomycin. Cells were incubated at 37 °C in a humidified 5% CO_2 atmosphere. Culture medium was replaced every two days. To maintain the cell line, cells were sub-cultured when reaching 80% confluence by removing culture medium, rinsing cells three times in 1 x phosphate buffered saline (1x PBS: 137 mM NaCl, 2.7 mM KCl, 8.1 mM Na_2HPO_4 □ $12H_2O$, 1.8 mM KH_2PO_4, pH 7.4) before adding 1.5 ml Trypsin: EDTA (0.25% Trypsin: 0.02% EDTA in Hanks' Balanced Salt Solution) and incubating at 37 °C for 3-5 minutes. After cells had detached, 250 µl of cell suspension was added to 8 ml of fresh culture medium and the medium was changed the day after seeding cells.

2.3. RNA extraction

To extract RNA from cells, cells were seeded equally in 100 mm dishes, medium changed every two days and cultured until 60-80% confluent before harvesting. Cells were washed, on ice, three times in cold 1 x PBS. Trizol® reagent was added to each dish (1 ml) to disrupt cells, dissolve cell components and maintain the integrity of RNA. The contents of the cell culture dish were transferred to a microcentrifuge tube, vortexed for 30 seconds and then left at room temperature (RT) for four minutes. Chloroform (200 µl) was added to the samples to denature and solubilise proteins in the organic phase, and mixed by vigorous shaking for 15 seconds, left at RT for three minutes and centrifuged for 15 minutes at 12 000 rpm at 4 ^{o}C. The RNA-containing top phase was transferred to a new microcentrifuge tube, isopropanol (500 µl) was added and samples left at RT for 10 minutes, to precipitate RNA. Following centrifugation for 10 minutes at 12 000 rpm at 4 ^{o}C, the supernatant was discarded, the RNA pellets washed with 1 ml 75% ethanol and again centrifuged for five minutes at 12 000 rpm. The ethanol was removed and the pellet left to air-dry for 20 minutes at RT. To resuspend RNA pellets, RNase-free water (50 µl) was added and the solution was incubated in a 60 °C water bath for 10 minutes. RNA was quantified using a NanoDrop ND-1000 Spectrophotometer (Thermo Fisher Scientific). In order to determine the integrity of the RNA, a sample was electrophoresed through a 1% agarose gel containing ethidium bromide (10 mg/ml) (EtBr) to ensure the presence of clear, sharp 28S (5 kb) and 18S (1.9 kb) rRNA bands with a 2:1 intensity ratio.

2.4. Agarose gel electrophoresis

To make a 1% agarose gel, 1x Tris-acetate-EDTA (TAE) buffer (40 mM Tris, 0.1% glacial acetic acid, 0.2 % 0.5 M EDTA pH 8) was added to 0.5 g agarose and heated in a microwave to dissolve agarose. Once cooled, 1 µl EtBr (of a 10 mg/ml stock solution) was added to the agarose solution before pouring into a gel-casting tray and allowing to set at RT. Once the gel had set, it was immersed in 1x TAE buffer and electrophoresis was carried out at 100 V (constant) for approximately 40 minutes. For band size

determination, 4 µl GeneRuler 1 kb DNA ladder (Thermo Fisher Scientific) was loaded into one well of the gel for reference. All RNA and PCR products were pre-mixed with 2 µl of 6x DNA loading dye (0.25% xylene cyanol, 0.25% bromophenol blue, 30% glycerol, pH 7). Following electrophoresis, gels were viewed under the ultraviolet (UV) light of a Bio-Rad Gel Doc XR System and images were captured using Image Lab software.

2.5. cDNA synthesis

cDNA was reverse transcribed from RNA using the RevertAid™ First Strand cDNA Synthesis Kit (Thermo Fisher Scientific). After thawing kit components, in a sterile, nuclease-free PCR tube on ice, 1 µl oligo (dT)18 primer was added to 1 µg total RNA. Diethyl pyrocarbonate (DEPC) treated water was added to bring the sample volume to 12 µl. Following incubation in a 2720 Thermal cycler (Applied Biosystems) at 65 °C for five minutes, PCR tubes were placed briefly on ice, centrifuged for a few seconds then placed back on ice. The following components were then added in the indicated order: 4 µl 5x reaction buffer, 1 µl RiboLock RNAse inhibitor (20 U/µl), 2 µl 10 mM dNTP mix, 1 µl RevertAid reverse transcriptase (200 U/µl), to a total volume of 20 µl. The samples were then mixed gently, briefly centrifuged and again incubated in the thermal cycler (42 °C for one hour and 70 °C for five minutes).

2.6. PCR

PCR was used to test for the expression of specific mRNA in the cell lines and also to amplify DNA regions for cloning. PCR was performed using 2x PCR Master Mix (Thermo Fisher Scientific) following manufacturer's instructions. For a total 25 µl reaction mixture, the following components were added to a sterile, nuclease-free PCR tube: 12.5 µl master mix, 0.5 µl each of 10 µM forward and reverse primers, 1 µl template cDNA and 10.5 µl nuclease-free water. The samples were gently vortexed, briefly centrifuged and incubated in a thermal cycler under the necessary cycling conditions. All PCR products were pre-mixed with 2 µl 6x DNA loading dye before loading onto

1% agarose gels. PCR products were resolved on a 1% agarose gels and viewed under UV light, as previously described (section 2.4. pg 32).

2.6.1. Glyceraldehyde 3-phosphate dehydrogenase PCR

PCR of a housekeeping/reference gene (genes involved in basic cellular processes that are used as a control for uniform gene expression) was used to confirm successful cDNA synthesis. Primers (supplied in the RevertAid™ First Strand cDNA Synthesis Kit to give a 496 bp amplicon) specific to the glyceraldehyde 3-phosphate dehydrogenase (*GAPDH*) gene were used to perform PCR following cDNA synthesis (Table 2.1). Cycling conditions for GAPDH PCR were as follows: Initial denaturation at 94 °C for three minutes; 30 amplification cycles made up of denaturation at 94 °C for 30 seconds, annealing at 58 °C for 30 seconds and extension at 72 °C for 15 seconds; and final extension at 72 °C for seven minutes.

2.6.2. Peroxidasin primer design and PCR

PXDN-specific primers were designed to test for mRNA expression of *PXDN* by PCR. *PXDN* expression primers were designed using Integrated DNA Technologies' (IDT) PrimerQuest PCR design tool. The Basic Local Alignment Search Tool (BLAST) was used to ensure minimal non-specific binding of primers to other genes. The expected amplicon size of the primers was 636 bp. Primers (Table 2.1) were synthesised by Inqaba Biotechnical Industries (South Africa). *PXDN*-specific PCR was performed as described above (section 2.6. pg 33) using 2x PCR Master Mix and *PXDN*-specific primers. Cycling conditions for PXDN PCR were as follows: Initial denaturation at 95 °C for three minutes; 30 amplification cycles made up of denaturation at 95 °C for 30 seconds, annealing at 59 °C for 30 seconds and extension at 72 °C for 50 seconds; and final extension at 72 °C for 10 minutes. PCR products were resolved on a 1% agarose gel and viewed under UV light, as previously described (section 2.4. pg 32).

Table 2.1: GAPDH and PXDN mRNA expression primer sequences

Region	Primer sequences
GAPDH	Forward: 5′ CAAGGTCATCCATGACAACTTTG 3′ Reverse: 5′ GTCCACCACCCTGTTGCTGTAG 3′
PXDN mRNA expression	Forward: 5′ TATTGAGGGCCAGACCGTGGATTT 3′ Reverse: 5′ ATCATTTGGAGAACGAGGACGGCT 3′

2.7. Protein expression determination by western blot

To determine the expression of specific proteins in cell lysates (cytoplasmic and nuclear fractions) and changes in the expression level of the proteins, protein concentration was determined by western blot. In order to determine the level of protein expression in each cell sample, cells were lysed in lysis buffer with protease inhibitors. Whole cell protein was quantified in order to determine protein concentration for all samples. Proteins were then denatured under reducing conditions and resolved (separated by molecular weight) on a sodium dodecyl sulfate (SDS) polyacrylamide gel. Resolved proteins were then transferred (electroblotted) to a membrane that was subsequently incubated with target-specific primary antibodies, which were then detected by using a corresponding secondary horseradish peroxidase (HRP) conjugated antibody. In the presence of a substrate, the HRP emits light, which is captured on X-ray film and the film developed. The bands on the X-ray film were then quantified and equalized against a control protein (β- actin) of known concentration. The abovementioned steps are described below.

2.7.1. Cell preparation and lysis

Cells were seeded equally in 100 mm cell culture dishes, medium changed every two days, and cultured until 80% confluent. Cells were then placed on ice and washed three times with cold 1x PBS. Cells were then collected by scraping in 1 ml of 1x PBS and centrifuged at 10 000 rpm for 10 minutes at 4 ^{o}C. The pellet was re-suspended in either triple detergent lysis buffer (50 mM Tris-HCl pH 8, 150 mM NaCl, 0.1% SDS, 1% Triton X-100, 0.5% sodium deoxycholate) or ½ triple detergent lysis buffer (25 mM Tris-HCl pH 8, 75 mM NaCl, 0.05% SDS, 0.5% Triton X-100, 0.25% sodium deoxycholate) with

protease inhibitors (1 mM PMSF, 10 µM leupeptin, 10 mM sodium fluoride, 1 mM sodium orthovanadate), to lyse cells and release cytoplasmic (½ triple detergent lysis buffer) and/or nuclear proteins (full strength buffer). Lysates were left in lysis buffer, on ice, and vortexed for five seconds, every five minutes. After 45 minutes, cell lysates were centrifuged at 12 000 rpm for five minutes at 4 ^{o}C to pellet cell debris and collect the protein-containing supernatant.

2.7.2. Protein concentration determination

Cellular protein was quantified by the Bradford assay (Bradford, 1976) for cytoplasmic fraction or the Bramhall assay (Bramhall *et al*., 1969) for whole cell lysates containing the nuclear fraction.

2.7.2.1. Bradford assay

The Bradford method involved setting up a dilution series of known standard concentrations (ranging from 4 µg/ml to 50 µg/ml) of bovine albumin serum (BSA) dissolved in dH_2O. A dilution series of protein samples in ½ triple detergent lysis buffer (with protease inhibitors, as previously described in section 2.7.1. pg 35) were also prepared (1/100 and 1/200 dilutions in dH_2O), and 160 µl each of BSA standards, protein sample dilutions and lysis buffer dilutions were dispensed in triplicate into a 96-well microplate. Bio-Rad protein assay dye reagent (Bio-Rad) was added to each sample (40 µl), mixed by pipetting, then absorbance was read at 595 nm using a Multiskan GO microplate reader (Thermo Fisher Scientific). A standard curve of absorbance vs. BSA protein concentration was constructed using Microsoft Excel, and by fitting a linear trendline to the data points, the cellular protein concentration was determined by using the recorded absorbance values and the standard curve equation.

2.7.2.2. Bramhall assay

The Bramhall (Bramhall *et al*., 1969) method of protein quantification was used for cell samples lysed in triple detergent buffer (with protease inhibitors), as previously described (section 2.7.1. pg 35). Since this lysis buffer has a higher SDS content than ½ triple detergent lysis buffer, it is incompatible with the Bradford reagent which is inhibited by the higher SDS content in the full strength lysis buffer. To quantify protein after lysis of cells, a sheet of Whatman filter paper was placed in dH_2O on a shaker (30 rpm) for 20 minutes. The filter paper was then transferred to 95% ethanol, then 100% ethanol and finally, 100% acetone, for five minutes each, still on a shaker. The filter paper was air-dried before blotting with BSA solution (1 µl, 3 µl, 6 µl, 12 µl, 16 µl, and 20 µl of 1 mg/ml BSA dissolved in lysis buffer) and protein samples (2 µl in triplicate). After completely drying the filter paper, it was placed in 7.5% trichloroacetic acid (TCA) for 45 minutes on a shaker to fix proteins to the paper. The filter paper was stained in Coomassie brilliant blue gel staining solution (3 mM Coomassie blue; 50% methanol; 10% acetic acid) for one hour and destained in destain solution (12 % glacial acetic acid, 10 % methanol in dH_2O) for another hour. After drying filter paper completely, each BSA and protein sample was cut out of the filter paper and individually incubated overnight in elution solution (66 % methanol, 1 % of 25 % ammonium solution, in dH_2O) in the dark. After vortexing each tube, the absorbance value of each solution was read against a blank (elution solution alone) at 595 nm on a Multiskan GO microplate reader. A standard curve was plotted as described for the Bradford assay (section 2.7.2.1. pg 36).

2.7.3. SDS polyacrylamide gel electrophoresis

To separate equal amounts of protein (from total cellular protein samples) by molecular weight, samples were resolved by SDS polyacrylamide gel electrophoresis (SDS-PAGE) using the Mini-PROTEAN® Electrophoresis System (Bio-RAD). Gels were prepared depending on the size of the protein to be detected. Higher molecular weight proteins (>100 kDa) were resolved in a 4%-8% discontinuous SDS polyacrylamide gel (recipe: Table 2.2), while lower molecular weight proteins (<100 kDa) were resolved in a 5%-10% discontinuous SDS polyacrylamide gel (recipe: Table 2.2).

Table 2.2: Recipes for SDS-polyacrylamide gels. Gel percentage was selected based on the molecular weight of the protein being probed for. Higher molecular weight proteins were resolved in a 4% stacking gel and 8% resolving gel, while lower molecular weight proteins required a 5% stacking gel and 10% resolving gel.

	4% stacking gel	**5% stacking gel**	**8% resolving gel**	**10% resolving gel**
Reagent	(µl)	(µl)	(µl)	(µl)
29:1 acrylamide/bis-acrylamide	850	830	2667	3300
1.5 M Tris pH 8.8	0	0	2500	2500
1 M Tris pH 6.8	625	630	0	0
10% Ammonium persulfate (APS)	50	50	100	100
10% SDS	50	50	100	100
Tetramethyl-ethylenediamine (TEMED)	5	5	5	5
	Make up to 5 ml with dH_2O		Make up to 10 ml with dH_2O	

Prior to loading protein samples in the gels, samples were mixed with 4x protein loading buffer (0.2 M Tris-HCl pH 6.8, 8% SDS, 40% glycerol, 4% β-mercaptoethanol, 50 mM EDTA, 0.08% bromophenol blue) and heated to 100 °C for five minutes. SDS-PAGE was conducted in running buffer (0.1% SDS, 192 mM glycine, 25 mM Tris, pH 8.8) at

200 V (constant) until the loading buffer dye front reached the bottom of the gel. Spectra Multicolor Broad Range Protein Ladder (Thermo Fisher Scientific) was loaded onto SDS polyacrylamide gels to determine the molecular weight of electrophoresed proteins.

2.7.4. Electroblotting

Following electrophoresis, gels were removed from the system and submerged in transfer buffer (192 mM glycine, 25 mM Tris, 20% methanol, pH 8.3) for five minutes. This was to allow for equilibration of the gel and removal of residual SDS from the gel before electroblotting of proteins to Immobilon polyvinylidene fluoride (PVDF) transfer membranes (Merck Millipore). Gels were cut to remove the unrequired portions and these were stained in Coomassie brilliant blue gel staining solution for one hour and destained in destain solution (10% acetic acid, 10% methanol) overnight, to ensure even electrophoresis. Gel portions with the required proteins were placed onto activated PVDF membrane and sandwiched between filter paper and foam pads before placing in the electroblotting cassette. The cassette was placed into the transfer tank along with an ice pack and magnetic stir bar, topped up with transfer buffer and placed in a cold room, on a magnetic stirrer. Protein transfer time and current was dependent on the size of the protein being probed for: <100 kDa (200 mA constant current for 30 minutes), >100 kDa (200 mA constant current for one hour).

2.7.5. Blocking and antibody binding

Following electroblotting, non-specific regions of membranes were blocked by incubating membranes in 5% fat-free milk powder dissolved in Tris buffered saline with 0.1% Tween®20 (1x TBS/T: 200 mM Tris-HCl, 500 mM NaCl, 0.1% Tween®20, pH 7.6) at RT for one hour on a shaker at 40 rpm. Membranes were subsequently washed three times in cold 1x TBS/T, for five minutes per wash, at RT on a shaker at 100 rpm; then incubated in primary antibody. Primary antibodies used in this study (for western blots) include: goat anti-PXDN (1:200) (Santa Cruz Biotechnology), rabbit anti-Snai1 (1:1000) (Santa Cruz Biotechnology), rabbit anti-β-actin (1:500) (Santa Cruz

Biotechnology), rabbit anti-E-cadherin (1:1000) (Cell Signaling Technology) and rabbit anti-vimentin (1:1500) (Cell Signaling Technology). Primary antibodies were diluted in either 5% fat-free milk in 1x TBS/T (anti-PXDN and anti-Snai1) or 5% BSA in 1x TBS/T (anti-β-actin, anti-E-cadherin and anti-vimentin); and membranes left overnight at 4 °C on a shaker at 40 rpm. Before incubating in HRP-conjugated secondary antibodies: donkey anti-goat IgG or goat anti-rabbit IgG (both from Santa Cruz Biotechnology) diluted in 5% fat-free milk in 1x TBS/T, membranes were washed five times as described before primary antibody incubation. Secondary antibody incubation was at RT, in the dark for one hour. Membranes were again washed five times before detection of protein bands.

2.7.6. Chemiluminescence band detection and quantification

Proteins were detected using chemiluminescence substrate, SuperSignal West Pico (Thermo Fisher Scientific). To do this, a working solution of substrate was prepared (by mixing equal parts the Stable Peroxide Solution and the Luminol Enhancer Solution), and used to completely cover the membranes. The working solution was left on the membrane for five minutes at RT before pouring off and wicking off access solution with a paper towel. The membranes were then covered with cling film and the emitted light signal was captured on X-ray film. X-ray film signals were developed (developer solution: 6.4 M metol, 0.6 M sodium sulphite anhydrous, 80 mM hydroquinone, 450 mM sodium carbonate anhydrous, 34 mM potassium bromide) and fixed (fixer solution: 800 mM sodium thiosulphate, 200 mM sodium metabisulphite) in the dark. Densitometry (quantitative measurement of the optical density of the bands) was performed using Image Studio Lite Software (version 5.2.5).

2.8. TGF-β1 cell treatments

For TGF-β1 treatments to induce EMT, cells were seeded equally in 100 mm tissue culture dishes and medium changed every two days until cells were 60% confluent. At 60% confluence, cells were then cultured in low serum (1% FBS) medium overnight

followed by the addition of 5 ng/ml TGF-β1 (recombinant human expressed in CHO cells) for 24 or 48 hours.

2.9. Differential interference contrast microscopy

DIC images were captured to study changes in cell morphology. Cells ($8x10^4$) were seeded equally on coverslips in 24-well tissue culture plates and medium changed on the second day. After treating (as described in section 2.8. pg 40) live cells were then rinsed with cold 1x PBS and visualised on an Olympus BX63 microscope.

2.10. Immunoprecipitation to enrich for peroxidasin

In order to improve the yield of PXDN from total cell protein, PXDN was first immunoprecipitated (IP) from cell lysates prior to western blotting. Cells were lysed in native lysis buffer (25 mM Tris pH 8, 75 mM NaCl, 0.5% Triton X-100) with protease inhibitors, as previously described (section 2.7.1. pg 35). Protein was quantified by Bradford method as previously described (section 2.7.2.1. pg 36). To precipitate PXDN, 1 µg anti-PXDN antibody was added to 150 µg total protein lysates, made up to 1 ml with IP buffer (200 mM Tris-HCl pH 8, 150 mM NaCl, 0.5% Triton-X100) and left rotating (30 rpm) overnight at 4 °C. Samples were then rotated for four hours at 4 °C after the addition of 30 µl (resuspended volume) protein A/G-plus agarose beads (Santa Cruz Biotechnology) to bind the immunocomplexes. Beads were pelleted by centrifugation at 5000 rpm for two minutes, supernatant was removed and beads washed with IP buffer with protease inhibitors (three washes for five minutes each at 4 °C on rotation). After washing, beads were heated to 100 °C for 10 minutes in 4x denaturing protein loading buffer. Following centrifugation at 6000 rpm for five minutes, the supernatant was removed and electrophoresed in a 4-8% SDS-PAGE, electroblotted onto PVDF membrane and detected by chemiluminescence, as previously described (sections 2.7.3. – 2.7.6. pg 38).

2.11. Immunofluorescence microscopy

In order to visualise the expression and localisation of proteins in cells, confocal IF microscopy was performed. Cells (1.5 x 10^5) were seeded equally on 22 mm glass coverslips in 6-well tissue culture treated plates. Culture medium was changed the following day before treating cells (transfecting with vectors or siRNA, or TGF-β1 treatment, as described in section 2.8. pg 40 and section 2.15. pg 52, respectively). When the required time had lapsed (based on treatment of cells), cells were washed once with cold 1x PBS for five minutes on a shaker (30 rpm) and then fixed with 3% formaldehyde (v/v) in 1x PBS, for 15 minutes at RT on slow rotation (60 rpm). Formaldehyde was removed and cells washed three times in cold 1x PBS for five minutes per wash, on a shaker (30 rpm). Cell membranes were permeabilised by incubating in 0.25 % Triton X-100 in 1x PBS for one hour and washed again as previously described. Non-specific sites were blocked with 0.5% BSA in 1x PBS for 30 minutes at RT and washed once as previously described. Expression of PXDN, Snai1, E-cadherin and vimentin were detected with the respective primary antibodies; antibodies were diluted in a 1x PBS, 0.5% BSA solution and incubated overnight at 4 °C on a shaker (30 rpm). Coverslips were washed in 0.5 % BSA in 1x PBS, three times for five minutes per wash before incubating with the corresponding secondary antibodies: donkey anti-goat IgG-fluorescein isothiocyanate (FITC), goat anti-rabbit IgG-FITC, goat anti-rabbit IgG-Texas Red (TR) (all from Santa Cruz Biotechnology). Secondary antibodies were also diluted in a 1x PBS, 0.5% BSA solution and slides were incubated at RT in a moist container and protected from light by covering with foil. Three more five-minute 1x PBS washes were performed before incubating slides in 0.1 µg/ml of 4',6-diamidino-2-phenylindole (DAPI), diluted in 1x PBS, for five minutes in the dark. After three more 1x PBS washes, coverslips were mounted onto slides with Fluoromount, and sealed with clear nail polish. Cells were visualised with a Zeiss LSM 780 confocal microscope at 630x magnification and images captured using Zen 2010 software. Fluorophores were detected at the following wavelengths: FITC- $488_{exitation}/525_{emission}$, TR-

$561_{excitation}/615_{emission}$ and DAPI- $405_{excitation}/454_{emission}$. Background controls were incubated in secondary antibody only (no primary antibody).

2.12. Chromatin immunoprecipitation

To determine Snai1 interaction with the *PXDN* gene promoter, ChIP followed by PCR was performed. The principle of ChIP is based on the interaction of transcription factors with the promoter region of a gene. Proteins are cross-linked to the DNA with which they interact in the nucleus, then the protein is immunoprecipitated using a specific antibody along with the DNA fragments attached to the protein. The protein-DNA cross-link is then reversed and the DNA is used as the template for PCR to test for the presence a specific region of DNA. In this experiment, the E-cadherin promoter region served as a positive control as this gene is an established target of Snai1 (Batlle *et al.*, 2000; Cano *et al.*, 2000; Peinado *et al.*, 2004).

2.12.1. Cell collection and sonication

Cells were seeded equally in 100 mm tissue culture dishes, and medium changed every two days until cells were 60% confluent. Cells were either left untreated or treated with TGF-β1 (as described in section 2.8. pg 40) for 24 hours. Protein-DNA interactions were cross-linked by added formaldehyde directly to the culture medium to a final concentration of 1%. Cells were left rotating gently for 10 minutes at RT on a shaking platform (60 rpm). Formaldehyde was quenched by adding glycine to the culture medium to a final concentration of 0.12 M and left for five minutes, again shaking at RT. Cells were washed three times with cold 1x PBS, scraped in 1 ml of 1x PBS and collected in a microcentrifuge tube. Centrifuging at 4000 rpm for five minutes, in a cold room, collected the cell pellet. Cell pellets were resuspended in triple detergent lysis buffer and sonicated, to shear chromatin (sheared to 200-1000 bp fragments, confirmed by resolving a sample of sheared chromatin in a 1% agarose gel as previously described in section 2.4. pg 32) using a Misonix Ultrasonic Liquid Processor XL-2000, 15 pulses for 15 seconds each, with cooling on ice in between pulses. Cell debris was removed by

centrifuging at 10 000 rpm for 10 minutes in a cold room, leaving the chromatin containing supernatant.

2.12.2. Genomic DNA extraction

To quantify genomic DNA in the supernatant, genomic DNA was extracted by phenol-chloroform extraction method. A sample of the supernatant (50 µl) was transferred to a microcentrifuge tube and to this, 2 µl RNAse A (10 mg/ml, Thermo Fischer Scientific) was added and the tube incubated for one hour in a 37 °C water bath. Proteinase K (2 µl of 20 mg/ml, Thermo Fisher Scientific) was added and incubation adjusted to 50 °C for two hours, with gentle swirling of the supernatant every 20 minutes. An equal volume of phenol:chloroform:isoamyl alcohol (25:24:1) was added and the solution vortexed vigorously for 30 seconds before centrifuging at 13 000 rpm for 25 minutes at RT. The upper phase was carefully removed without contamination from the lower phases and transferred to a new microcentrifuge tube. An equal volume of phenol:chloroform:isoamyl alcohol (25:24:1) was again added to the previously extracted upper phase and again vortexed and centrifuged as previously described. The upper phase was again removed and to this an equal volume of chloroform:isoamyl alcohol (24:1) added, and vortex and centrifugation steps repeated. The upper phase was again removed and to this 0.1 volume 3 M sodium acetate and two volumes absolute ethanol were added and the solution mixed by inversion. After incubation at -20 °C overnight to precipitate DNA, DNA was pelleted by centrifuging at 13 000 rpm for 20 minutes in a cold room. The DNA pellet was washed three times with cold 70% ethanol, air-dried and resuspended in nuclease-free water. Assessment of DNA quality and fragment sizes was through agarose gel electrophoresis (1% agarose gel, as previously described in section 2.4. pg 32) and quantification using the NanoDrop. This DNA was used as the input sample for PCR.

2.12.3. Immunoprecipitation

DNA (15 -25 µg) was diluted up to 1 ml with dilution buffer (1% Triton-X 100, 2 mM EDTA pH 8, 20 mM Tris-HCl pH 8, 150 mM NaCl) with protease inhibitors (1 mM PMSF, 10 µM leupeptin, 10 mM sodium fluoride and 1 mM sodium orthovanadate), and pre-cleared with 20 µl (resuspended volume) protein A/G plus agarose beads for one hour in a cold room on a vertical rotator (50 rpm). Beads were collected by centrifuging at 2 500 rpm for five minutes. The supernatant was collected and to this, 4 µg anti-Snai1 antibody was added. The DNA-antibody solution was left rotating overnight at 4 ^{o}C. A no antibody, beads and DNA only, control sample was also prepared in the same way. After overnight incubation, 40 µl (resuspended volume) protein A/G plus agarose beads were then added to the immunocomplexes with rotation for two hours at 4 ^{o}C and beads were subsequently pelleted as previously described. Pelleted beads were washed three times with 1 ml wash buffer (0.1% SDS, 1% Triton-X 100, 2 mM EDTA pH 8, 20 mM Tris-HCl pH 8, 15 mM NaCl), once with 1 ml final wash buffer (0.1% SDS, 1% Triton-X 100, 2 mM EDTA pH 8, 20 mM Tris-HCl pH 8, 500 mM NaCl) and twice with 1 ml TE buffer (10 mM Tris-HCl pH 8, 1 mM EDTA pH 8).

2.12.4. Elution and PCR

After the final wash, 200 µl pre-warmed elution buffer (1% SDS, 100 mM $NaHCO_3$) was added to the centrifuged beads and incubated at 65 ˚C for 6 hours to reverse cross-links. Following protein digestion with Proteinase K (final concentration, 0.1 mg/ml) for two hours at 50 °C, DNA was purified using the GeneJet PCR Purification kit (Thermo Fisher Scientific), according to manufacturer's instructions. Eluted DNA was analysed by PCR, and for this, two sets of primers were designed for each of the PXDN and E-cadherin gene promoter regions (Table 2.3).

Table 2.3: Primer sets for Snai1 vector, ChIP and luciferase reporter assay constructs.

Region	Primer sequences
pcDNA-Snai1	Forward: 5′ATCGCTAGCATGCCGCGCTCTTTCCTCG 3′ Reverse: 5′ATCTGATATCTCAGCGGGGACATCCTGAGCA 3′
ChIP PXDN^{Snai1+}	Forward: 5′ GAACGTTAAATAATTTCCTACGT 3′ Reverse: 5′GGCGCAGAACAGCACGAGCG 3′
ChIP PXDN^{Snai1-}	Forward: 5′GTTTGCGACGGGAACACGCC 3′ Reverse: 5′AAAGCCCCTCATTCCTTTTGAGGA 3′
*ChIP E-cadherin^{Snai1+}	Forward: 5′GGCCGGCAGGTGAAC 3′ Reverse: 5′GGGCTGGAGTCTGAACTGAC 3′
ChIP E-cadherin^{Snai1-}	Forward: 5′GCTGGTCAGTGTCAAATGCT 3′ Reverse: 5′CCTCAGTTTCTCCACCCTCC 3′
Luciferase PXDN^{Snai1+}	Forward: 5′ATAGCTAGCGAACGTTAAATAATTTCCTACGTGGT 3′ Reverse: 5′ATTAGATATCGGCGCAGAACAGCACGAGCG 3′
Luciferase PXDN^{Snai1-}	Forward: 5′ATAGCTAGCGTTTGCGACGGGAACACGCC 3′ Reverse: 5′AAAGATATCAAAGCCCCTCATTCCTTTTGAGGA 3′
Luciferase E-cadherin^{Snai1+}	Forward: 5′ATTTAGCTAGCGGCCGGCAGGTGAAC 3′ Reverse: 5′TCGTAGATATCGGGCTGGAGTCTGAACTGAC 3′
Luciferase E-cadherin^{Snai1-}	Forward: 5′ATTTAGCTAGCGCTGGTCAGTGTCAAATGCT 3′ Reverse: 5′TCGTAGATATCCCTCAGTTTCTCCACCCTCC 3′
T7	Forward: 5′TAATACGACTCACTATAGGG 3′

*Primers from Vandewalle *et al*. span across three E-boxes in the *E-cadherin* promoter (Vandewalle *et al.*, 2005).

For the *PXDN* promoter, we identified three E-boxes close to the transcription start site (Fig. 2.1) and designed one set of primers that amplified across these putative Snai1 binding sites (Snai1+) and another set that amplified across a region in the *PXDN* promoter with no E-boxes (Snai1-) (Fig. 2.1). The same method was used to design primers for the E-cadherin promoter region. Primers were designed using IDT's PrimerQuest and BLAST to ensure specific binding to the identified regions.

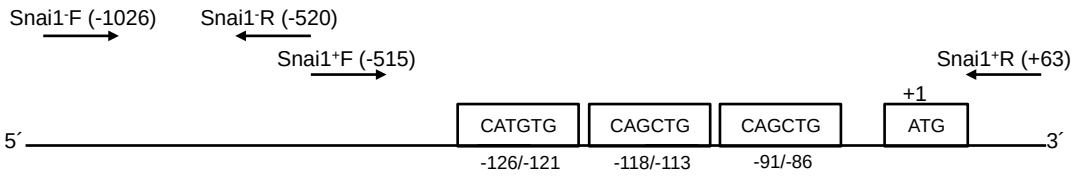

Figure 2.1: PXDN promoter region depicting three E-boxes as putative Snai1 binding sites. One set of primers was designed to span across these three sites (Snai1+) and another set of primers was designed to amplify across a region with no identified E-boxes (Snai1-) for use in ChIP and luciferase reporter assays.

PCR was conducted using 2x PCR Master Mix, as previously described in section 2.6. pg 33, with the following cycling conditions:

PXDN^{Snai1+}: Initial denaturation at 95 °C for two minutes; 35 amplification cycles made up of denaturation at 95 °C for 30 seconds, annealing at 64 °C for 30 seconds and extension at 72 °C for 40 seconds; and final extension at 72 °C for two minutes (producing a 578 bp amplicon).

PXDN^{Snai1-}: Initial denaturation at 95 °C for two minutes; 35 amplification cycles made up of denaturation at 95 °C for 30 seconds, annealing at 61 °C for 30 seconds and extension at 72 °C for 40 seconds; and final extension at 72 °C for two minutes (producing a 507 bp amplicon).

E-cadherin^{Snai1+}: Initial denaturation at 95 °C for two minutes; 35 amplification cycles made up of denaturation at 95 °C for 30 seconds, annealing at 58 °C for 30 seconds and extension at 72 °C for 15 seconds; and final extension at 72 °C for two minutes (producing a 168 bp amplicon).

E-cadherin^{Snai1-}: Initial denaturation at 95 °C for two minutes; 35 amplification cycles made up of denaturation at 95 °C for 30 seconds, annealing at 52 °C for 30 seconds and extension at 72 °C for 40 seconds; and final extension at 72 °C for two minutes (producing a 544 bp amplicon).

2.13. pcDNA-Snai1

In order to increase Snai1 expression in cells, we constructed a Snai1 expression vector with which to transfect cells. For this purpose, we selected the mammalian expression vector, pcDNA3.1 (Invitrogen). The full-length Snai1 expressing pcDNA3.1 vector (pcDNA-Snai1) was constructed by firstly isolating total RNA from HeLa cells using the Trizol® and phenol/chloroform method as previously described (section 2.3. pg 32). Then mRNA was converted to cDNA using the RevertAid First Strand cDNA synthesis kit with the Oligo dT primer, as previously described (section 2.5. pg 33). The full-length Snai1 coding region was amplified by PCR (Snai1 primers, Table 2.3, designed using IDT's PrimerQuest tool and BLAST search to minimise non-specific binding) using KAPA High Fidelity (HiFi) HotStart ReadyMixPCR Kit (Kapa Biosystems) and producing an 814 bp amplicon. For a total 25 µl reaction mixture the following components were added to a sterile, nuclease-free PCR tube: 12.5 µl 2x KAPA HiFi HotStart ReadyMix, 1 µl each of 10 µM forward and reverse primers, 100 ng template DNA and nuclease-free water up to 25 µl. The sample was gently vortexed, briefly centrifuged and incubated in a thermocycler under the following cycling conditions: initial denaturation at 95 °C for three minutes, 30 amplification cycles made up of denaturation at 98 °C for 20 seconds, annealing at 66 °C for 15 seconds and extension at 72 °C for one minute; and final extension at 72 °C for one minute. Following PCR, a small quantity of the PCR product was resolved in a 1% agarose gel to ensure successful PCR and the correct amplicon size. Snai1 insert was purified from the PCR mix using the GeneJet PCR Purification Kit (Thermo Fisher Scientific), according to manufacturer's instructions, and quantified using the NanoDrop. Vector and DNA insert were restricted in double-digestion reactions using Nhe1 and EcoRV enzymes, according to manufacturer's instructions (Thermo Fisher Scientific); Nhe1 and EcoRV restrictions sites were engineered into the primers (as underlined in the primer sequences in Table 2.3). Following restriction, vector and DNA insert were again purified using the GeneJet PCR Purification Kit, and quantified using the NanoDrop, before ligating Snai1 insert into the pcDNA3.1 vector using T4 DNA ligase (5 U/µl)

(Thermo Fisher Scientific). Recombinant DNA was transformed into *E.coli* JM109 cells using a chemical transformation method. Ligation of insert DNA to vector, bacterial transformation and isolation of plasmid DNA from bacteria (minipreparation) are described in more detail below.

2.13.1. Ligation (T4 DNA ligase)

The insert to vector ratios used were 3:1 and 5:1. For a 20 µl reaction, 10 µl of ligation buffer was added to a nuclease-free PCR tube. To this, the required amount of linear DNA insert (depending on DNA concentration) and 50 ng vector DNA were added. After adding 1 µl of T4 DNA ligase, the reaction mixture was made up to 20 µl with nuclease-free water. After mixing well and briefly centrifuging, the reaction mixture was incubated in a thermal cycler for one hour at 22 °C and ligase was inactivated at 70 °C for five minutes.

2.13.2. Chemical transformation of *E.coli* JM109

In order to make bacteria competent to take up recombinant DNA, *E.coli* was grown overnight in lysogeny broth (LB broth). While bacteria was still in exponential growth phase (absorbance falling between 0.5 and 0.6 when read at 600 nm), 1 ml bacterial culture was chilled on ice for five minutes before pelleting cells by centrifugation for five minutes at 10 000 rpm in a cold room. After discarding the supernatant, the bacterial pellet was resuspended in transformation buffer (100 mM $CaCl_2$, 100 mM Tris-HCl pH 8) and left on ice for 10 minutes. Cells were again pelleted by centrifugation before being resuspended in 200 µl transformation buffer and left on ice for two hours. Recombinant DNA (5 ng) was then added to 50 µl competent bacteria and after gentle tapping of the tube was left on ice for 30 minutes. Bacteria were heat shocked in a 42 °C waterbath for 90 seconds before placing back on ice. Following addition of 500 µl super optimal broth (SOB) (LB, 2.5 mM KCl, 10 mM $MgCl_2$), bacteria were incubated for one hour on rotation (220 rpm) at 37 °C. Transformed bacteria were selected for on LB agar plates containing ampicillin (100 µg/ml).

2.13.3. Minipreparation of plasmid DNA by alkaline lysis method

Transformed bacterial colonies were individually selected from ampicillin-containing LB agar plates and used to inoculate fresh ampicillin-containing LB broth which was left on rotation (30 rpm) overnight at 37 °C. Bacteria were isolated by centrifuging at 12 000 rpm for one minute and discarding the broth supernatant. The bacterial pellet was resuspended by vortexing in 110 µl resuspension buffer (25 mM Tris-HCl pH 8, 10 mM EDTA, 0.1 mg/ml RNAse A). Lysis buffer (400 mM NaOH, 2% SDS) was then added to the bacterial suspension and mixed by gentle inversion. After addition of 120 µl neutralizing buffer (ice-cold 5 M potassium acetate pH 5.5), bacterial suspension was left at RT for three minutes. Plasmid-containing supernatant was removed after centrifuging the mixture at 13 000 rpm for five minutes and to this, 200 µl isopropanol was added and left for two minutes at RT to precipitate DNA. The DNA pellet was isolated after centrifuging at 13 000 rpm for one minute and removing supernatant. DNA was washed with 70% ethanol before dissolving in nuclease-free water and quantifying using the NanoDrop. The presence and orientation of DNA inserts in the vector (recombinant vectors) was confirmed by Sanger sequencing (Inqaba Biotechnical Industries, South Africa), using the T7 forward primer (Table 2.3). We then confirmed that the recombinant vectors were functional by transfecting HeLa and SiHa cells with the vectors, using TurboFect (ThermoFisher Scientific) according to manufacturer's instructions. Transient transfections were performed over 24-48 hours as indicated, then protein expression and localisation determined IF microscopy (as previously described in section 2.11. pg 42).

2.14. Luciferase reporter assay

In order to assess the ability of Snai1 to repress *PXDN* gene expression from the *PXDN* promoter, luciferase reporter assay was performed using the Steady-Glo® Luciferase assay system (Promega). Two regions of the *PXDN* promoter, one with ($PXDN^{Snai1+}$) and one without ($PXDN^{Snai1-}$) putative Snai1 E-boxes were selected by identifying the Snai1 consensus binding sequence, CANNTG, in the PXDN promoter region. We then

re-designed the primer sets used for ChIP by engineering EcoRV and NheI restriction sites into the primers (Table 2.3). The PXDN^{Snai1-} primers were used to amplify the Snai1 E-box null region by HiFi PCR, as previously described (section 2.13. pg 48), under the following cycling conditions: Initial denaturation at 95 °C for three minutes; 35 amplification cycles (denaturation at 98 °C for 20 seconds, annealing at 61 °C for 15 seconds and extension at 72 °C for 40 seconds) and final extension at 72 °C for five minutes. PCR of this region produced a 525 bp amplicon which was restricted through the NheI and EcoRV restriction sites (the vector was also restricted in the same way). Cloning of the insert into the vector was as previously described (section 2.13.1. pg 49). The PXDN^{Snai1+} region was amplified by PCR (597 bp PCR product), restricted and cloned into the pGL4.10 vector by Biomatik (Ontario, Canada). As a positive control, we performed the abovementioned protocol to construct luciferase reporter assay vectors of the E-cadherin promoter. The cycling conditions for E-cadherin^{SnaiI+} (promoter region containing Snai1 E-box elements) were as follows: Initial denaturation at 95 °C for two minutes; 35 amplification cycles (denaturation at 98 °C for 20 seconds, annealing at 59 °C for 15 seconds and extension at 72 °C for 20 seconds) and final extension at 72 °C for five minutes (producing a 190 bp amplicon). The cycling conditions for E-cadherin^{SnaiI-} (promoter region with no Snai1 binding sites) were as follows: Initial denaturation at 95 °C for two minutes; 35 amplification cycles (denaturation at 98 °C for 20 seconds, annealing at 58 °C for 15 seconds and extension at 72 °C for 45 seconds) and final extension at 72 °C for five minutes (producing a 566 bp amplicon). Sanger sequencing (Inqaba Biotechnical Industries, South Africa) was used to confirm the recombinant vector sequences prior to transfections.

Cells (8 x 10^3) were seeded equally in 96-well tissue culture plates and maintained for 48 hours before transfecting. The vectors pGL4.10- PXDN^{SnaiI+}, pGL4.10- PXDN^{SnaiI-}, pGl4.10- E-cadherin^{Snai1+} and pGl4.10- E-cadherin^{Snai1-} were each co-transfected with pcDNA-Snai1 into HEK293 cells using TurboFect transfection reagent, according to manufacturer's instructions. After 24 hours, the luciferase assay was performed using the Steady-Glo Luciferase assay system. Cells were removed from the incubator and left

to reach RT. Luciferase reagent (prepared according to manufacturer's instructions) was added (100 µl, equivalent to amount of cell culture medium in each well) to each well, mixed thoroughly and incubated at RT for five minutes. The content of each well was then transferred to a luciferase plate and luminescence quantified using a GloMax-96 Microplate Luminometer (Promega).

2.15. Peroxidasin siRNA

In order to determine the effects of changes in PXDN expression on EMT related features such as migration, attachment and invasion, PXDN expression was knocked down using MISSION® esiRNA Human PXDN and TransIT-X2® System transfection reagent (Mirus Bio LLC, Madison, Wisconsin, USA). Cells ($8x10^4$) were seeded equally in 24 well tissue culture plates and left to attach for 12 hours before changing medium. For cell transfection, 1 µg siRNA was combined with 2.5 µl of transfection reagent, in serum-free medium, incubated at RT for 30 minutes then applied to cells, according to manufacturers instructions. Cells were then transfected for 24 hours prior to use in downstream assays. For samples where cells were to be treated with TGF-β1, 5 ng/ml TGF-β1 was added to cells three hours post-transfection. The negative control included in all experiments was MISSION® esiRNA Fluc targeting firefly luciferase gene. PXDN knockdown was visualised by IF microscopy and measured by ELISA.

2.16. ELISA

The ELISA is technique that can be used to detect and quantify protein. It is plate based in that the antigen is immobilised on a solid surface. In this experiment, PXDN-specific antibody (capture antibody) was immobilised on the bottom of the wells of a 96-well plate. The sample (cell lysate) is added to each well allowing PXDN in the lysate to bind to the immobilised antibody. An antibody (biotin conjugated) is added and binds to the captured PXDN. Avidin-HRP is added which binds to the biotin, then tetramethylbenzidine (TMB) is added and reacts with HRP to produce a color reaction (stopped by the addition of an acid) and absorbance is measured.

The Human PXDN/MG50 ELISA kit (LS-F12454, LifeSpan BioSciences, Inc.) was used to quantify changes in PXDN protein expression following knockdown of *PXDN* and/or treatment with TGF-β1. Cells ($8x10^4$) were seeded equally into 24-well tissue culture plates and maintained until 60% confluent. Transfection with siRNA, and TGF-β1 treatments were as previously described (section 2.8. pg 40 and 2.15. pg 52, respectively). When treatment time had lapsed, cells were washed three times with cold 1x PBS with protease inhibitors added (1 mM PMSF, 10 µM leupeptin), scraped in 1 ml 1x PBS and collected in a microcentrifuge tube. Cells were sonicated using a 750W Ultrasonic Processor (Sigma Aldrich) and sonication was performed on ice, for 10 seconds at 30% power, and then placed back on ice. The lysates were then centrifuged at 4 000 rpm for 10 min at 4 °C to remove cell debris. In order to derive protein concentration from absorbance readings, a standard curve was constructed beforehand by measuring the absorbance of known concentrations of PXDN protein (50 ng/ml - 0.782 ng/ml). Sample dilutions (dilutions of lysates) were also prepared in order to determine which dilution (undiluted, 1:10, 1:100 or 1:1000) would fall on the standard curve. For the assay, 100 µl of sample/standard/blank was added to the wells of the PXDN ELISA plate, in triplicate. The plate was sealed with a plate sealer and left to incubate at 37 °C for two hours. After aspirating all the liquid, a proprietary detection reagent was added and the plate left to incubate again for one hour at 37 °C. The plate was then washed three times before the addition of a second detection reagent, and again incubated for an hour at 37 °C. The plate was then washed five times before the addition of TMB substrate, which was left to act for 15-20 minutes at 37 °C. After optimal colour development was achieved, the reaction was stopped and absorbance at 450 nm measured using a Multiskan GO microplate reader. Total protein concentration of the samples was determined by Bradford assay (as previously described in section 2.7.2.1. pg 36) and the ELISA readings were corrected accordingly.

2.17. MTT cell proliferation assay

In order to determine the possible involvement of PXDN in cell proliferation, the MTT assay was used. The assay is colourmetric and cell metabolic activity is quantified by the reduction of MTT to formazan. Proliferating cells are able to reduce MTT to form purple formazan crystals. The formazan crystals are then dissolved and the optical density is measured to determine concentration. Cells ($8x10^3$) were seeded equally in 96-well tissue culture plates and left to attach and proliferate for 48 hours. Cells were transfected and treated as previously described (section 2.8. pg 40 and 2.15. pg 52). After the required incubation time the medium was removed from the wells and replaced with 100 µl of MTT solution (0.5 mg/ml MTT in cell culture medium) and incubated at 37 °C for one hour. The MTT solution was then removed (90 µl) without disturbing any formazan crystals, which were dissolved by the addition of 100 µl (dimethyl sulfoxide) DMSO and incubated for five minutes at 37 °C. After shaking the plate for 10 minutes at RT in the dark, absorbance was measured at 570 nm using a Multiskan GO microplate reader.

2.18. Attachment assay

In order to observe the changes in the ability of cells to attach to tissue culture plates, cell attachment assay was used. Cells ($8x10^4$) were seeded equally into 24-well tissue culture plates and maintained until 60% confluent. Cells were then transfected or treated with TGF-β1 as described in section 2.8. pg 40 and section 2.15. pg 52 After 24 hours, cells were trypsinised and after cells had detached the trypsin was neutralized with cell culture medium. Cells were then centrifuged at 2 500 rpm for five minutes in a cold room. Trypsin and culture medium was aspirated from the cell pellet and cells were washed twice in cold 1x PBS and centrifuged at 2 500 rpm for 5 minutes in a cold room, after each wash. After resuspending in culture medium, cells were counted with a haemocytometer, and $1x10^4$ cells/well were seeded equally into 96-well tissue culture plates. Cells were seeded equally for each of 4 time points (15 minutes, 30 minutes, 45 minutes and 60 minutes). After 15 minutes, unattached cells were removed from the 15

minutes time point wells by aspirating cell culture medium and gently rinsing wells with cold 1x PBS to remove unattached cells. Fresh culture medium (100 µl) was then added to the remaining attached cells. The same method of removing unattached cells was done after 30, 45 and 60 minutes for each of the relevant wells. An MTT assay was performed, as described in section 2.17. pg 54, to quantify the number of proliferating cells in each well at the four time points.

2.19. Invasion assay

Invasion of cells through a reconstituted BM was performed to assess the role of PXDN in cellular invasion in EMT. The invasion assay involves cells invading through a reconstituted BM (in this experiment we used ECM gel from Engelbreth-Holm-Swarm murine sarcoma). The plate used for the assay has two chambers (upper and lower), separated by a permeable support/insert on which the reconstituted BM is set. The cells are seeded in the upper chamber in low serum (1% FBS) medium, while the 10% FBS medium in the lower chamber acts as a chemoattractant that attracts the cells into the lower chamber, requiring the cells to invade the ECM gel.

All reagents and equipment used were kept cold to prevent setting of the ECM gel. The upper chamber of permeable supports of a 96-well Corning® HTS Transwell® plate were coated with 200 µg/ml ECM gel (diluted in cold serum-free culture medium) and incubated overnight at 37 °C to allow ECM gel to set. The residual medium was then removed and the ECM gel layers were re-hydrated with serum-free culture medium for one hour before seeding cells. Cells were trypsinised, collected and centrifuged for five minutes at 1 500 rpm at 4 °C. After re-suspending the pellet in 10% FBS culture medium, cells were counted using a haemocytometer and $1x10^4$ cells/well were seeded equally in the upper chambers of the Transwell® plate, the lower chambers were filled with 10% FBS culture medium. After 24 hours, the culture medium in the upper chamber was removed and replaced with low serum (1% FBS) culture medium. Cells were then transfected with PXDN siRNA or treated with TGF-β1, as previously

described (section 2.8. pg 40 and section 2.15. pg 52). After 24 hours, cells that did not invade (cells in the upper chamber) were removed using a cotton swab and cells that had invaded through the ECM gel were fixed to the inserts in 100% ice-cold methanol for 15 minutes and stained with crystal violet (0.2% w/v in 20% v/v ethanol) for 20 minutes at RT. The permeable inserts were then washed with dH_2O until the water ran clear and left to dry overnight. The crystal violet stain was dissolved in 10% acetic acid until all dye was removed from the inserts. Absorbance was measured at 590 nm using a Multiskan GO microplate reader.

2.20. Scratch assay

Scratch assays were performed to determine the effect of PXDN on cell movement/migration (the ability of cells to close a scratch made in the cell monolayer). Cells ($8x10^5$) were seeded equally into 24-well tissue culture plates and culture medium changed every two days until cells were 80% confluent. Transfections with PXDN siRNA and treatment TGF-β1 treatment were as previously described (section 2.8. pg 40 and section 2.15. pg 52). After 24 hours, a p200 pipette tip was used to create a scratch in the cell monolayer. Cells were then rinsed with 1x PBS to remove detached cells and fresh culture medium was added. The cells were visualised under the bright field of an Olympus BX63 microscope at 40x magnification. Cells were visualised after scratching (time point 0 hours) and then returned to the incubator and again viewed and images recorded after 12, 24 and 48 hours.

2.21. Statistical analysis

All results are representative of a minimum of three independent experiments and are expressed as means ± standard deviation (SD). Data obtained from treated and untreated samples were analysed using unpaired Student's t-test; a p-value of < 0.05 was considered significant. Stars represent the following p-values:

* $p \leq 0.05$ ** $p \leq 0.001$ ***$p \leq 0.001$

Chapter 3: Peroxidasin is regulated by the master EMT regulator, Snai1, during TGF-β1-induced EMT

3.1. Introduction

In order to ensure and maintain homeostasis in tissues, the interaction between cells and the ECM must be strictly controlled and balanced. Cytokines, acting through specific cell surface receptors, are essential in maintaining this balance. One of the most important cytokines in this regard is TGF-β1, a growth factor of the TGF family of cytokines (Blobe, Schiemann and Lodish, 2000).

The TGF-β family consists of five isoforms, with TGF-β1, TGF-β2 and TGF-β3 expressed in mammals (Blobe, Schiemann and Lodish, 2000). These three mammalian isoforms share 80% polypeptide sequence identity and have similar biological activities. However, expression of each isoform is tissue-specific: *TGF-β1* mRNA is expressed in endothelial, hematopoietic and connective-tissue cells; *TGF-β2* mRNA in epithelial and neuronal cells; and *TGF-β3* mRNA in mesenchymal cells (Blobe, Schiemann and Lodish, 2000). Since these mammalian isoforms are highly conserved, this may suggest a critical shared biologic function, as they all bind TGF-β receptors but differ in their binding affinities (Elliott and Blobe, 2005). TGF-β1, the most abundant and universally expressed isoform, can act both as a stimulator or inhibitor of cellular growth, depending on cell type and the state of cellular differentiation (Elliott and Blobe, 2005; Soulitzis *et al.*, 2006). TGF-β1 is able to effect cell proliferation by inhibiting growth via a reversible arrest of the cell cycle at G1 phase (Blobe, Schiemann and Lodish, 2000). In the ECM, TGF-β1 also regulates the formation of stroma and multiple ECM components since in the presence of TGF-β1, fibroblasts and other cells are stimulated to produce ECM proteins such as collagens, fibronectin and laminin (Hazelbag *et al.*, 2002). Understanding the function of TGF-β is important since changes in TGF-β gene expression such as transcriptional modifications or mutations, protein modifications such as mutations affecting translation and post-translational modifications, and cellular concentration levels have been linked to several disease states, including

atherosclerosis, fibrotic disease and cancer. Indeed, the significance of TGF-β signaling has been highlighted by mutations that affect TGF-β, TGF-β receptors and signaling molecules that associate with TGF-β, which are particularly important in the pathogenesis of diseases such as cancer (Blobe, Schiemann and Lodish, 2000).

The function of TGF-β in cancer is cell and stage specific and in the early stages of tumourigenesis TGF-β acts as a tumour suppressor (Elliott and Blobe, 2005). At this time, TGF-β acts directly on the cancer cell to suppress tumour outgrowth by inhibiting cell proliferation or by promoting cellular differentiation or apoptosis (Blobe, Schiemann and Lodish, 2000). At the later stages of tumour progression, the role of TGF-β changes to that of a stimulator of tumour proliferation, invasion and metastasis (Akhurst and Derynck, 2001). These changes usually occur as a result of cancer cells gaining mutations in the genes coding for proteins involved in the TGF-β signaling pathway, mutations that subsequently affecting the function of these proteins (Blobe, Schiemann and Lodish, 2000), allowing cancer cells to evade the growth inhibiting effects of TGF-β while exploiting the effects that promote tumour proliferation and metastasis. For example, TGF-β promotes angiogenesis and cancer cells exploit this as it allows new vessels to bring nutrients and oxygen to tumour cells. TGF-β also enhances the invasiveness and metastatic ability of malignant cells through its ability to modify the ECM by increasing deposition of ECM proteins (Soulitzis *et al.*, 2006). Löhr et al. (2001) showed that TGF-β1 from pancreatic cancer cells induced extensive, collagenous and cell-rich deposition in pancreatic carcinoma (Lohr *et al.*, 2001). Frazier *et al*. (1997) showed a connection between increased collagen deposition in mammary cancer and the production of TGF-β1 and TGF-β1–induced connective tissue (Frazier and Grotendorst, 1997). On the other hand, TGF-β is also able to mediate the production of enzymes that degrade the ECM, allowing cancer cells to invade the ECM and metastasise (Elliott and Blobe, 2005). For example, Safina *et al*. (2007) found that TGF-β stimulates MMP-dependent degradation of the ECM at the cell–matrix focal contacts of breast cancer MDA-MB-231 cells (Safina, Vandette and Bakin, 2007).

TGF-β signals by binding to three high-affinity TGF-β cell-surface receptors: types I, II, and III. TGFβRIII (type III receptors) are the most abundant type and they bind TGF-β and transfer it to its signaling receptors, type I and II receptors (TGFβRI and TGFβRII, respectively) (Blobe, Schiemann and Lodish, 2000). TGFβRI and TGFβRII are serine/threonine kinases, and once TGF-β binds to a receptor, TGFβRII recruits, binds and transphosphorylates TGFβRI which then phosphorylates cytoplasmic proteins, Smad2 and Smad3. The activated Smad2/3 then form complexes with Smad4, which translocates to the nucleus and binds to chromatin to regulate expression of genes involved in the regulation of cell proliferation, differentiation, apoptosis and cell migration (Fig. 3.1).

TGF-β signaling can also act through receptors that activate alternative signaling effectors, such as MAPK, phosphoinositide 3-kinase and small GTPases of the Rho family. These signaling molecules then contribute to regulation of genes controlling, amongst other cellular processes, cell motility, apoptosis and metastasis-promoting EMT (Blobe, Schiemann and Lodish, 2000; Moustakas and Heldin, 2007).

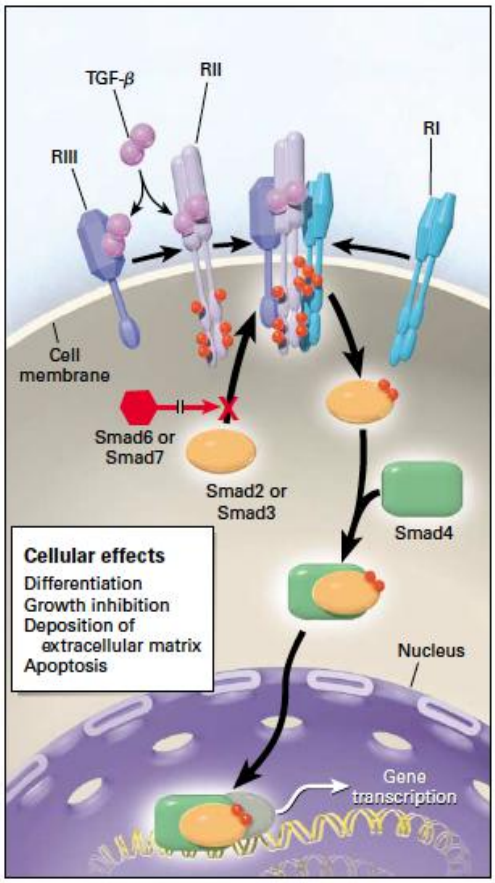

Figure 3.1: Smad-dependent TGF-β signaling mechanism. TGF-β ligand binds to either TGFβRII or TGFβRIII. If TGF-β binds to TGFβRIII, this receptor presents the ligand to TGFβRII. This then leads to TGFβRI binding to the complex, which causes transphosphorylation of TGFβRI. Phosphorylation (red spheres) of TGFβRI activates its protein kinase , which then phosphorylates the transcription factor Smad2 or Smad3. Smad4 then binds to phosphorylated Smad2/3, and the resulting complex moves from the cytoplasm into the nucleus. The nuclear Smad complex associates with various other transcription factors to regulate the transcription of TGF-β-responsive genes. Smad6 and Smad7 function to inhibit the phosphorylation of Smad2/3 by TGFβRI (taken from Blobe *et al*., 2000).

TGF-β mediates EMT by upregulating the expression of the EMT master regulator, Snai1, which belongs to the Snail family of transcription factors. This family consists of Snail, Snai2 and Snai3 (also known as Snai1, Slug and Smuc, respectively). They have a highly conserved carboxy-terminal region, containing four to six C_2H_2 type zinc fingers, and an amino-terminal region with a SNAG domain (Fig. 3.2). The zinc fingers function as the DNA-binding domains that recognise a sequence-specific consensus E-box: C/A(CAGGTG). The SNAG domain is the repressor domain and is evolutionarily conserved (Schwab, 2011). In addition, Snail has a nuclear localisation signal located within the zinc finger region (Lee and Shen, 2012).

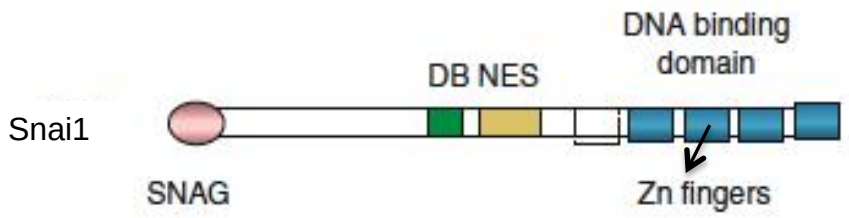

Figure 3.2: Diagram of the main structural features of Snai1. The DNA-binding domain is made up of four zinc finger motifs and the dotted box indicates the presence of a fifth zing finger in Snail1 protein in some invertebrates. The SNAG domain represses gene expression. Domains specific to Snai1 are a destruction box (DB) which mediates ubiquitylation and subsequent proteolysis of Snai1 and the nuclear export signal (NES) which mediates nuclear export of Snai1 (taken from Schwab, 2011).

Snai1 activates EMT during development, fibrosis and cancer (Naber *et al.*, 2013) and is the focus of this study. The significance of Snai1 as a master regulator of EMT in cancer has been shown through Snai1 silencing, which leads to inhibition of tumour growth and metastasis (Kudo-Saito *et al.*, 2009). Snai2 also functions to suppress epithelial markers and activate mesenchymal genes, although it has a lower affinity for the Snail consensus binding site than Snai1 (De Craene *et al.*, 2005; Schwab, 2011). Snai3 is a novel member of the Snail family and regulates basic helix-loop-helix transcription factors by

controlling differentiation processes through the competition of zinc finger domains for E-box binding (Kataoka *et al.*, 2000).

Snai1-induced EMT involves a complex genetic programme that results in the downregulation of epithelial genes, such as *E-cadherin* (Lamouille, Xu and Derynck, 2014) and the upregulation of mesenchymal and migratory genes such as the cytoskeletal protein, vimentin (De Craene *et al.*, 2005; Schwab, 2011). Snai1-mediated gene repression involves the recruitment of specific co-repressor complexes, and HDAC1 and HDAC2 to gene promoter regions (Peinado *et al.*, 2004; Lee and Shen, 2012). Snai1 is also able to recruit histone and DNA methylases to mediate epigenetic silencing of target genes (Schwab, 2011). On the other hand, Snai1 has also been found to upregulate gene expression by recruitment of differential transcriptional machinery and chromatin remodeling complexes (Lee and Shen, 2012). Vetter *et al*. (2009) found that morphological changes that occur in cells as a result of EMT, such as mesenchymal properties (flattening of cells and loss of cell–cell contacts), were visible within a time frame of 12–24 hours after Snai1 expression. Snai1 was expressed as early as 4 hours after induction by removing tetracycline from cell culture medium. Before 12 hours post-induction of Snai1 expression, transcriptional modifications that trigger EMT occur and precede phenotypic change (Vetter *et al.*, 2009). Expression of Snai1 in E-cadherin positive cells was found to induce expression of mesenchymal markers such as fibronectin and vimentin (Lee and Shen, 2012).

Epithelial cells arrange in layers of cells, tightly connected, laterally, by adherens junctions, desmosomes, tight junctions and gap junctions. The position of epithelial cells is maintained by their anchoring to the BM, ensuring that the cells can only migrate laterally along the basal surface, preventing them from entering the ECM. Additionally, the apical-basal polarity of epithelial is established through association with the BM and BM production and assembly is disrupted when cancer cells metastasise (Yang and Weinberg, 2008). Snai1 also promotes EMT by affecting cell adhesion; Snai1-expressing cells downregulate E-cadherin, migrate and become invasive through changes in their

cytoskeleton and the induction of MMPs (Barrallo-Gimeno, 2005). Haraguchi *et al*. (2008) found that exogenous expression of Snai1 in epithelial MDCK and A431 cells enhanced trypsin-induced cell detachment from the ECM; suggesting that Snai1 affects cell-to-ECM adhesion possibly through alteration of ECM components in the BM, secreted by the cells (Haraguchi *et al.*, 2008). Furthermore, a reduction in collagen IV (the main constituent of the BM) in Snail-expressing MDCK cells, leads to increased detachment (Haraguchi *et al.*, 2008). Perhaps the reduction of collagen IV in Snai1 expressing cells may be mediated by downregulation of *PXDN* expression by Snai1 since PXDN has been shown to consolidate collagen IV protomers (Bhave *et al.*, 2012).

In this chapter, we aimed to determine if there is a link between PXDN and TGF-β1-mediated EMT in HeLa and SiHa cells. To this end, we first established whether or not HeLa and SiHa cells undergo EMT in the presence of TGF-β1. We then investigated if PXDN expression changes in response to TGF-β1 exposure. Finally, since Snai1 is the main transcription factor regulating TGF-β1-induced EMT, we sought to determine if Snai1 regulates *PXDN* expression.

3.2. Methodology

Objective 1: Determine if PXDN is a feature of TGF-β1-induced EMT in HeLa and SiHa cervical carcinoma cells.

For TGF-β1 treatments, cells were cultured in low serum (1% FBS) overnight followed by the addition of 5 ng/ml TGF-β1 (recombinant human expressed in CHO cells) for 24 or 48 hours (as described in section 2.8. pg 40).

i. Observe EMT phenotype in response to TGF-β1 through changes in cell morphology.

- Changes in cell morphology were observed by DIC microscopy as described in section 2.9. pg 41.
  Briefly, cells were seeded on coverslips and treated with TGF-β1. The live cells were visualised on an Olympus BX63 microscope at 400x magnification.

ii. Confirm EMT induction by TGF-β1 through EMT marker expression and cellular localisation, namely Snai1, E-cadherin, and vimentin.

- Changes in expression of EMT markers were quantified by western blot as described in section 2.7. pg 35.
  Briefly, cells were seeded and treated with TGF-β1. Cells were lysed and total protein concentration determined by Bradford or Bramhall assays. Proteins were denatured under reducing conditions, resolved by SDS-PAGE and transferred to PVDF membrane. The membrane was incubated with Snai1, E-cadherin and vimentin primary antibodies. Membrane bound primary antibodies were detected by HRP-conjugated secondary antibodies. In the presence of a substrate, the HRP emits light, which is captured on X-ray film, and the film developed. The bands on the X-ray film were then quantified and equalised against a β-actin band of known concentration.
- Changes in cellular localisation of EMT markers were observed by IF

microscopy, as described in section 2.11. pg 42.

Briefly, cells were seeded on coverslips and treated with TGF-β1. Cells were fixed with formaldehyde and cell membranes were permeabilised in 0.25 % Triton X-100. Non-specific sites were blocked with 0.5% BSA before incubating in primary antibody (Snai1, E-cadherin or vimentin). Coverslips were then incubated in the corresponding HRP-conjugated secondary antibody. Coverslips were incubated in DAPI before mounting onto slides, sealing and visualising.

iii. Investigate changes in PXDN expression and cellular localisation in response to TGF-β1 treatment.

- Changes in PXDN expression and localisation were determined by western blot and IF microscopy, respectively, as described above for EMT markers. The exception to PXDN protein quantification was that PXDN was first immunoprecipitated before western blot, as described in section 2.10. pg 41.

  Briefly, cells were lysed in native lysis buffer and protein quantified by Bradford method. Anti-PXDN antibody was added to total protein lysates, and left rotating overnight. Samples were then rotated for four hours at after the addition of protein A/G-plus agarose beads. Beads were heated to 100 °C in denaturing protein loading buffer. The supernatant was removed and electrophoresed in a 4-8% SDS-PAGE, electroblotted onto PVDF membrane and detected by chemiluminescence, as described in section 2.7.3. pg 38.

Objective 2: Investigate whether the Snai1 transcription factor plays a role in regulating *PXDN* gene expression.

i. Design a Snai1 over expression vector and confirm functional vector by Sanger sequencing and IF microscopy.

- A Snai1 overexpression vector was designed and constructed as described in section 2.13. pg 48.

The Snai1 coding region was inserted into the mammalian expression vector, pcDNA3.1. Briefly, total RNA was isolated from HeLa cells using the Trizol® and phenol/chloroform method. Then mRNA was converted to cDNA and the full-length Snai1 coding region was amplified by PCR. This Snai1 insert was purified from the PCR mix, quantified, then both vector and DNA insert were restricted by an EcoRV/Nhe1 double-digestion reaction and subsequently ligated. Recombinant constructs were transformed into *E.coli* JM109 cells using a chemical transformation method and colonies selected by ampicillin resistance. Recombinant vectors were isolated from *E.coli* and Sanger sequencing was used to confirm the nucleotide sequence and orientation of the DNA insert in the vector.

- Confirmation of functional vector was by transfection of HeLa and SiHa cells followed by IF microscopy, as previously described above in section 2.11. pg 42.

ii. Observe the effect of Snai1 overexpression on PXDN expression and cellular localisation.

- After transfecting cells with Snai1 overexpression vector, changes in PXDN cellular localisation were observed by IF microscopy, as previously described above and in section 2.11. pg 41.

iii. Identify whether TGF-β1 causes Snai1 to interact with the *PXDN* promoter.

- The interaction of Snai1 with the *PXDN* promoter region was achieved through ChIP as described in section 2.12. pg 43.

  Briefly, cells were seeded and treated with TGF-β1, as previously described. Protein-DNA interactions were cross-linked by adding formaldehyde to the culture medium, which was quenched by the subsequent addition of glycine. Cells were lysed and sonicated to shear chromatin. Genomic DNA was extracted by phenol-chloroform extraction method and quantified. DNA was pre-cleared with protein A/G plus agarose and after collection of the supernatant, anti-Snai1 antibody was added. Protein A/G plus agarose beads were then added to the

immunocomplexes with subsequent pelleting of beads. DNA was eluted from beads and protein-DNA cross-links were reversed before digesting protein. DNA was eluted and analysed by PCR, with primers designed for each of the *PXDN* and *E-cadherin* gene promoter regions with and without Snai1 E-box binding sites.

iv. Determine the effects of Snai1 overexpression on driving *PXDN* gene expression.

- The effect of TGF-β1 and Snai1 overexpression on driving *PXDN* gene expression was investigated by luciferase reporter assay as described in section 2.14. pg 50. Briefly, two regions of the *PXDN* promoter, with and without putative Snai1 E-boxes were selected and engineered into a luciferase vector. In the same manner, luciferase reporter vectors of the *E-cadherin* promoter were designed. Sanger sequencing confirmed the recombinant vector sequences prior to transfections. Cells were either treated with TGF-β1 or co-transfected with pcDNA-Snai1 and the PXDN or E-cadherin luciferase vectors. After 24 hours luciferase reagent was added and the cell solution was transferred to a luciferase plate and luminescence quantified.

3.3. Results

3.3.1. TGF-β1 induces epithelial-to-mesenchymal transition and decreases peroxidasin expression in HeLa and SiHa cell lines

We first determined the effect of TGF-β1 treatment on EMT induction in HeLa and SiHa cervical carcinoma cells. EMT is characterised by the loss of the epithelial, and acquisition of a mesenchymal, phenotype. Morphologically this involves less cell-to-cell contacts with cells having a cobblestone-like appearance (Kalluri and Weinberg, 2009). We showed that TGF-β1 caused these morphological changes in both HeLa and SiHa cells (Fig. 3.3).

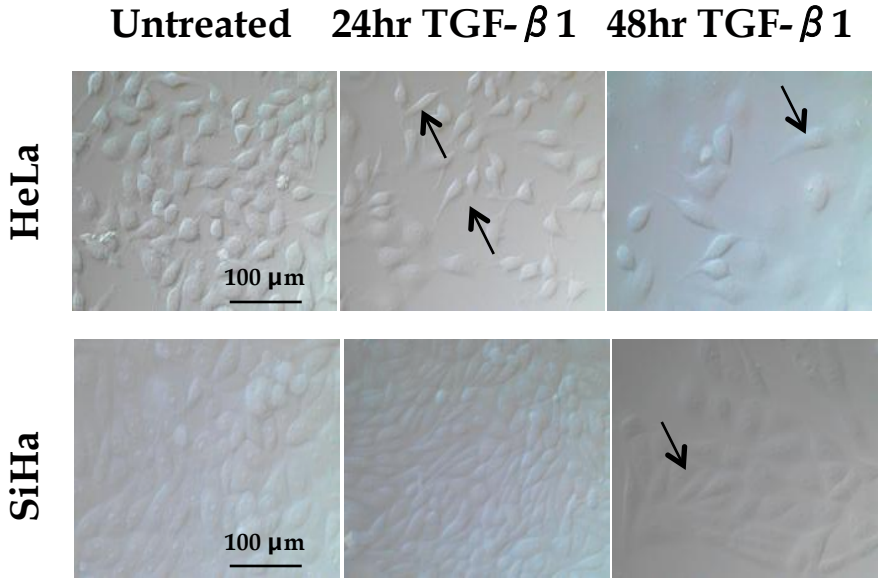

Figure 3.3: The morphology of TGF-β1–treated HeLa and SiHa cells. Morphological changes following treatment of cells with TGF-β1 for 48 hours depict long fibroblast-like features (indicated by arrows) and loss of cell-cell contacts. Cells were visualised on an Olympus BX63 microscope at 400x magnification.

These morphological changes are usually accompanied by modified expression of various EMT markers, including decreased expression of E-cadherin, which is a

classical marker of the epithelial phenotype (Cano *et al.*, 2000) and increased expression of Snai1 and vimentin (Huber, Kraut and Beug, 2005), which reflect the mesenchymal properties of cells undergoing EMT. To assess these, together with looking at the effect of TGF-β1 on PXDN expression, we looked at the level of PXDN, Snai1, E-cadherin and vimentin, by western blotting and IF microscopy. First, by western blot, we quantified the changes in expression levels of PXDN and the EMT markers Snai1, E-cadherin and vimentin in response to TGF-β1 treatment over 24 and 48 hours. Interestingly, TGF-β1 treatment resulted in significantly decreased expression of PXDN in HeLa cells by 26% to 74 ± 10.5% after 24 hours, relative to untreated cells. A similar trend of decreased PXDN expression was observed after 48 hours exposure to TGF-β1 with PXDN expression decreased by 28% to 72% ± 17.9%, relative to untreated cells, although this was not statistically significant (Fig. 3.4A). As expected, in response to TGF-β1 treatment, Snai1 expression in HeLa cells increased by 38% to 138 ± 16.1%, relative to untreated cells, at 24 hours then decreased (not statistically significant) to untreated levels by 48 hours (Fig. 3.4A). As expected in cells undergoing TGF-β1-induced EMT, we found that E-cadherin expression decreased in response to TGF-β1, to 57 ± 9.6% and 35 ± 12.4%, relative to untreated cells, over 24 and 48 hours, respectively in HeLa cells. Vimentin, which acts as a marker for the mesenchymal phenotype, showed increased protein expression by ~22% (123 ± 15.2% at 24 hours and 121 ± 7.2% at 48 hours relative to untreated control) over 48 hours (Fig. 3.4A).

We also used IF microscopy to determine the localisation, and changes thereof, of the proteins of interest and this confirmed that cells treated with TGF-β1 over 48 hours showed reduced PXDN expression in HeLa cells (Fig. 3.4B), which is in agreement with the western blotting results. IF microscopy results showed that PXDN expression and localisation is more organised and defined in HeLa cells. We also saw the expected increase in Snai1 expression (Fig. 3.4B) with distinct nuclear localisation being apparent in HeLa cells. Accordingly, with the increase in Snai1 expression when cells undergo TGF-β1-induced EMT, E-cadherin was decreased and vimentin expression was increased in their respective cellular locations (Fig. 3.4B).

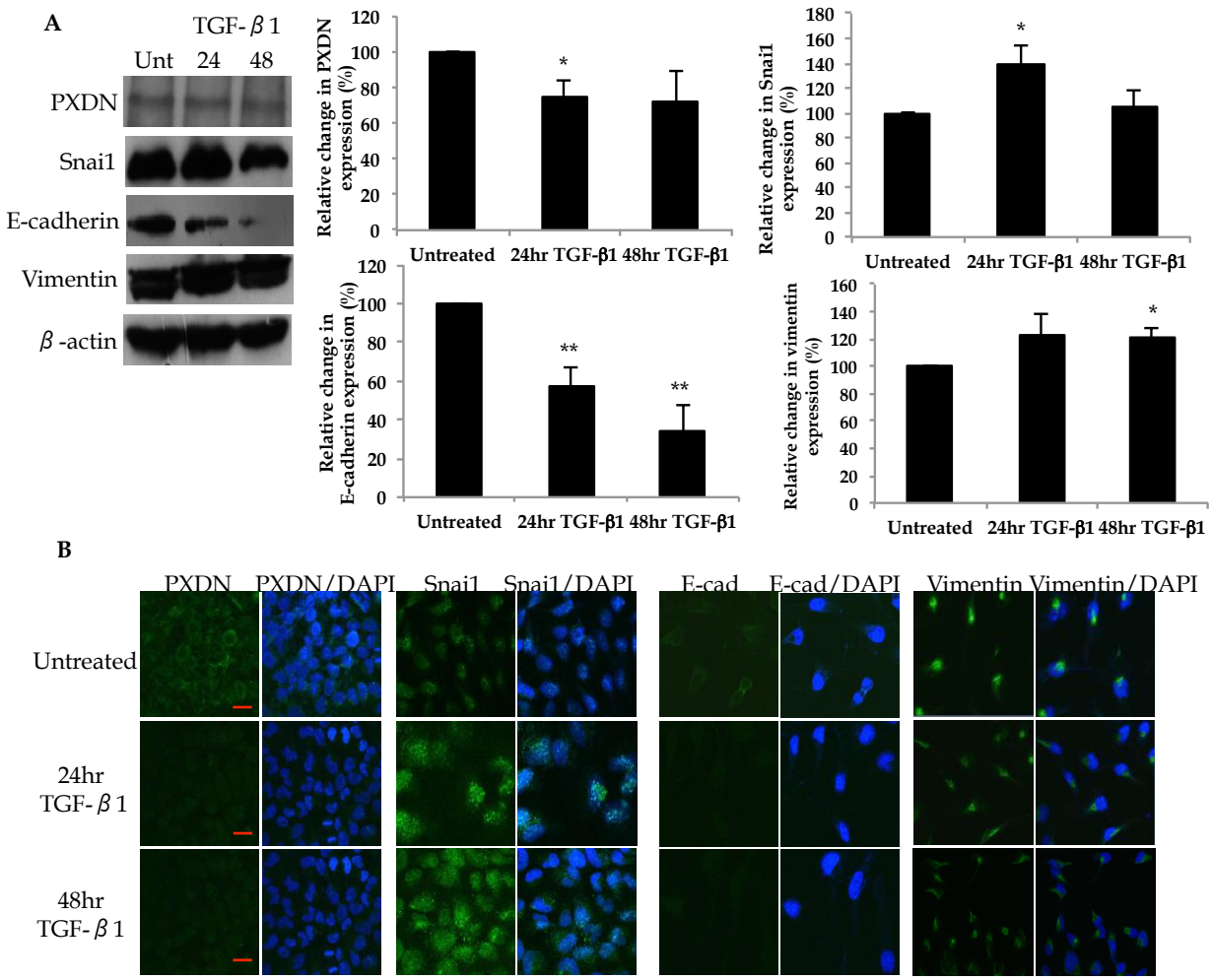

Figure 3.4: PXDN and EMT marker expression in response to TGF-β1 in HeLa cells, over 24 and 48 hours. A) Western blot analysis of the effect of TGF-β1 showed PXDN expression decreased significantly after 24 hours. As expected, Snai1 expression increased in response to TGF-β1 treatment; with a concomitant decrease in E-cadherin and increase in vimentin expression (β-actin was used as a loading control; n = 3 ± SD) Significance stars represent p-values compared to untreated cells, all other comparisons between treatments were not significant. B). IF microscopy of protein localisation in response to TGF-β1-induced EMT showed PXDN expression was reduced with a disruption in organisation of PXDN in the extracellular environment. There was increased nuclear translocation of Snai1 with reduced E-cadherin and increased vimentin, over 24 and 48 hours. Nuclei were counterstained with DAPI (630x magnification; scale bar = 20 µm).

In SiHa cells, PXDN expression decreased to 75 ± 2.9% at 24 hours and 53 ± 10.6% at 48 hours, relative to untreated cells (Fig. 3.5A). As expected, in response to TGF-β1 treatment, Snai1 expression increased to 146 ± 9.2 % and 109 ± 1.1% at 24 and 48 hours, respectively, relative to untreated cells (Fig. 3.5A). As expected in cells undergoing TGF-β1-induced EMT, we found that E-cadherin expression decreased in response to TGF-β1, to 71 ± 12.9% and 54 ± 4.4%, at 24 and 48 hours, respectively, relative to untreated cells (Fig. 3.5A). Vimentin, a marker for the mesenchymal phenotype, showed increased protein expression to 127 ± 13.5% and 142 ± 8.9% over 24 and 48 hours, respectively, relative to untreated cells (Fig. 3.5A).

IF microscopy also showed that SiHa cells treated with TGF-β1 over 48 hours have reduced PXDN expression (Fig. 3.5B), which is in agreement with the western blotting results. PXDN expression and localisation is less organised and defined in SiHa cells when compared to the distribution pattern in HeLa cells. We also saw the expected increase in Snai1 expression (Fig. 3.5B) although nuclear localisation was less apparent in SiHa cells when compared to HeLa cells. Accordingly, with the increase in Snai1 expression when cells undergo TGF-β1-induced EMT, E-cadherin was decreased and vimentin expression was increased in their respective cellular locations (Fig. 3.5B).

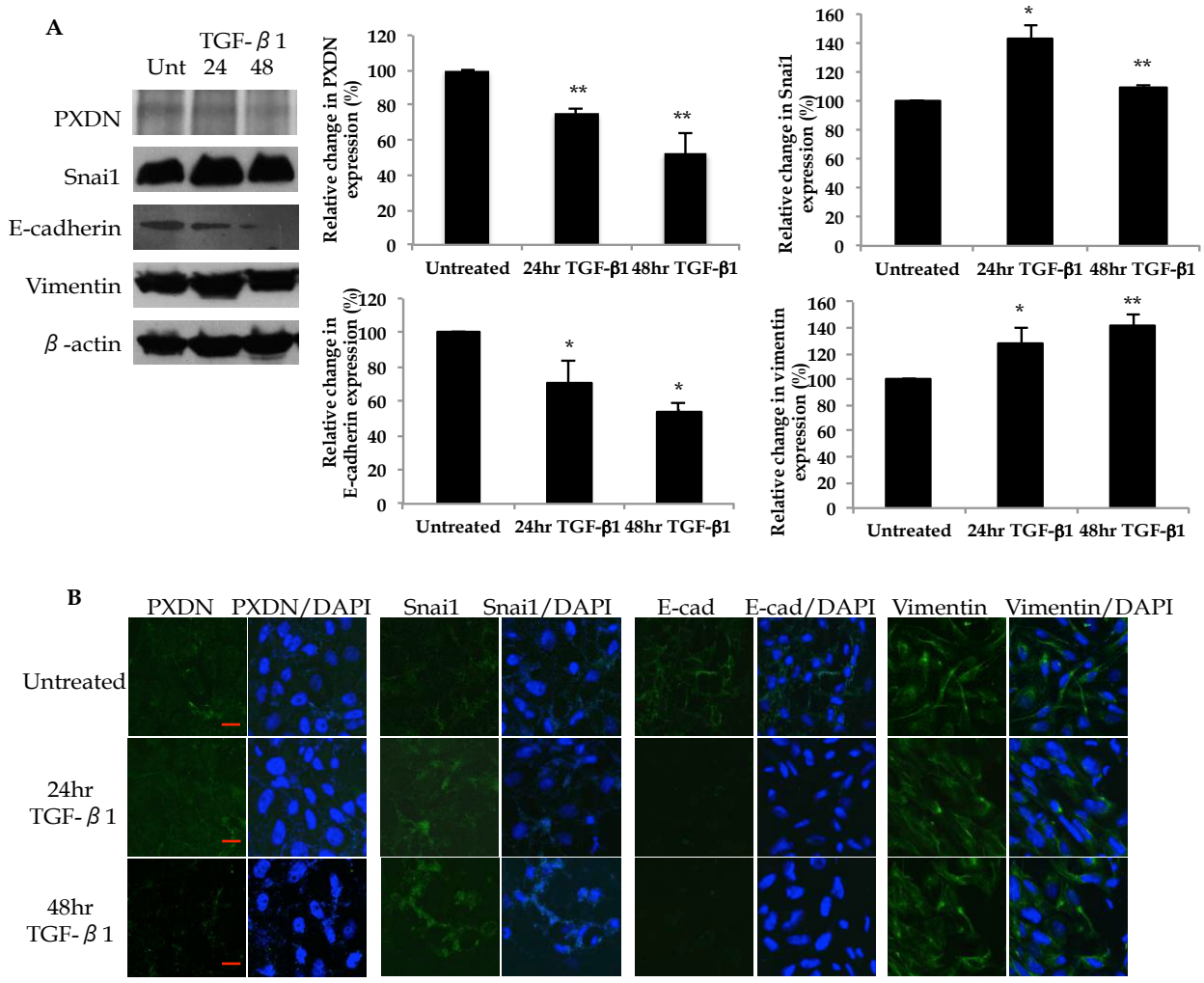

Figure 3.5: PXDN and EMT marker expression in response to TGF-β1 in SiHa cells, over 24 and 48 hours. A) Western blot analysis of the effect of TGF-β1 on protein expression of PXDN and EMT markers Snai1, E- cadherin, vimentin. PXDN expression decreased over this time period. Snai1 and vimentin expression increased while E-cadherin expression decreased (β-actin was used as a loading control; n = 3 ± SD). Significance stars represent p-values compared to untreated cells, all other comparisons between treatments were not significant. B) IF microscopy of protein localisation in response to TGF-β1-induced EMT. TGF-β1 treatment showed PXDN expression was reduced with a disruption in organisation of PXDN in the extracellular environment. There was increased nuclear translocation of Snai1 with reduced E-cadherin and increased vimentin, over 24 and 48 hours. Nuclei were counterstained with DAPI (630x magnification; scale bar = 20 µm).

3.3.2. Snai1 binds to the *peroxidasin* promoter in TGF-β1-treated HeLa and SiHa cells

ChIP is a technique used to identify DNA associated with specific proteins. In order to investigate whether Snai1 is involved in TGF-β1-induced regulation of *PXDN*, we performed ChIP-PCR to establish if Snai1 binds to the *PXDN* promoter in response to TGF-β1. This was achieved by immunoprecipitating Snai1-bound DNA after treating cells with TGF-β1. Snai1 is known to interact with E-boxes in target gene promoters, which have the consensus sequence CANNTG. Through a manual search of the PXDN promoter region, we identified that *PXDN* contains three such E-boxes proximal to the transcription start site (Fig. 2.1). As such, for the ChIP-PCR analysis, Snai1-bound DNA immunoprecipitated from TGF-β1-treated HeLa and SiHa cells was amplified by PCR using primers specific to two regions of the *PXDN* promoter region; one set that amplified across the putative Snai1 binding sites ($PXDN^{Snai1+)}$ and one that amplified a region with no E-boxes ($PXDN^{Snai1-}$) (Fig. 2.1). The $E\text{-}cadherin^{Snai1+}$ promoter region was used as a positive control for TGF-β1-induced Snail binding to DNA, as this interaction has previously been well established (Peinado, Quintanilla and Cano, 2003; Lamouille, Xu and Derynck, 2014).

In both cell lines, amplification of the $PXDN^{Snai1+}$ region of the promoter was seen in TGF-β1 treated cells only (Fig. 3.6A). In both cell lines, the $E\text{-}cadherin^{Snai1+}$ promoter region was positive for PCR products with TGF-β1 treatment (Fig. 3.6B). Primer sets designed to flank the $PXDN^{Snai1-}$ and $E\text{-}cadherin^{Snai1-}$ promoter regions were negative by PCR, indicating that Snai1 was not bound to these DNA regions and therefore did not immunoprecipitate during ChIP, as expected (Fig. 3.6). PCR on input DNA, which had not been processed by immunoprecipitation, confirmed the presence of the target DNA sequences in the genomic DNA and the successful PCR for each primer set (Fig. 3.6). The negative control containing only the protein A/G agarose beads gave no PCR products indicating that there was no non-specific binding of DNA to the beads, therefore all precipitated DNA was bound to cellular protein and not to the beads.

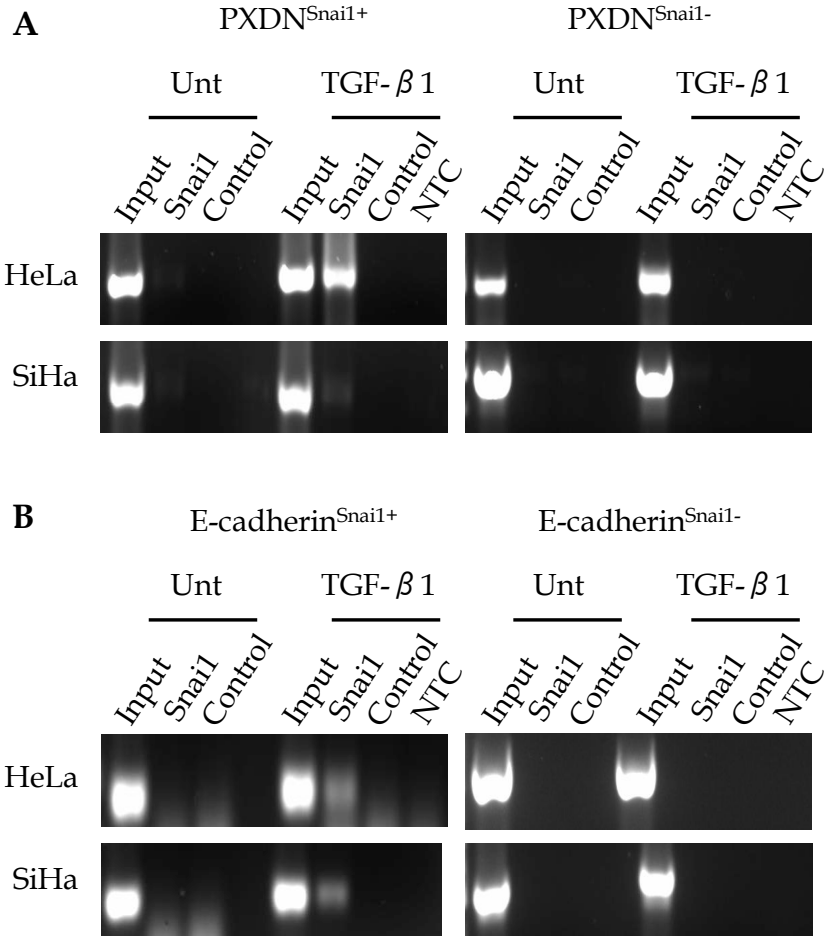

Figure 3.6: ChIP-PCR analysis of the Snai1 bound regions of *PXDN* promoter after TGF-β1 treatment of HeLa and SiHa cells. Cells were treated with TGF-β1 for 24 hours and Snai1-bound DNA was immunoprecipitated and used as template for PCR. A) PCR was conducted with primers spanning across Snail E-box binding sites (PXDN^{Snai1+}) and regions without Snai1 binding sites (PXDN^{Snai1-}). PCR products were generated for the *PXDN*$^{Snai1+}$ region when cells were exposed to TGF-β1 treatment. B) E-cadherin^{Snai1+} and E-cadherin^{Snai1-}promoter primers were used as a positive and negative control for Snai1 binding. Results represent three independent experiments.

3.3.3. Snai1 represses *peroxidasin* expression

We conducted luciferase reporter assays to ascertain whether Snai1 repressed *PXDN* expression by directly binding to Snai1 E-box binding sites within the *PXDN* gene promoter. To achieve this, we cloned two regions of the *PXDN* promoter either with or without the Snai1 consensus E-boxes, PXDN $^{Snai1+}$ and PXDN $^{Snai1-}$, respectively, into the luciferase gene reporter vector pGL4.10. Similarly, luciferase reporter gene constructs were generated for E-cadherin^{Snai1+} and E-cadherin^{Snai1-} regions, to serve as positive controls for the down-regulation of expression by Snai1. Luciferase assays were conducted using HEK293 cells transiently transfected with each of the luciferase reporter vectors (pGL4.10-PXDN^{Snai1+}, pGL4.10-PXDN^{Snai1-}, pGL4.10-E-cadherin^{Snai1+}, and pGL4.10-E-cadherin^{Snai1-}) and treated with TGF-β1. Furthermore, to conclude that Snai1 is indeed directly responsible for *PXDN* gene repression through these putative binding sites, we created a pcDNA-Snai1 over-expression vector that was used in co-transfections with the aforementioned luciferase reporter constructs. In this way we could determine the difference in Snai1 repression of *PXDN* expression in TGF-β1 treated cells and in cells where Snai1 is over-expressed.

First, we tested and established the effect of Snai1 overexpression using the pcDNA-Snai1 construct, on protein expression and localisation of PXDN, E-cadherin and vimentin by confocal IF microscopy. HeLa and SiHa (Fig. 3.7) cells transfected with the pcDNA-Snai1 vector cells exhibited protein expression patterns similar to those of TGF-β1-treated cells, in that E-cadherin and PXDN were downregulated with increased Snai1, while vimentin expression increased.

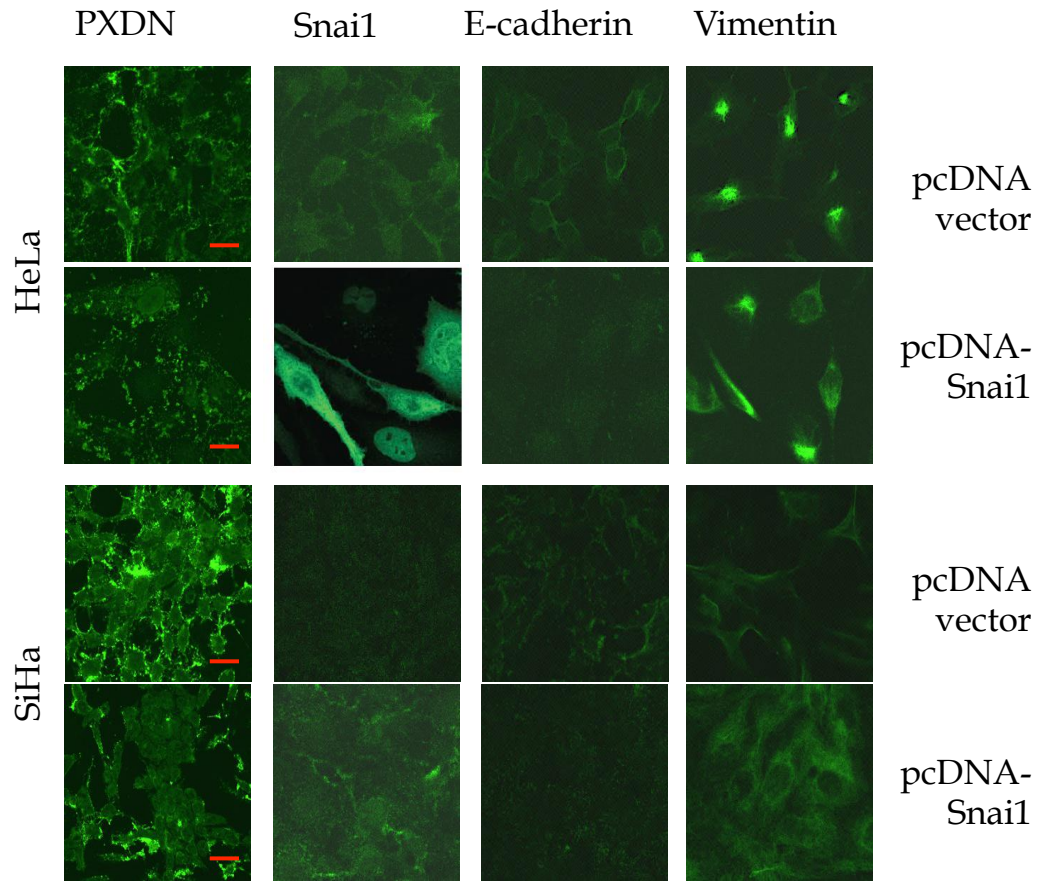

Figure 3.7: The effect of Snai1 overexpression on PXDN and EMT markers, E-cadherin and vimentin. Cells were grown on coverslips then transfected for 24 hours with Snai1 expression vector, pcDNA-Snai1. IF microscopy indicated that transiently transfected cells exhibited an increase in Snai1 and vimentin expression and a decrease in E-cadherin, as expected. Both cell lines showed a decrease in PXDN with Snai1 overexpression (630x magnification, scale bar = 20 µm).

Once we had established that the Snai1 overexpression could induce EMT-markers, we performed the luciferase reporter assays. In TGF-β1-treated cells, luciferase expression from the $PXDN^{Snai1+}$ promoter region (pGL4.10-$PXDN^{Snai1+}$) was reduced significantly to 33 ± 5.9% compared to untransfected, untreated cells (Fig. 3.8A). Similarly, co-transfection of HEK293 cells with pcDNA-Snai1 and pGL4.10-$PXDN^{Snai1+}$ resulted in a 71% decrease in relative light units as an indication of luciferase reporter gene

expression and 29 ± 5.1% compared to untransfected cells (Fig. 3.8A). For the E-cadherin control, pGL4.10-E-cadherin^{Snai1+} with TGF-β1 gave a 79% reduction to 21 ± 1.1%, relative to untreated, untransfected cells, and pcDNA-Snai1 co-transfected cells showed a 94% decrease in luciferase reporter gene expression to 6 ± 0.8%, relative to untransfected cells (Fig. 3.8B). Regions of both *PXDN* and *E-cadherin* promoters that do not contain E-boxes (pGL4.10-PXDN^{Snail-} and pGL4.10-E-cadherin^{Snail-}) did not show any significant changes in luciferase reporter activity with TGF-β1, treatment. Co-transfection with pcDNA-Snai1 decreased luciferase reporter activity to 69 ± 0.3% for PXDN^{Snail-} and 96 ± 3.6% for E-cadherin^{Snail-}, relative to untreated and untransfected cells (Fig. 3.8).

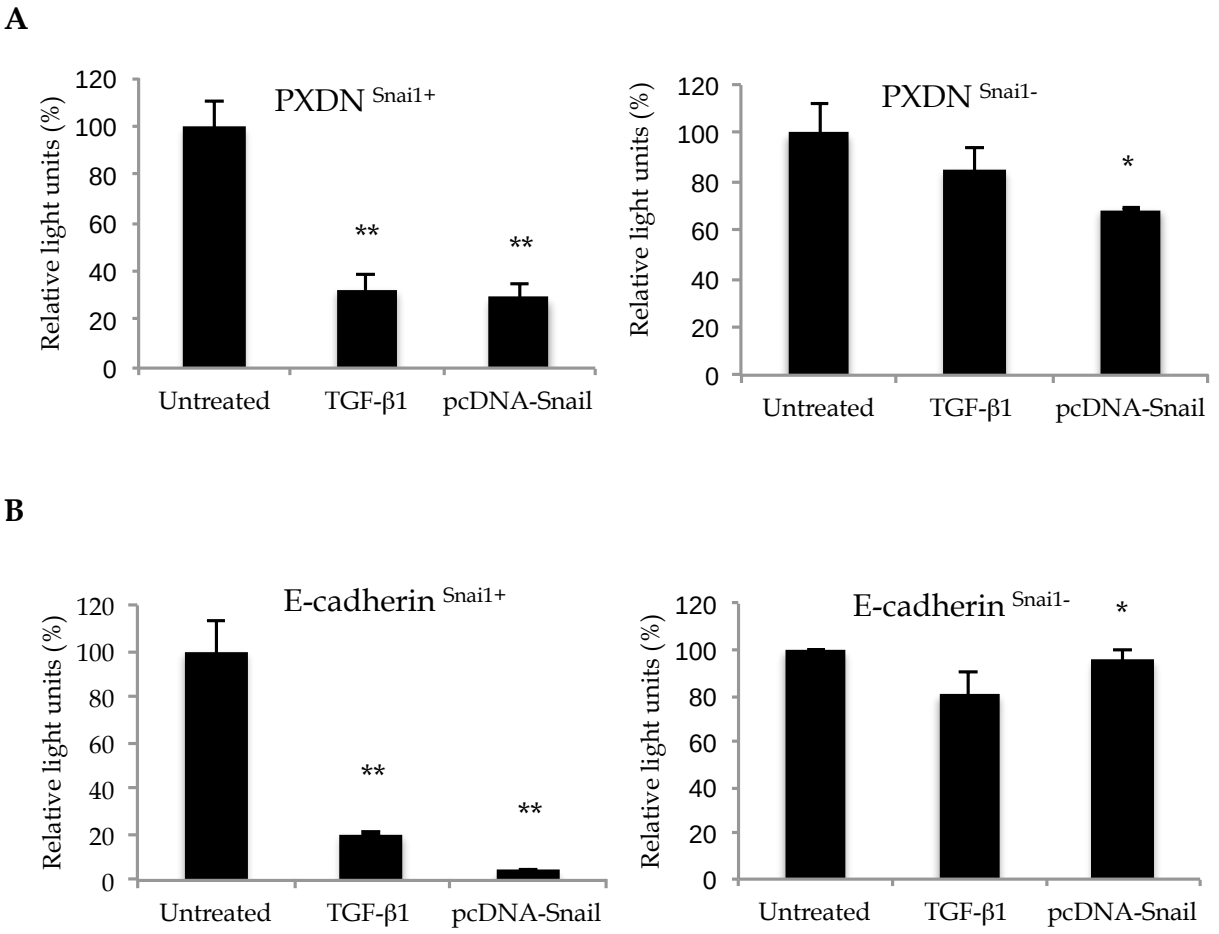

Figure 3.8: PXDN expression decreases in response to Snai1 overexpression. Luciferase reporter assay for regulation of PXDN expression by Snai1 shows that Snai1 downregulates PXDN expression. PXDN promoter regions, with and without Snai1 E-boxes were ligated into pGL4.10 luciferase vector (pGL4.10-PXDN^{Snai1+} and pGL4.10-PXDN^{Snai1-}, respectively) and transfected into HEK293 cells, either in the presence of TGF-β1 or co-transfected with Snai1 expression vector, pcDNA-Snai1. A) Snai1 binds to the promoter region of PXDN to downregulate expression, while a Snai1-null region of the promoter shows no binding of Snai1. B) E-cadherin promoter regions with (pGL4.10-E-cadherin^{Snai1+}) and without (pGL4.10-E-cadherin^{Snai1-}) Snai1 E-boxes were used as positive and negative controls for Snai1 binding, respectively. Significance stars represent p-values compared to untreated cells, all other comparisons between treatments were not significant (n = 3 ± SD.)

3.4. Discussion

In this chapter, using the cervical carcinoma cell lines HeLa and SiHa, we sought to determine if PXDN expression is modified during TGF-β1-induced EMT and ultimately whether the EMT master regulator, Snai1, regulates *PXDN* gene expression. We investigated this by first observing any modifications to PXDN expression after exposing HeLa and SiHa cells to TGF-β1, an EMT effector. We then considered that PXDN might be regulated by the EMT master regulator, Snai1 transcription factor.

We first established that our model cells, the cervical carcinoma cell lines HeLa and SiHa, undergo EMT when exposed to TGF-β1 over 48 hours, which is in line with previously observed effects of TGF- β1 on HeLa and SiHa cells (Cheng and Hao, 2016). In both cells lines PXDN expression was decreased at 24 and 48 hour time points, after treating cells with 5 ng/ml of TGF-β1. We also observed changes in Snai1 expression in these cells, and as expected, and expression of the EMT markers, E-cadherin and vimentin were also affected by TGF-β1 accordingly. In both cell lines, Snai1 expression increased the most 24 hours after treatment, with levels returning to just above normal after 48 hours. This pattern is not surprising since Snai1 expression has more recently been determined to act over a shorter time period than previously thought, although the downstream effects of Snai1 are longer lasting (Vetter *et al.*, 2009). Predicted expression of Snai1 targets, E-cadherin and vimentin, was observed, with E-cadherin expression decreased and vimentin increased (Soini *et al.*, 2011). This agrees with previous findings that show TGF-β1 leads to decreased E-cadherin and promotes an EMT phenotype in HeLa and SiHa cells (Yi *et al.*, 2002; Kloth *et al.*, 2005; Cheng and Hao, 2016). IF microscopy results were in agreement with the western blotting results and together confirmed that PXDN expression is decreased in the presence of TGF-β1 in these cells during TGF-β1-induced EMT.

In line with our hypothesis, we expected and found that PXDN decreases upon EMT induction. Since PXDN has being found to consolidate collagen IV and possibly other

ECM proteins (Bhave *et al.*, 2012), we hypothesised that during type 3 EMT that occurs in cancer, PXDN would decrease. This is because PXDN consolidates collagen IV in the BM and the BM functions to stabilise epithelium to connective tissue. In cancer cells undergoing EMT for the purposes of metastasis, for example, cells would need to detach from the primary tumour, which would require disrupting the BM. In this instance PXDN expression would be downregulated since there would be less need for BM consolidation. Additionally, when metastasising cells reach the secondary tumour site and undergo MET in order to establish at the secondary tumour site, PXDN expression may then be restored or overexpressed in order to establish the tumour cells at the new site. The precise roles of PXDN in cancer are as yet unclear and, perhaps unsurprisingly, there does not seem to be a consistent and established pattern of modification of PXDN expression. Some studies have found an upregulation in PXDN while others show a downregulation in gene expression (Castronovo *et al.*, 2006; Desmond *et al.*, 2007; Péterfi *et al.*, 2009; Liu *et al.*, 2010; Tauber *et al.*, 2010; Bai *et al.*, 2011; Barnett *et al.*, 2012; Young *et al.*, 2015; Jayachandran *et al.*, 2016). For example, PXDN expression is highly upregulated in androgen refractory cancer of the prostate *(*ARCaP*)* cells stably transfected with constitutively active Snail cDNA (Barnett *et al.*, 2012); in mesenchymal-like melanoma cells (Jayachandran *et al.*, 2016) and in malignant primary glial and secondary metastatic brain tumours (Liu *et al.*, 2010). PXDN was also found to be differentially expressed in breast cancer cell lines where PIK3CA (the gene encoding the p110α catalytic subunit of phosphoinositide 3-kinase) was mutated (Young *et al.*, 2015). Although these mutations are present in all breast cancer subtypes, Young *et al*. (2015) found that even within the basal or luminal subtypes, expression differed significantly from highly expressed to not at all. PXDN was also found to be overexpressed in a choriocarcinoma cell line stably expressing the adhesion molecule, HO-1 (Tauber *et al.*, 2010). On the other hand, expression of PXDN was significantly deceased in a subset of AML patients and PXDN was therefore thought to be a tumour suppressor, which is epigenetically silenced by methylation (Desmond *et al.*, 2007). These differences in expression could be attributed to the type and stage of cancer, which is not unusual. In addition, the reverse process of EMT, were cells undergo MET,

must also be considered. Therefore, the changes in PXDN expression could also quite possibly be attributed to MET.

Although several transcription factors are required for TGF-β1-induced EMT, Snai1 is considered the master regulator of this process (Cano *et al.*, 2000; Barberà *et al.*, 2004; Naber *et al.*, 2013). Although conventionally understood to act as a transcriptional repressor by recruiting HDACs to target gene promoters, such as *E-cadherin* (Cano *et al.*, 2000; Peinado *et al.*, 2004), Snai1 has also been found to upregulate expression of genes that favour the mesenchymal phenotype (Miyoshi *et al.*, 2005). Our ChIP-PCR results showed that in the presence of TGF-β1, Snai1 binds to the *PXDN* promoter region. We then determined that Snai1 causes repression from the *PXDN* promoter, through luciferase reporter assays. Since TGF-β1 is able to activate several transcription factors, we further confirmed the ability of Snai1 to downregulate *PXDN* expression by the use of a Snai1 overexpression vector. We showed that TGF-β1 treatment represses luciferase reporter gene expression from the *PXDN* promoter, and that this repression is mostly likely mediated by Snai1, since a similar level of repression was observed in pcDNA-Snai1 co-transfected cells. Furthermore, cells transfected with the Snai1 expression vector show decreased expression of PXDN by IF microscopy.

Snai1 regulated genes usually contain more than one Snai1 E-box proximal to the transcription start site (Beach *et al.*, 2008; Whiteman *et al.*, 2008). In the *PXDN* promoter region we identified three such E-boxes proximal to the transcription start site (Fig. 2.1, pg 47). Whilst it has not yet been determined why multiple sites exist for Snai1 binding, Batlle *et al*. (2000) found that mutation of one or several of these sites still confers the ability to repress gene expression via Snai1; only when all sites were mutated was there no regulation by Snai1 of the target genes. The scope of our study did not extend to whether Snai1 binds to all three E-boxes and which of these are more integral to Snai1 regulation of *PXDN* expression. Further studies may determine the importance of each E-box and the level to which each is responsible for regulating *PXDN* expression.

Chapter 4: The functional role of peroxidasin in EMT

4.1. Introduction

The ECM is a major component of tumour stroma and is a key regulator of cell and tissue function (Fang *et al.*, 2014). It provides a physical scaffold for cell adhesion and migration. Proteolysis of the ECM regulates cellular migration by modifying the structure of the ECM scaffold and is therefore tightly controlled in normal tissues but usually deregulated in tumours (Egeblad, Rasch and Weaver, 2010).

A specialised form of ECM lining epithelial sheets and blood vessels is the BM and is composed predominantly of collagen IV, laminin and proteoglycans (Petitclerc *et al.*, 2000). The BM is found at the basal surface of epithelial and endothelial cells and plays an important role in cell adhesion, proliferation, migration and tumour angiogenesis and is essential for tissue polarity (Fang *et al.*, 2013). The BM promotes adhesion and motility of various normal and also tumour cells and is the first barrier that cells must traverse to undergo metastasis and as such, acts as a physical barrier that prevents cancer invasion (Cortes-Reynosa *et al.*, 2008).

In cancer cells, the balance of degrading and re-depositing the tumour stroma is broken and this can actively induce and allow for EMT of cancer cells (Fang *et al.*, 2013). The BM defines the tumour microenvironment and provides significant host-derived regulatory signals during progression of tumour growth and metastasis (Tanjore and Kalluri, 2006). PXDN stabilises the BM by reinforcing the collagen IV network (Bhave *et al.*, 2012) and catalyzing dityrosine formation and consequently promoting ECM protein cross-linking (Cheng *et al.*, 2011). Therefore, the significance of PXDN may be reflected in the diverse and essential functions of collagen IV, the BM and the ECM. Collagen IV is the major component of BM, therefore, the destabilisation of collagen IV may be an important prerequisite for cancer invasion and metastasis (Fang *et al.*, 2013).

Collagen IV is the most abundant constituent of the ECM and is considered to account for the major function of the ECM (Fang *et al.*, 2014). Collagen IV belongs to the larger group of collagens, which are highly abundant in humans, accounting for one-third of total proteins. The collagen superfamily consists of 28 different types and type IV collagen is a unique in that it only occurs in the BM. Collagen IV comprises six genetically distinct α-chains, α1(IV) to α6(IV). The interaction of these chains is very specific and they assemble to form only three distinct heterotrimers (α1α1α2, α3α4α5, and α5α5α6). The α1(IV) and α2(IV) chains, are present in the BM of all tissues, and α3(IV) – α6(IV) are restricted in their tissue distribution during development (Khoshnoodi, Pedchenko and Hudson, 2008).

Collagen IV (α1) is downregulated in all 3 types of EMT (Zeisberg and Neilson, 2009) and changes in the deposition of collagen can be associated with increased malignancy (Fang *et al.*, 2014). During cancer invasion, structural changes that remodel the ECM occur in the tumour stroma, including degradation, re-depositing, cross-linking and stiffening of collagens (Khoshnoodi, Pedchenko and Hudson, 2008; Fang *et al.*, 2014). This results in a reorganised microenvironment to promote tumour progression by destabilising cell polarity and cell–cell adhesions. The morphological changes are characterised by linearisation of interstitial collagens at the tumour invasion front, which affects cellular processes such as gene expression, cell differentiation, proliferation, migration and responses to cancer treatments (Fang *et al.*, 2014). In cervical carcinoma, collagen IV shows a loose and stratified structure constraining tumour nests, with many obscure collagen fragments distributed discretely at the site of the BM (Fang *et al.*, 2013). Collagen IV may play a direct role in the adhesion, migration, and invasion of tumour cells since tumour cell adhesion to the BM is critical in invasion (Chelberg *et al.*, 1989). For example, Xu *et al*. (2006) found ECM protein remodeling in non-small cell lung carcinoma (NSCLC), with collagen IV highly expressed in NSCLC stroma and increased cell adhesion of NSCLC (Xu *et al.*, 2006).

During malignant transformation, tumour cells are able to secrete signaling molecules, such as TGF-β1, that disrupt normal tissue architecture (Tanjore and Kalluri, 2006). Although TGF-β1 plays a role in regulating BM integrity, there is a threshold at which increased TGF-β1 causes discontinuous BM formation, despite increased expression of the BM component molecules (Stahl and Felsen, 2001). MMPs are also upregulated in cancer, in both cells of the tumour and those of the tumour microenvironment, and are responsible for loss of BM architecture (Tanjore and Kalluri, 2006). MMPs play an essential role in the destruction of collagen IV in the BM (Fang *et al.*, 2013) and TGF-β1 upregulates expression of type IV collagenases, MMP-2 and MMP-4 (Stahl and Felsen, 2001). MMP-2 mediates the proteolytic alteration of collagen IV and this significantly positively impacts the migration of transdifferentiated cells (Stahl and Felsen, 2001). Interestingly, peroxidases such as MPO and EPO have been found to upregulate expression of MMPs (Davies *et al.*, 2008; Panagopoulos *et al.*, 2017). HOCl and HOBr produced by peroxidases can activate the inactive pro-forms of MMPs via the conversion of a key cysteine residue in the cysteine switch domain of pro-MMP-7 to a sulfinic acid derivative (Davies *et al.,* 2008). Therefore, as a peroxidase, PXDN may also reorganise the ECM by producing HOX that upregulate expression of MMPs.

Collagens are also essential for tumour angiogenesis. The formation and survival of blood vessels are vitally connected with the proper synthesis and deposition of collagen at the BM, since inhibition of collagen metabolism has been demonstrated to have anti-angiogenic effects (Maragoudakis *et al.*, 1993). Collagen IV is synthesised during angiogenesis and is deposited around endothelial cells and pericytes, which may explain the high expression of PXDN in vasculature (Liu *et al.*, 2010) and could be considered as a marker of angiogenic activity (Öhlund *et al.*, 2013). Type IV collagen can therefore either promote or inhibit endothelial cell growth and proliferation (Fang *et al.*, 2014).

Attachment to the BM is crucial for the survival and growth of epithelial cells. Cells attach to the BM via integrins. Integrin receptors provide essential survival signals and

are critical in anchoring cells because apoptosis is initiated if epithelial cell loses contact with the BM (Öhlund *et al.*, 2013). Integrins are heterodimeric, transmembrane adhesion receptors that bind to ligands including, collagens, laminins and fibronectin in the ECM (Scanlon *et al.*, 2013). Integrins mediate interactions between cells and the ECM by making transmembrane connections between the cytoskeleton and the ECM. When integrins bind to ligands, signaling cascades are induced that affect cell polarity, motility, survival, morphology, proliferation and differentiation (Scanlon *et al.*, 2013). In addition to the binding to the CB3 region of collagen IV, integrin receptors bind the NC1 domain (Öhlund *et al.*, 2013), the site of the sulfilimine bond catalysed by PXDN (Bhave *et al.*, 2012). Therefore it is possible that PXDN may play a role in attachment, migration and invasion of tumour cells since the BM plays an essential role in the tumour microenvironment.

In this chapter, our aim was to elucidate the role of PXDN in EMT by functional studies, wherein PXDN expression was knocked down. We investigated the effect of *PXDN* knockdown on morphology, proliferation, attachment characteristics, invasion ability and migration of HeLa and SiHa cells. Determining the importance of PXDN in these cellular activities may be significant in elucidating the role of PXDN in EMT of cancer cells.

4.2. Methodology

Objective 3: Elucidate the role of PXDN in EMT by functional studies, wherein *PXDN* expression is knocked down (silenced).

All functional assays were performed on:

- Cells in which PXDN expression was knocked down by transfecting cells with MISSION® esiRNA Human PXDN as described in section 2.15. pg 52.
- Cells were treated with TGF-β1 as described in section 2.8. pg 40.
- Cells were silenced for PXDN expression and treated with TGF-β1 (also referred to as siRNA/TGF-β1) as described in section 2.15. pg 52.
- Transfection of control of cells was with MISSION® esiRNA Fluc as described in section 2.15. pg 52.

i. Quantify PXDN expression levels in PXDN siRNA-transfected cells, TGF-β1 treated cells and siRNA-transfected cells concomitantly treated with TGF-β1.

- ELISA was performed as described in section 2.16. pg 52.
  Cells were seeded and treated as previously described. Cells were sonicated and lysates were added to the wells of the ELISA plate and left to incubate before detection reagent was added. After addition of the second detection reagent, TMB substrate was added and following optimal colour development, the reaction was stopped and absorbance at 450 nm measured. Total protein concentration was determined by Bradford assay and the ELISA readings were corrected accordingly.

ii. Investigate the proliferation of cells by MTT assay, after knockdown of *PXDN* expression.

- MTT assay was performed as described in section 2.17, pg 54.
  Briefly, cells were seeded and treated as previously described. Culture medium was removed from wells and replaced with MTT solution. MTT solution was

then removed without disturbing formazan crystals, which were dissolved with DMSO and absorbance measured at 570 nm.

iii. Observe changes in cell morphology and protein localisation after knocking down PXDN expression.

- DIC microscopy and IF microscopy were performed as described in section 2.9. pg 41 and section 2.11. pg 42, respectively. Briefly, for DIC, cells were seeded on coverslips and visualised as previously described. For IF microscopy, cells were seeded on coverslips and treated. Cells were fixed onto coverslips with formaldehyde and permeablised before blocking non-specific sites with BSA. Cells were incubated in primary antibody overnight and then in secondary antibody. After staining nuclei with DAPI, coverslips were mounted onto glass slides, sealed and cells visualised.

iv. Observe the effect of PXDN knock down on the attachment characteristics of cells to tissue culture treated plates.

- Cell attachment assay was performed as described in section 2.18, pg 54.
  Briefly, cells were seeded and treated as previously described. After treatments, cells were trypsinised and seeded in 96-well plates and attachment monitored at four time points (15 minutes, 30 minutes, 45 minutes and 60 minutes). Unattached cells were removed every 15 minutes for the relevant time points. Fresh culture medium was added to cells for the remaining time (up to 60 minutes) at which time the MTT assay was performed as an indication of number of attached cells.

v. Observe the effect of PXDN knock down on the invasion ability of cells by invasion assay using reconstituted BM.

- Invasion assays were performed as described in section 2.19. pg 55.
  Briefly, the upper chamber of the permeable supports of a 96-well Corning® HTS Transwell® plate were coated with ECM gel. Cells were then seeded in the upper

chamber on the ECM gel, in 10% FBS culture medium. The same culture medium was added to the lower chamber and incubated overnight. The medium in the upper chamber was changed to 1% FBS culture medium and cells were then treated and transfected as previously described. Cells that had not invaded the ECM gel were removed and cells in the lower chamber fixed with methanol and stained with crystal violet solution. After washing off residual stain, the supports were left to dry before dissolving crystal violet stain in acetic acid solution. Absorbance was measured at 590 nm.

vi. Observe the effect of PXDN knock down on migration ability of cells by scratch assay.

- Scratch assays was performed as described in section 2.20. pg 56.
  Briefly, cells were seeded and treated as previously described. After 24 hours, a p200 pipette tip was used to create a scratch in the cell monolayer. Scratch closure was monitored by visualising cells at 12, 24 and 48 hours post scratch.

4.3. Results

4.3.1. Peroxidasin expression is knocked down by transfection with siRNA

We sought to elucidate the role of PXDN in HeLa and SiHa cells by observing changes in EMT features of cells after knocking down PXDN expression by transient transfection of cells with MISSION® esiRNA Human PXDN. The ELISA was used to quantify the knock down of PXDN expression in PXDN siRNA-transfected cells, TGF-β1 treated cells and PXDN siRNA-transfected cells treated with TGF-β1.

PXDN expression was decreased to 69 ± 7.6% in HeLa cells transfected with PXDN siRNA, relative to untreated cells. TGF-β1 treatment did not significantly affected PXDN expression (decrease to 81 ± 14.9%) and in siRNA/TGF-β1 cells PXDN expression was also not significantly affected (decreased to 84 ± 21.1%), relative to untreated cells (Fig. 4.1A). HeLa cells transfected with negative control Fluc esiRNA also did not show a significant change in PXDN expression (decrease to 80 ± 20.6%), relative to untreated cells (Fig. 4.1A). IF microscopy images also showed that PXDN expression is knocked down to a different extent for transfection with siRNA and treatment with TGF-β1 (Fig. 4.1B). Along with knockdown of PXDN in siRNA-transfected cells, the localisation of PXDN protein was disrupted and lacked the pattern seen in untreated cells. In siRNA/TGF-β1 treated cells, the distribution pattern of PXDN was not as disrupted as in siRNA-transfected cells, even though PXDN expression was lower. Background control of secondary antibody only showed a lack of background fluorescence signal from non-specific binding (Fig. 4.1B).

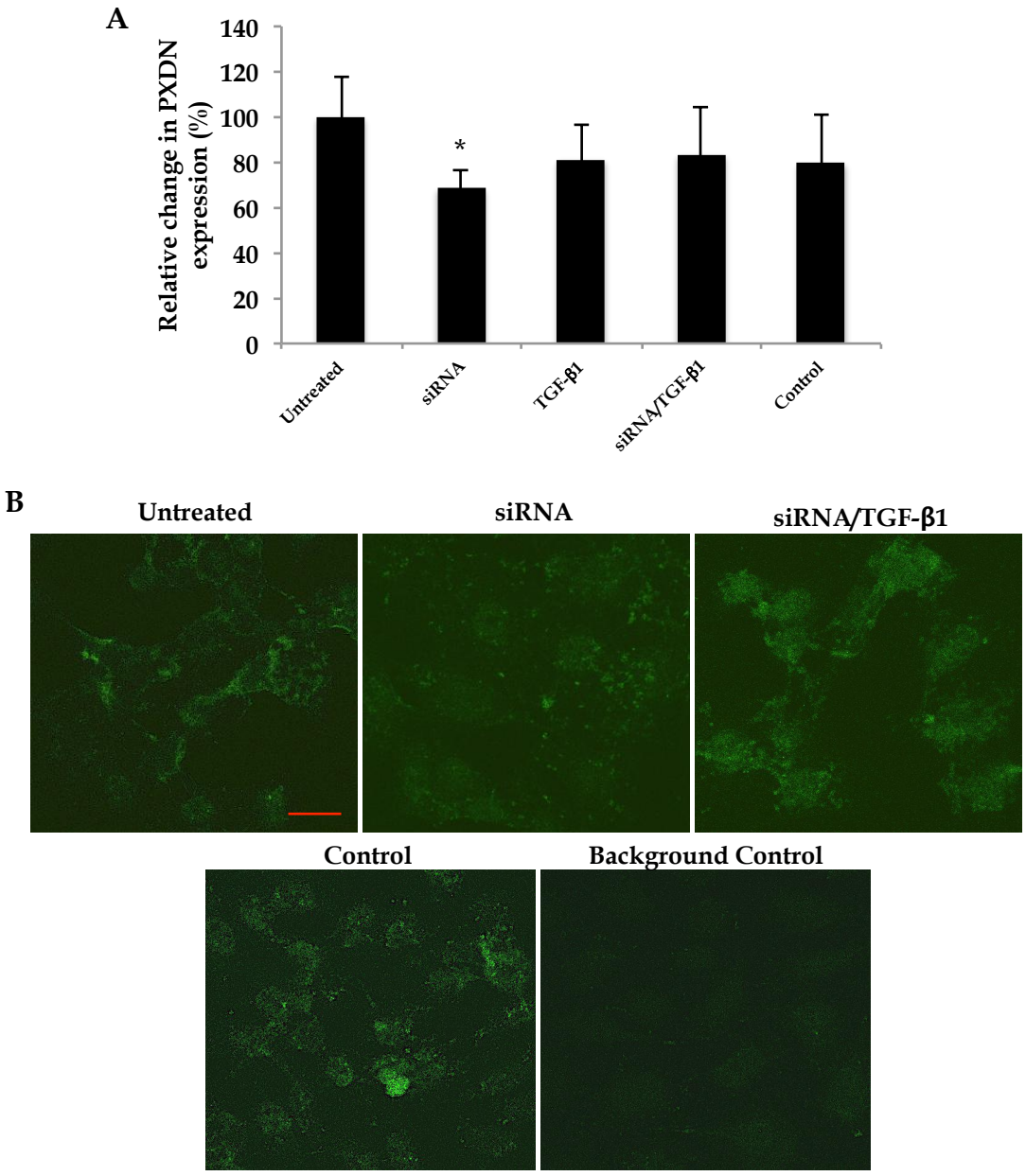

Figure 4.1: siRNA-mediated knockdown of PXDN expression in HeLa cells. PXDN expression is knocked down after transient transfection of cells with siRNA, as observed by A) ELISA and B) IF microscopy. The combination of transfecting HeLa cells treated with TGF-β1 did not cause a significant decrease in PXDN expression. Significance stars represent p-values compared to untreated cells, all other comparisons between treatments were not significant (n = 3 ± SD, scale bar = 20 μm).

PXDN expression was also knocked down in SiHa cells transfected with PXDN siRNA, PXDN expression decreased to 83 ± 6.0%, relative to untreated cells. While PXDN siRNA caused a larger decrease in PXDN expression than TGF-β1 in HeLa cells, the opposite effect was seen in SiHa cells. TGF-β1 treatment of SiHa cells caused PXDN expression to decrease to 64 ± 16.5% relative to untreated cells, a 19% difference in the decrease of PXDN expression than siRNA-mediated knock down. The combination of siRNA transfection and TGF-β1 treatment knocked down PXDN expression to 72 ± 14.5% in SiHa cells, relative to untreated cells (Fig. 4.2A). In SiHa cells, the negative control siRNA (Fluc) had the opposite effect to that seen in HeLa cells, causing an increase in PXDN expression of 31% to 131 ± 17.0% when compared to untreated cells (Fig 4.2A). IF microscopy images of siRNA-transfected and TGF-β1-treated SiHa cells corroborate the ELISA results, in that PXDN expression is shown to be knocked down in siRNA-transfected cells, with disruption of the cellular localisation and distribution of PXDN in these cells. PXDN siRNA-transfected and siRNA/TGF-β1 cells show similar patterns of PXDN localisation and cellular distribution, there is less PXDN extracellularly and PXDN does not appear to localise to the ECM and cell-to-cell contacts. The control, using the secondary antibody only, showed no non-specific binding as seen from the lack of background fluorescence signal (Fig 4.2B).

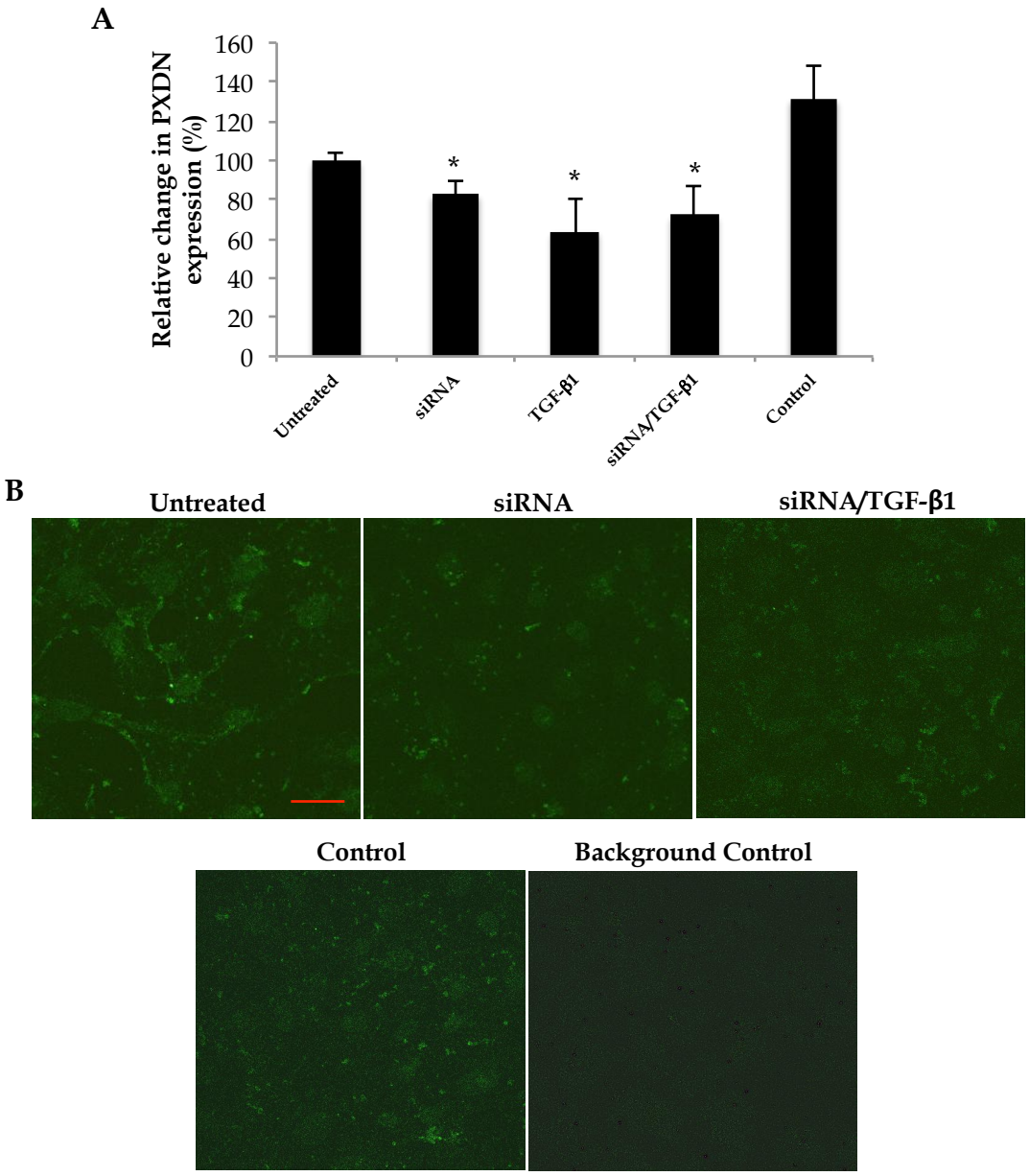

Figure 4.2: siRNA-mediated knockdown of PXDN expression in SiHa cells. PXDN expression is knocked down after transient transfection of cells with siRNA, as observed by A) ELISA and B) IF microscopy. In SiHa cells, TGF-β1 decreased PXDN expression more than transfection with PXDN siRNA. The combination of siRNA and TGF-β1 resulted in a significant decrease in PXDN expression when compared to untreated cells. Fluc esiRNA was used as a negative control. Significance stars represent p-values compared to untreated cells, all other p-values of comparisons between treatments were not significant (n = 3 ± SD, scale bar = 20 μm).

4.3.2. Knocking down peroxidasin expression alters the morphology of HeLa and SiHa cells

We sought to investigate if silencing PXDN expression in HeLa and SiHa cells would affect the morphology of cells and cell-cell interactions. Untreated HeLa cells have a slightly rounded shape, most especially when cells are in close contact with one another. Single cells not tightly packed have projections extending towards other cells in the vicinity. When PXDN expression was knocked down in HeLa cells, by transfection with PXDN siRNA, the cells appeared smaller and less round and with fewer cell-to-cell contacts. The HeLa cells developed projections extending out towards other cells, when compared to untreated cells. Treating HeLa cells with TGF-β1 significantly decreased cell-to-cell contacts and a small number of cells retained their rounded shape. In addition, a minor proportion of cells remained attached to the coverslips compared to untreated and siRNA-transfected cells. When siRNA transfection was combined with TGF-β1 treatment, almost all cell-to-cell contacts were lost and cells appeared more stressed (Fig. 4.3).

Untreated SiHa cells have a less rounded morphology than HeLa cells, but can be as tightly packed, without any projections. Transfecting SiHa cells with PXDN siRNA resulted in reduced cell-to-cell contacts and a higher proportion of cells developed filopodia than untreated cells. Cells also began to form clusters rather than a monolayer and there was a reduced number of cells in the dish, despite equal seeding density. When SiHa cells were exposed to TGF-β1, as expected, cells formed even more clusters than siRNA-transfected cells and became rounded. When siRNA transfection and TGF-β1 treatment were combined, cells took on a combination of siRNA-transfection features and TGF-β1-treatment features (Fig. 4.3). Overall, PXDN downregulation in HeLa and SiHa cells alters the morphology of cells to a mesenchymal phenotype. HeLa and SiHa cells transfected with control siRNA (Fluc) did not show altered cell morphology (Fig. 4.3).

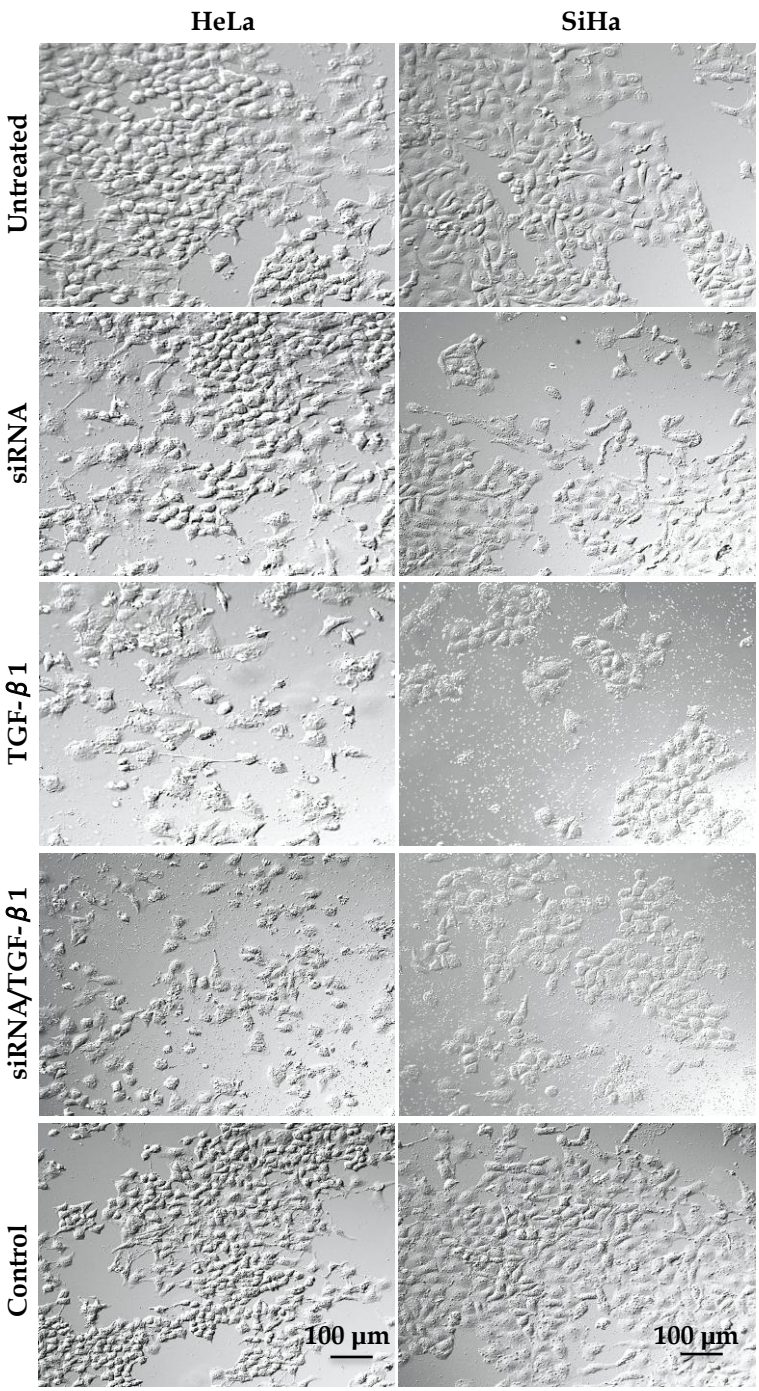

Figure 4.3: The morphology of HeLa and SiHa cells changes when PXDN expression is knocked down. Knocking down PXDN expression by siRNA transfection, TGF-β1 treatment, and a combination of transfection and TGF-β1 treatment alters the morphology of HeLa and SiHa cells. Cells were visualised on an Olympus BX63 microscope at 100x magnification (scale bar = 100 µm).

4.3.3. Peroxidasin may contribute to the proliferation of HeLa and SiHa cells

We performed an MTT assay to determine the effect of silencing PXDN expression on cell proliferation. Cell proliferation was also determined for cells treated with TGF-β1 and cells treated with TGF-β1 and concomitantly transfected with PXDN siRNA. When compared to untreated cells, transfection of cells with PXDN siRNA resulted in a 15% decrease in cell proliferation to 85 ± 2.9%, relative to untreated. TGF-β1 treatment caused cell proliferation to decrease by 12% to 88 ± 1.3% relative to untreated, while the combination of siRNA transfection and TGF-β1 treatment resulted in a 26% decrease in the proliferation of HeLa cells to 74 ± 0.5%, relative to untreated cells (Fig. 4.4A). Transfecting cells with control siRNA also caused a similar decrease in cell proliferation as with PXDN siRNA, 17% decrease to 83 ± 0.7%, relative to untreated cells.

As with HeLa cells, silencing of PXDN expression in SiHa cells resulted in a decrease in cell proliferation by 9% to 91 ± 1.0% relative to untreated cells. When SiHa cells were treated with TGF-β1, the opposite effect was seen as with HeLa cells. TGF-β1 treatment caused a 4% increase in proliferation of SiHa cells to 104 ± 1.9%, relative to untreated cells. When PXDN siRNA transfection was combined with TGF-β1 treatment, once again, the effect of TGF-β1 treatment alone was mitigated, resulting in an 11% decrease in proliferation to 89 ± 3.1%, relative to untreated, which is a 2% decrease compared to cells in which PXDN was silenced without concomitant TGF-β1 treatment. Transfection with control siRNA showed similar results as with HeLa cells, with a 14% decrease in cell proliferation to 86 ± 1.3% relative to untreated (Fig. 4.4B). Overall, these results show that silencing PXDN expression decreases proliferation of HeLa and SiHa cells, and that combined with a decrease in PXDN expression, treating cells with TGF-β1 lowers the rate of proliferation even more. However, transfecting cells with control siRNA also caused a similar decrease in cell proliferation as with PXDN siRNA.

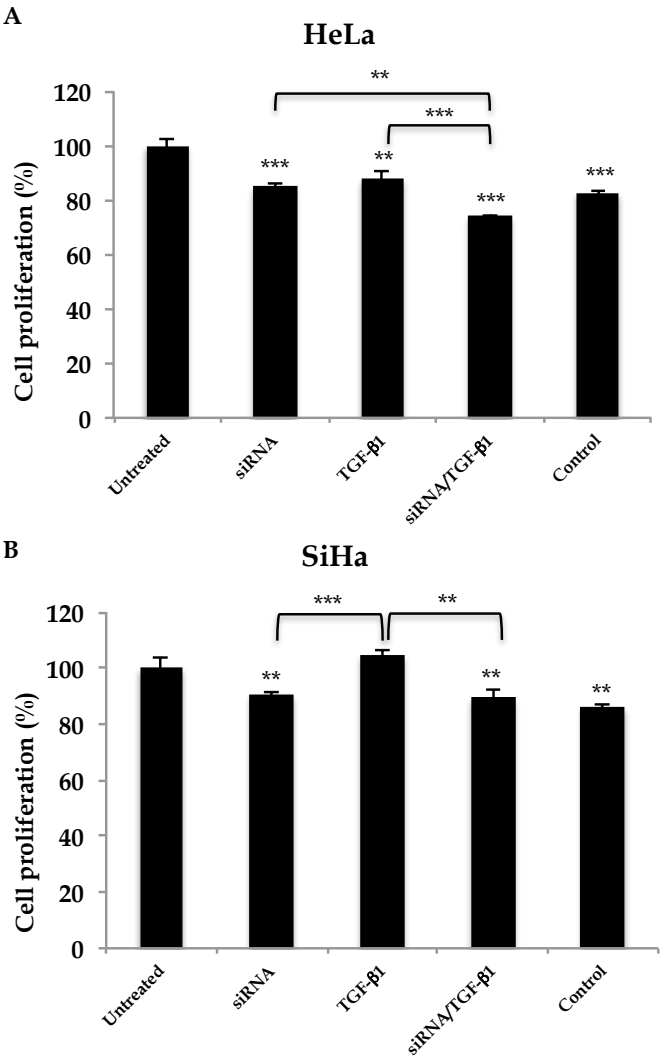

Figure 4.4: Silencing PXDN expression decreases proliferation of HeLa and SiHa cells. A) HeLa cell proliferation decreased when PXDN expression was reduced. TGF-β1 also decreased proliferation, although to a lesser extent than with PXDN siRNA. Combined PXDN siRNA transfection and TGF-β1 treatment reduced cell proliferation more than either treatment alone. B) Cell proliferation of SiHa cells was decreased when PXDN expression was knocked down. Treating cells with TGF-β1 had the opposite effect and increased cell proliferation. TGF-β1 treatment with siRNA transfection, showed decreased cell proliferation. Control siRNA resulted in a similar decrease in proliferation as with PXDN siRNA-transfected cells. Significance stars above error bars represent p-values compared to untreated cells, all other p-values were not significant (n = 3 ± SD).

4.3.4. Peroxidasin plays a role in cell attachment

PXDN stabilises the BM, an important effector of cell attachment properties. We sought to investigate if knocking down PXDN expression in HeLa and SiHa cells would affect the rate at which cells attach to tissue culture plates. The attachment assay was conducted over 60 minutes and attachment was observed at 15-minute intervals. In untreated HeLa cells, we observed the number of cells attaching to the culture plates increasing steadily at each time interval, with the most cells attached after 60 minutes (Fig. 4.5A). The number of siRNA-transfected cells attaching also increased in the first 45 minutes, following a similar pattern to untreated cells, although less siRNA-transfected cells were attached at each time point, compared to untreated cells. In siRNA-transfected cells, 29 ± 2.3% less cells were attached after 15 minutes, when compared to untreated cells. At the 30, 45 and 60-minutes time point, there were 25 ± 8.5%, 17 ± 9.3% and 29 ± 2.7% less cells attached, respectively, when compared to untreated cells (Fig. 4.5B). TGF-β1-treatment of cells increased the attachment potential of HeLa cells; although only 3% more cells had attached after 15 minutes, 97 ± 5.0% unattached compared to untreated cells. The proportion of attached cells increased to 13 ± 11.9% more at 30 minutes, 19 ± 8.3% more at 45 minutes and 23 ± 2.6% more cells attached after 60 minutes (Fig. 4.5B). When PXDN siRNA-transfected cells were treated with TGF-β1, the number of cells attaching at each time point was similar to that of untreated cells, until the 60 minute time point, where, 8 ± 1.5% less cells had attached compared to untreated cells (Fig 4.5B). These results showed that when PXDN expression is knocked down in HeLa cells, the cells are less able to attach to tissue culture dishes. And while TGF-β1 treatment increase the attachment properties of HeLa cells, silencing PXDN expression in the cells counteracts this effect. Although control siRNA increased the attachment of HeLa cells in the first 45 minutes, at 60 minutes the number of cells attached was not significantly different.

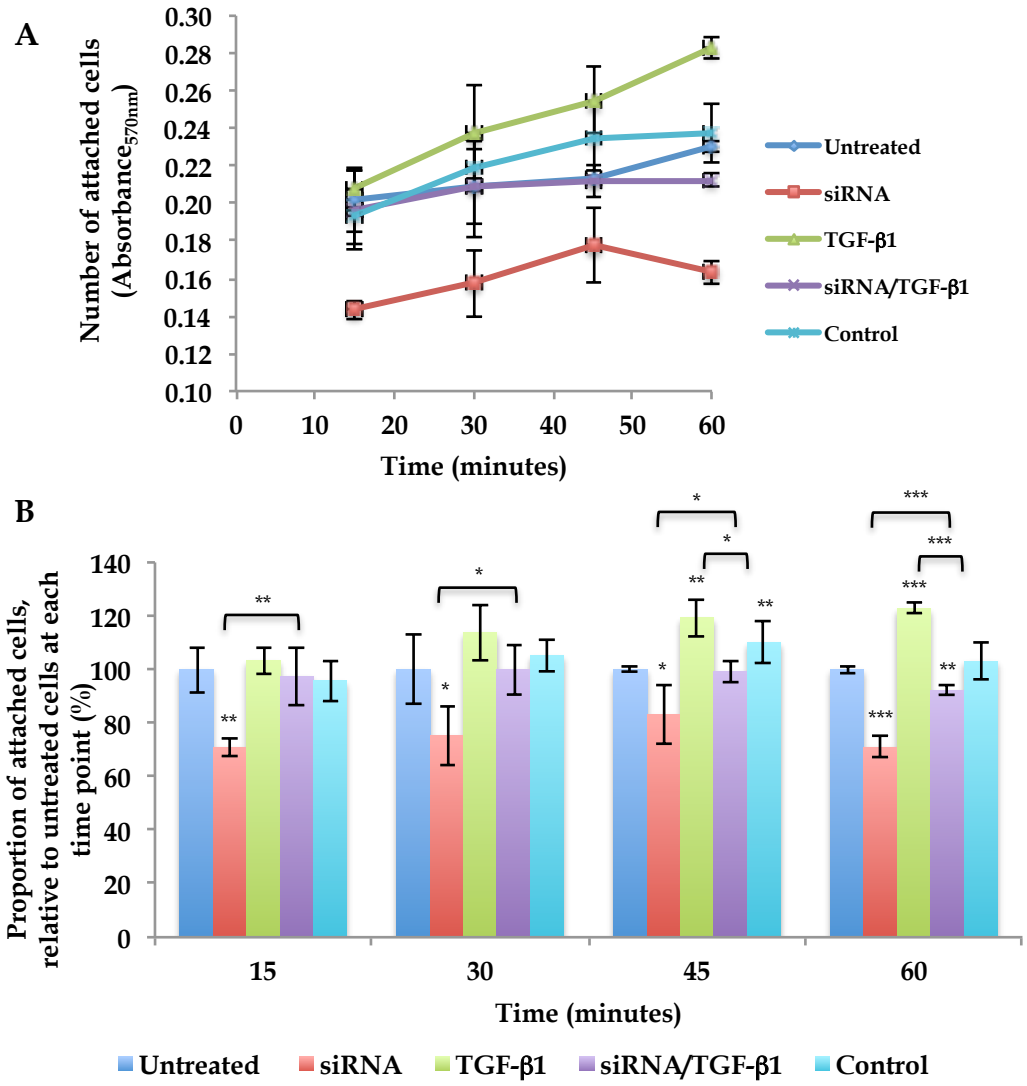

Figure 4.5: PXDN plays a role in HeLa cell attachment. A) A representation of the changes in cell attachment of HeLa cells over 60 minutes when cells were untreated, transfected with PXDN siRNA, treated with TGF-β1, and siRNA and TGF-β1 combined. B) A comparison of the proportion of attached cells at each time point, when compared to untreated cells. TGF-β1 increases attachment of HeLa cells, while silencing PXDN expression decreases the ability of cells to attach to culture plates. Treating siRNA-transfected cells with TGF-β1 neutralises the effect of the individual treatments, resulting in similar number of cells attaching as untreated cells. After 60 minutes, attached control siRNA cells are similar to untreated cells (n = 3 ± SD).

The number of untreated SiHa cells that attached to the tissue culture plate every 15 minutes increased between 15 and 45 minutes and leveled out at 60 minutes, with the highest number of cells attached at 60 minutes (Fig. 4.6A). When SiHa cells were transfected with PXDN siRNA, the number of attached cells decreased at each time point, until 45 minutes, at which point the number of attached cells increased (Fig. 4.6A). TGF-β1 increased the attachment properties of SiHa cells, resulting in more cells attaching at each time point when compared to untreated cells (Fig. 4.6A). The siRNA/TGF-β1 combination saw an increase in attached cells between 15 and 30 minutes. The cell count remained approximately the same between 30 and 45 minutes and then decreased between 45 and 60 minutes (Fig. 4.6A). When comparing each treatment to untreated cells, at each time point, the following observations were made: for siRNA-transfected cells, the number of cells decreased to 88 ± 13.0% at 15 minutes, 85 ± 2.9% at 30 minutes, 79 ± 11.1% at 45 minutes and 85 ± 5.1% at 60 minutes, relative to untreated cells. After TGF-β1 treatment, the number of attached cells increased to 103 ± 6.8%, 112 ± 5.9%, 111 ± 3.0% and 117 ± 8.4% at 15, 30, 45 and 60 minutes respectively, relative to untreated cells. When cells were transfected with siRNA and subsequently treated with TGF-β1, the number of attached cells was lowered to 83 ± 6.5% relative to untreated cells at 15 minutes. At 30 minutes the number of attached cells was 88 ± 5.7%, and 84 ± 2.3% at 45 minutes, relative to untreated cells. At the final time point, there were 80 ± 2.7% cells attached, relative to untreated. These results show that knocking down PXDN expression in SiHa cells results in a reduction in the ability of cells to attach to tissue culture plates. Additionally, TGF-β1 significantly increases attachment properties of SiHa cells and when siRNA-transfected cells are treated with TGF-β1 this does not return cell attachment levels to untreated levels, as seen in HeLa cells, but cells retain the properties of PXDN siRNA-transfected cells. For the control siRNA there was a trend towards decreased attachment and control siRNA significantly lowered attachment of SiHa cells by 20% at 15 minutes, 16% at 45 minutes and 11% at 60 minutes.

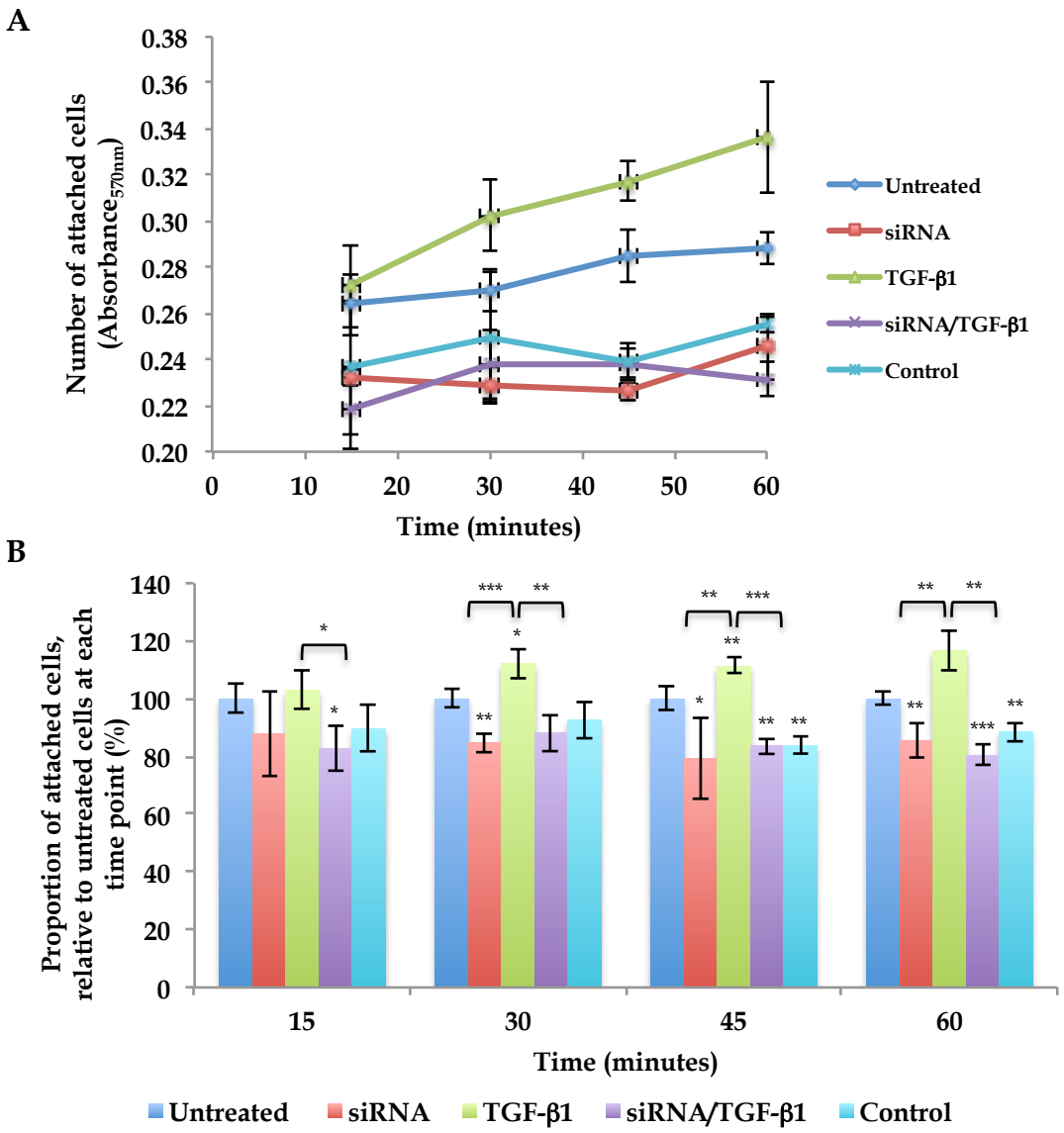

Figure 4.6: PXDN plays a role in SiHa cell attachment. A) A representation of the changes in SiHa cell attachment over 60 minutes when cells were untreated, transfected with PXDN siRNA, treated with TGF-β1 and siRNA and TGF-β1 combined. B) A comparison of the proportion of attached cells at each time point, relative to untreated cells. Downregulating PXDN expression decreases attachment of cells while TGF-β1 has the opposite effect. Treating siRNA-transfected cells with TGF-β1 does not mitigate the effect of the individual treatments. Control siRNA decreased the number of attached cells at three time points relative to untreated (n = 3 ± SD).

4.3.5. Peroxidasin promotes invasion of HeLa cells

Invasion assays were used to observe changes in the ability of HeLa and SiHa to invade through a reconstituted BM after knocking down PXDN expression. We also monitored changes in the invasion ability of cells treated with TGF-β1, and cells transfected with siRNA with concomitant treatment with TGF-β1. Knocking down PXDN expression resulted in less HeLa cells invading through the ECM gel; 82 ± 3.6% cells invaded the ECM gel over 24 hours relative to untreated cells (Fig. 4.7). Treating HeLa cells with TGF-β1 did not affect the number of cells invading through the ECM gel. The siRNA/TGF-β1 combination caused a decrease in the number of invading cells by 34% to 66 ± 1.7% relative to untreated cells (Fig 4.7). Therefore, overall, knocking down PXDN expression in HeLa cells resulted in less cells invading through the ECM gel. While treating cells with TGF-β1 caused HeLa cells to increase invasion potential, knocking down PXDN expression while exposing cells to TGF-β1 resulted in even less cells invading the ECM gel than those transfected with siRNA alone. Interestingly, transfection of HeLa cells with control siRNA decreased invasion of cells by 46% to 54 ± 2.2% relative to untreated, even more than for PXDN siRNA alone, indicating that this may not just be a feature of the transfection process.

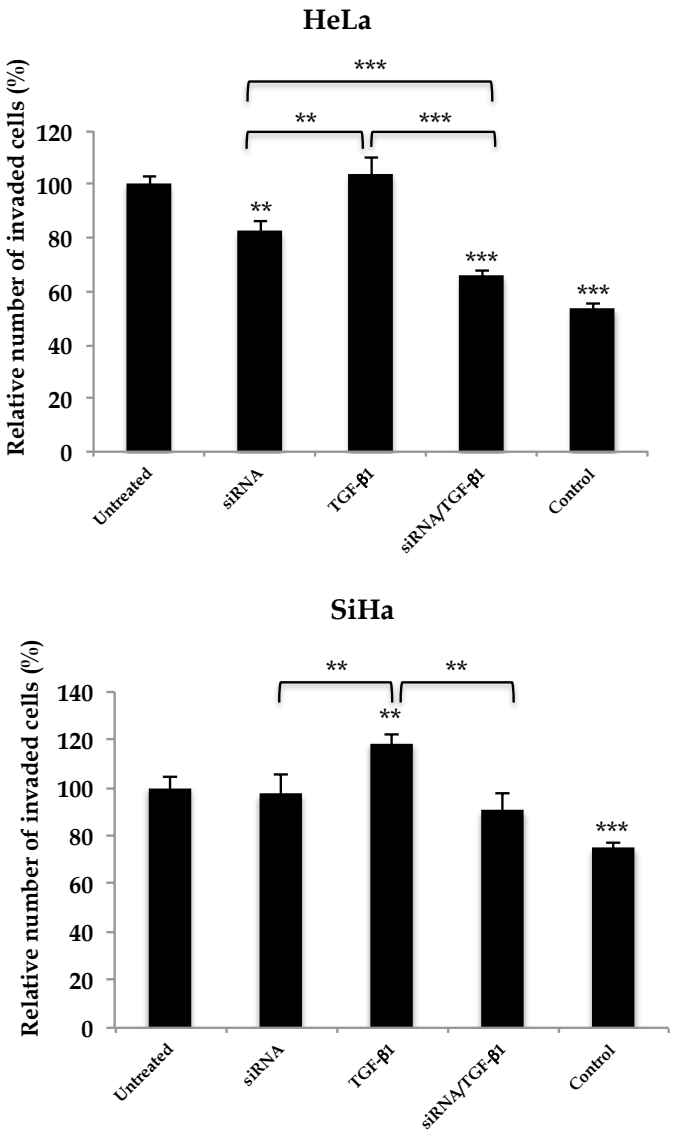

Figure 4.7: Silencing PXDN expression in HeLa cells causes a decrease in the number of cells invading through a reconstituted BM. HeLa and SiHa cells are able to invade through ECM gel towards a chemoattractant. Transfecting cells with PXDN siRNA results in a decrease in the invasion potential of the HeLa cells but not SiHa cells. When treated with TGF-β1, invasion potential is increased in SiHa cells. Although TGF-β1 did not significantly affect invasion of HeLa cells, a combination of TGF-β1 and siRNA transfection results in even less cells invading the ECM gel than siRNA-transfected cells. Significance stars above error bars represent p-values compared to untreated cells, all other p-values were not significant (n = 3 ± SD).

As mentioned, when PXDN expression is knocked down in SiHa cells, there is no change in the ability of the cells to invade the ECM gel. Treating SiHa cells with TGF-β1 resulted in 19% more cells invading through the ECM gel, 119 ± 4.0% relative to untreated cells. The siRNA/TGF-β1 combination did not significantly change the number of invading cells, compared to untreated cells. Control siRNA decreased invasion by 25% to 75 ± 1.8% relative to untreated cells (Fig 5.7). In summary, silencing PXDN expression decreases invasion of HeLa cells. In both cells, transfection with control siRNA significantly reduced the number of cells invading the ECM gel.

4.3.6. Peroxidasin affects migration of HeLa and SiHa cells

In order to determine if PXDN is involved in cell migration, we used the wound healing/scratch assay to observe the effect of knocking down PXDN expression on the rate of movement of HeLa and SiHa cells. The scratch assays showed that overall, SiHa cells migrate at a faster rate than HeLa cells, since the scratch created in untreated SiHa cells closed faster than those of untreated HeLa cells.

In the HeLa cell line, for untreated cells, the open scratch distance was 91 ± 7.0%, 82 ± 5.7 % and 51 ± 3.2 % after 12, 24 and 48 hours respectively, relative to the zero time point (Fig. 4.8 & Fig. 4.9). When transfected with PXDN siRNA, the widths at 12, 24 and 48 hours were 91 ± 12.0%, 75 ± 7.4% and 46 ± 3.4%, respectively, relative to the zero time point (Fig. 4.8 & Fig. 4.9). Treating cells with EMT-inducing TGF-β1 resulted in open wound widths of 92 ± 9.0% and 81 ± 1.8% over 12 and 24 hours respectively, relative to the zero time point. The fastest rate of wound closure in TGF-β1 treated cells occurred between 24 and 48 hours, when the open wound distance was 45 ± 5.5 %, relative to the zero time point. When siRNA transfection was combined with TGF-β1 treatment, cell movement rate increased and the open wound areas were 87 ± 7.6%, 65 ± 3.5% and 24 ± 1.9% over the three time points, relative to the zero time point (Fig. 4.8 & Fig. 4.9). Transfection of HeLa cells with control siRNA resulted in the scratch closing slower than in untreated cells. The scratch area in control cells closed to 87 ±1 0.0%, 76 ± 10.1% and 61 ± 8.9% over 12, 24 and 48 hours, respectively, relative to the zero time point.

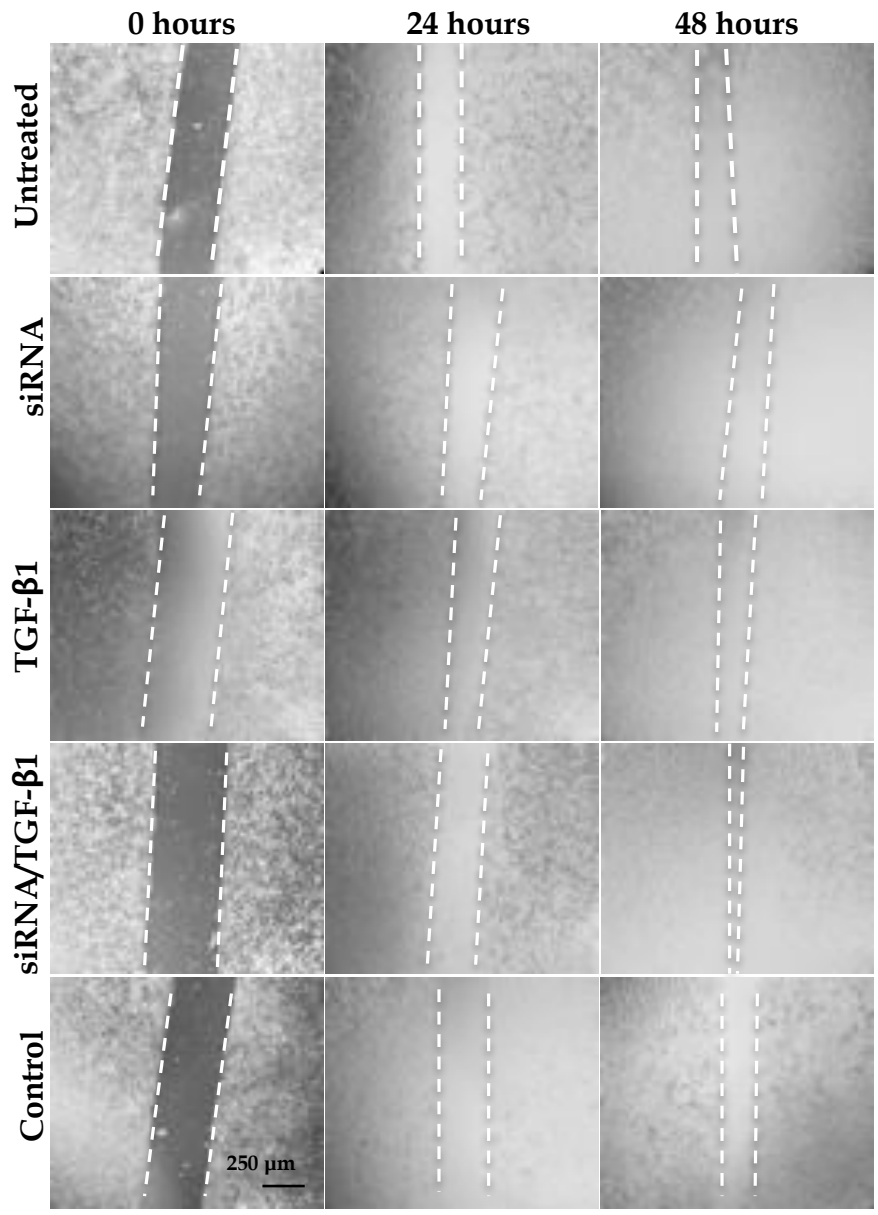

Figure 4.8: PXDN and TGF-β1 affect the rate of migration of HeLa cells. Untreated HeLa cells close a scratch in the cell monolayer by 50 % over 48 hours. Silencing PXDN expression also results in approximately 50 % scratch closure over 48 hours, and similar results are observed in TGF-β1-treated cells. The combination of transfection with PXDN siRNA and treatment with TGF-β1 resulted in 76 % scratch closure over 48 hours. Control siRNA cells close a scratch in the cell monolayer by 60 % over 48 hours Cells were visualised under the bright field of an Olympus BX63 microscope at 40x magnification (scale bar = 250 µm).

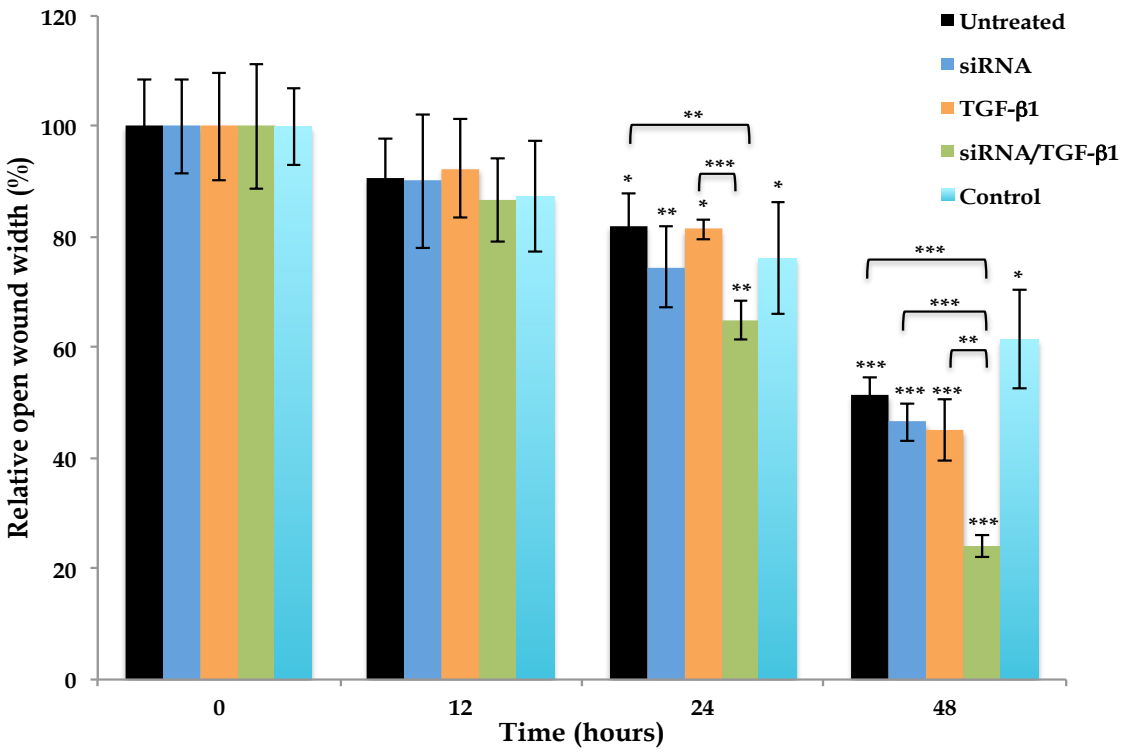

Figure 4.9: Silencing PXDN expression, in combination with TGF-β1 treatment, increases the rate of migration of HeLa cells. When comparing the rate of migration of siRNA-transfected cells and TGF-β1 treated cells, the combination of transfection and treatment increases migration rate more than siRNA transfection or TGF-β1 treatment alone. Significance stars above error bars represent p-values compared to untreated cells at zero time, all other p-values were not significant (n = 3 ± SD).

Untreated SiHa cells migrate at a faster rate than HeLa cells, and after 24 hours of scratching the cell monolayer, the scratch was closed. The scratch was closed by half, 46 ± 5.0% closed wound width, at 12 hours; and then almost completely at 24 hours, 94 ± 10.6% closed wound width (Fig. 4.10 & Fig. 4.11). Transfecting SiHa cells with PXDN siRNA slowed down the rate of migration, with 32 ± 9.4% open wound width 24 hours after wounding cells (63 ± 15.1% open wound width at 12 hours), relative to the zero time point. Treating SiHa cells with TGF-β1 increased the rate of migration, with complete wound closure at 24 hours post scratch (20 ± 7.4% open wound width at 12

hours, relative to zero time point). Transfecting cells with siRNA and then treating with TGF-β1 resulted in 95 ± 9.0% wound closure after 24 hours (43 ± 12.6% wound closure at 12 hours) (Fig. 4.10 & Fig. 4.11). Control cells transfected with Fluc esiRNA showed the slowest wound closure, 87 ± 10.0% and 76 ± 10.1% open wound width at 12 and 24 hours, respectively, relative to zero time point.

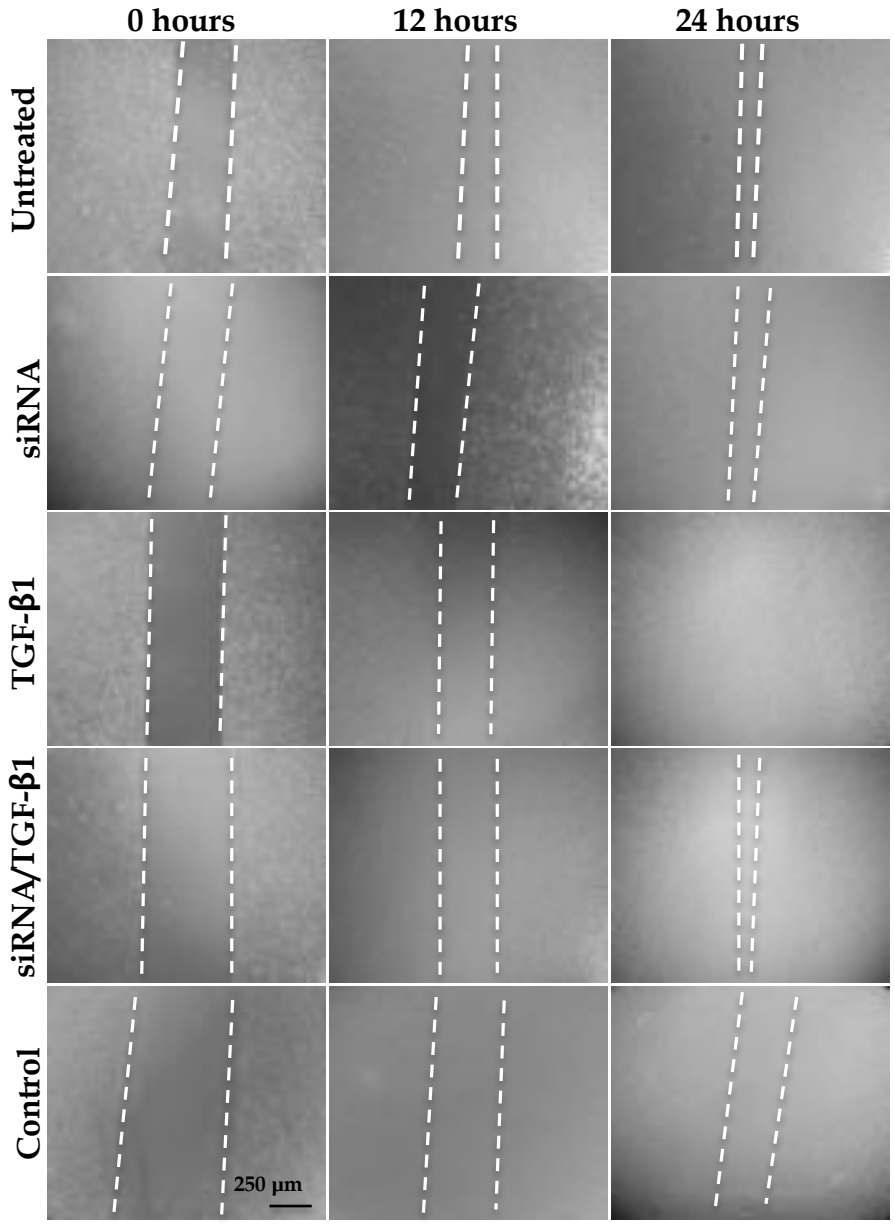

Figure 4.10: PXDN and TGF-β1 affect the rate of migration of SiHa cells. Untreated SiHa cells close a scratch in the cell monolayer after 24 hours. Silencing PXDN expression in SiHa cells also results in approximately 69% scratch closure over 24 hours, and in TGF-β1-treated cells, scratches are completely closed by 24 hours. The combination of transfection with siRNA and treatment with TGF-β1 results in 95% scratch closure over 24 hours. Control siRNA slowed the migration of cells. Cells were visualised under the bright field of an Olympus BX63 microscope at 40x magnification (scale bar = 250 µm).

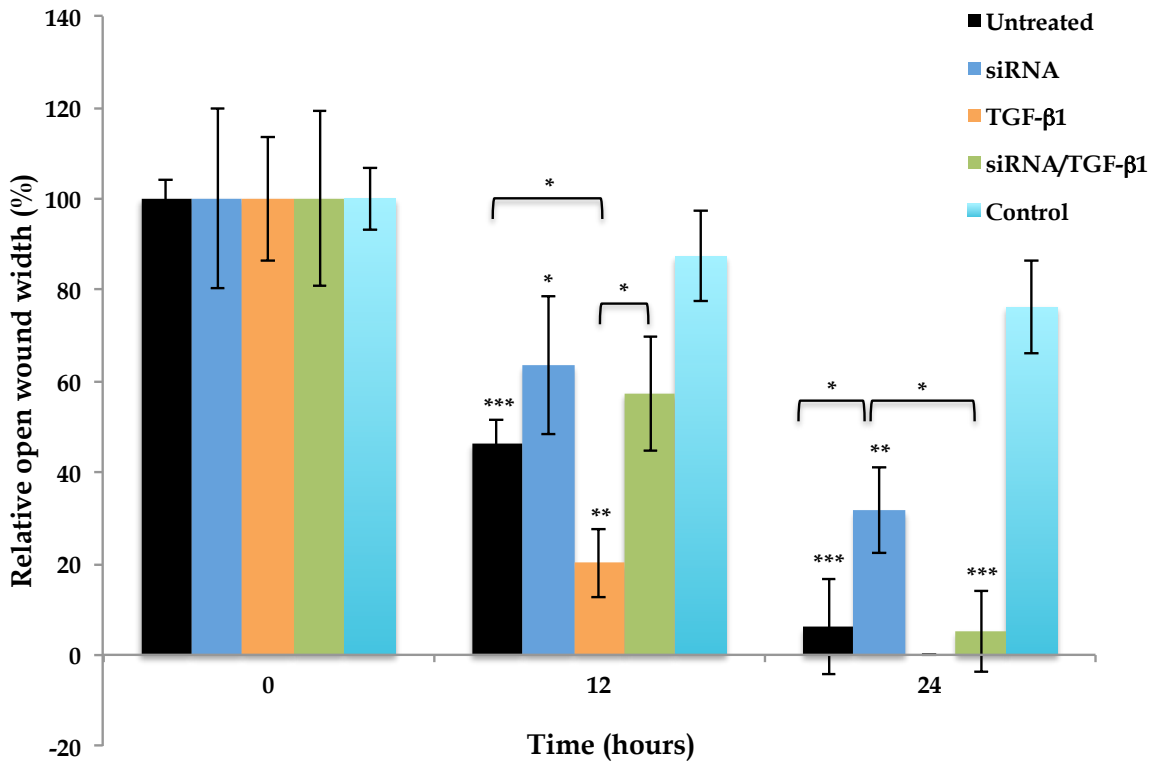

Figure 4.11: Silencing PXDN expression in SiHa cells slows down the rate of cell migration but this increases when transfected cells are exposed to TGF-β1. Transfecting SiHa cells with PXDN siRNA alone causes the cells to migrate at a slower rate than untreated cells. Treating cells with TGF-β1 acts in the opposite way by increasing the rate of cell migration. When PXDN is silenced in TGF-β1 treated cells, the effect of both (siRNA or TGF-β1) is mitigated by the effect of the other. Significance stars above error bars represent p-values compared to untreated cells at zero time point, all other p-values were not significant (n = 3 ± SD).

4.4. Discussion

In this chapter we sought to determine the role of PXDN in cellular processes that may be significant in EMT. We achieved this by performing functional studies to look at cell morphology, proliferation, attachment, invasion and migration of HeLa and SiHa cells in which PXDN expression was knocked down using an siRNA approach. PXDN expression was knocked down in both cell lines after transfecting cells with siRNA. The level of PXDN knockdown was lower than that seen in other studies where MISSION® esiRNA targeting other genes was used to transfect cancer cells (Arai *et al.*, 2011; Theis and Buchholz, 2011; Kim *et al.*, 2016) and specifically, HeLa cells (Theis and Buchholz, 2011). This difference may have been due to several factors such as the transfection reagent, siRNA concentration and cell culture medium composition, all of which may have had an effect on transfection efficiency and therefore, PXDN knockdown.

When the level of PXDN knockdown by TGF-β1 treatment was quantified by ELISA, we found that expression in SiHa cells was knocked down to similar levels as when PXDN was immunoprecipitated from the lysates of cells treated with TGF-β1 and quantified by western blot. In HeLa cells, the same trend was observed, although the level of PXDN expression when quantified by ELISA did not show a statistically relevant decrease. This could possibly be attributed to the difference in protein quantification between western blotting and ELISA for this cell line.

We found that silencing PXDN expression in HeLa cells changed cell morphology and made cells appear smaller and less round, and with fewer cell-to-cell contacts. In SiHa cells the same was also seen and in addition, cells were clustered together more. These properties and the observation of increased cell protrusions when PXDN expression is downregulated suggest that PXDN assists in maintaining the epithelial phenotype. The changes that occur after knockdown of PXDN expression may indicate that cells are taking on a more mesenchymal-like phenotype since the formation of a monolayer, which is seen with untreated cells, seems to be disturbed. Combining PXDN

knockdown and TGF-β1 treatment exacerbated the changes in cell morphology, confirming that indeed PXDN plays a role in maintaining the epithelial phenotype of HeLa and SiHa cells.

We next assessed cell proliferation to find that when PXDN was knocked down in HeLa and SiHa cells, cell proliferation was decreased. This is in line with other studies that found that knocking down PXDN expression decreased the proliferation of cancer cells (Tauber *et al.*, 2010; Young *et al.*, 2015). Young *et al.* (2015) found that silencing PXDN expression decreased growth factor-independent proliferation of PIK3CA mutant cells that have overexpressed levels of PXDN when compared to wild-type cells. Additionally, when basal-like breast cancer (BLBC) cells were transfected with PXDN-siRNA the four BLBC cell lines examined exhibited reduced proliferation (Young *et al.*, 2015). Moreover, in the luminal cell line, MDA-MB-361, which has low PXDN expression, proliferation was inhibited by siRNA knockdown (Young *et al.*, 2015). Tauber *et al.* (2010) found that silencing PXDN expression in a 607B melanoma cells overexpressing PXDN significantly reduced cell proliferation (Tauber *et al.*, 2010). TGF-β1 has been shown to increase the proliferation of HeLa and SiHa cells (Cheng and Hao, 2016). However, Kang *et al.* (1998) found that HeLa cells are in sensitive to the growth inhibitory effects of TGF-β1 and that TGF-β1 decreases proliferation of HeLa cells, while SiHa cells are not sensitive to this effect of TGF-β1 (Kang *et al.*, 1998). Maliekal *et al.* (2004) showed that TGF-β1 could promote and inhibit growth of HeLa cells and that the effect of TGF-β1 on proliferation of HeLa cells was time and concentration dependent (Maliekal, Anto and Karunagaran, 2004). In our study, TGF-β1 treatment decreased proliferation in HeLa cells, but did not significantly affect proliferation of SiHa cells. This may be due to the differing effects of TGF-β1 that are dependent on cell type, and TGF-β1 exposure time and concentration. Cell proliferation was decreased to the greatest extent when PXDN downregulation was combined with TGF-β1 treatment, in both cell lines. The effect of PXDN downregulation on cell proliferation could be attributed to detachment of cells from the culture dish and loss of contacts with adjacent cells, which may lead to cell death. Control siRNA also decreased proliferation

in both cell lines, to a similar extent as PXDN siRNA. The control siRNA may be binding non-specific targets and affecting downstream cellular processes (Persengiev, Zhu and Green, 2004). Tschuch *et al*. (2008) showed that siRNAs without a physiological target (such as green fluorescent protein) have sequence-specific off-target effects in mammalian cells (Tschuch *et al*., 2008). Given the unexpected effect of the control siRNA on cells, a BLAST of the mRNA target of the control siRNA was conducted and showed that surprisingly, the control siRNA binds to a 26 bp region of transforming growth factor-β–induced (TGFBI) mRNA (accession number NM_000358). TGFBI is induced by TGF-β and is secreted into the extracellular space (Zhao, Piao and Hei, 2002) where it binds to fibronectin, collagen and integrins (Wen *et al*., 2011). Therefore, this may be the reason for the decrease in PXDN expression seen in SiHa cells transfected with control siRNA. TGFBI has been found to promote proliferation of renal proximal tubular epithelial cells (Park *et al*., 2004). Additionally, upregulation of TGFBI in cancer cells may stimulate their survival via ECM-dependent signaling (Ivanov *et al*., 2008) and this may account for the decrease in proliferation that we observed in the control siRNA-transfected cells.

Since the BM plays a significant role in epithelial cell attachment (Fang *et al*., 2014), PXDN may play an important role in maintaining cell attachment to the BM by stabilising collagen IV and maintaining interactions between cells through its protein binding domains. PXDN knockdown in HeLa and SiHa cells reduced the ability of cells to attach to one another and to tissue culture plates. This effect may be due to the instability of collagen IV once PXDN expression is reduced. Furthermore, cells may produce collagen IV in order to attach to culture plates, thus a reduction in PXDN expression would adversely affect the ability of cells to attach. These findings concur with those reported by Tauber *et al*. (2010) where it was shown that the adhesion-promoting effects of HO-1 were dependent on PXDN expression. When PXDN was transiently overexpressed in choriocarcinoma cells, adhesion of cells to laminin and fibronectin coated wells was enhanced. Silencing PXDN expression reduced cell attachment and the effect was pronounced in tissue culture plates coated with laminin

and fibronectin (Tauber *et al.*, 2010). We found that TGF-β1 increased the attachment of HeLa and SiHa cells, and although we found that TGF-β1 decreases PXDN expression in HeLa and SiHa cells, TGF-β1 has been found to promote cell attachment by increasing the expression of ECM adhesion molecules such and laminin and fibronectin and upregulating expression of integrin receptors (Wang *et al.*, 2004). In the context of our study, perhaps the effect of TGF-β1 on increased cell attachment in HeLa and SiHa cells was due to an increase in the abovementioned ECM adhesion molecules, and while PXDN is knocked down in response to TGF-β1, the effect of cell detachment could be overcome by the increased expression of the ECM adhesion molecules. When PXDN expression was knocked down in HeLa and SiHa cells, with concomitant TGF-β1 treatment, the effect of TGF-β1 on cell attachment was somewhat mitigated. HeLa cells attachment was decreased, although not to the same extent as with PXDN knockdown alone. However, in SiHa cells, the eradication of the effect of TGF-β1 on cell attachment was more pronounced since attachment decreased to even lower levels than in PXDN siRNA-transfected cells. PXDN contributes to BM integrity by stabilising collagen IV, the major constituent of the BM (Bhave *et al.*, 2012) and since cells are anchored to the BM via collagen IV, a disruption in the stability of collagen would result in decreased ability of cells to attach (Fang *et al.*, 2014).

Cells undergoing EMT are able to invade the BM to enter the vascular system before spreading to secondary sites. We proposed that in cells undergoing invasion, PXDN is upregulated in order to destabilise the ECM by upregulation of ECM-degrading MMPs. We showed that decreasing PXDN expression in HeLa cells lowers the number of cells invading through a reconstituted BM. Similarly, Tauber *et al*. (2010) found that downregulation of PXDN expression significantly reduced invasion of BeWo choriocarcinoma cells (Tauber *et al.*, 2010), PIK3CA mutant cells overexpressing PXDN show an increased ability to invade through reconstituted BM (Young *et al.*, 2015) and PXDN silencing in melanoma cell lines significantly reduced invasion (Jayachandran *et al.*, 2016).

Invasion was not decreased significantly in SiHa cells when PXDN expression was knocked down. Perhaps this was due to the invasive ability of SiHa cells; since SiHa cells are more invasive than HeLa cells (Chatterjee and Chatterjee, 2001), knocking down PXDN expression alone may not be sufficient to impact invasion ability. It may be that PXDN may assist to maintain invasive potential of SiHa cells rather than promote it, with other cell proteins being responsible for promoting invasion. Where PXDN does affect invasion, perhaps when its expression is decreased, collagen IV integrity becomes compromised and cells are more able to invade the ECM. We found that TGF-β1 increases invasion of SiHa cells, which is been previously demonstrated by Yi *et al*. (2002), but did not affect HeLa cell invasion, although TGF-β1 has been shown to induce invasion in HeLa cells (Thacker and Karunagaran, 2015). We also observed a significant decrease in the number of invaded HeLa and SiHa cells when control siRNA was used to transfect cells. In both cell lines, these control samples showed less cells invading than in any of the experimental samples. It is likely this may be due to the effect of the control siRNA on the cells; since the control siRNA binds to TGFBI mRNA and cause downregulation of TGFBI protein, which is an ECM protein involved in increased cell invasion (Shang *et al.*, 2012; Ween, Oehler and Ricciardelli, 2012).

The rate at which cells migrate to close a scratch made in the cell monolayer can be used to measure cell motility and may point to their potential to migrate from one position to another in the tumour environment (Justus *et al.*, 2014). Knocking down PXDN expression increases the migration rate of HeLa cells but decreases that of SiHa cells, relative to untreated cells. Using a chicken transplantation model, Jayachandran *et al*. (2016) showed that silencing PXDN reduces migration of mesenchymal melanoma cells (Jayachandran *et al.*, 2016). As observed with the invasion of SiHa cells, PXDN knockdown did not affect migration of SiHa cells. Perhaps this can be attributed to the difference in the migration ability of the untreated cells, where we have found that SiHa cells migrate faster than HeLa cells (wound closure was achieved in 24 hours in SiHa cells). In both cell lines we observed a reduction in wound closure ability when compared to untreated cells. As previously mentioned, the control siRNA may be

downregulating expression of TGFBI and therefore affecting cell migration. TGFBI is secreted by colon cancer cells and increases migration of these cells (Ma *et al.*, 2008) as well as that of renal cell carcinoma cells (Shang *et al.*, 2012). The effects of the control siRNA on cell proliferation, morphology, invasion, attachment and migration necessitate the use of a different control siRNA that does not bind to any mammalian mRNA.

In summary, we found that silencing PXDN alters the morphology of HeLa and SiHa cells and causes cells to take on a more mesenchymal phenotype. Knocking down PXDN expression decreased the proliferation of HeLa and SiHa cells and also decreased attachment of both cell lines. Migration of HeLa cells was also affected by knockdown of PXDN, while the migration of SiHa cells was somewhat unchanged. Our results show that it is probable that PXDN plays a role in EMT of cancer cells, with some cancer stage and cell specific effects.

Overall, knocking down PXDN expression in HeLa and SiHa cells alters several cellular processes that are important for tumour progression. Tumour cells need to proliferate (in spite of cellular signals that attempt to induce cell death), attach stably to the BM, and migrate and invade when metastasising. If the manner in which PXDN exerts its function in these cellular processes in cancer cells is further elucidated, it may prove to be an important player in cancer therapy.

Chapter 5: Conclusion and Future Outlook

EMT-mediated metastasis of cancer cells in the body is responsible for the vast majority of cancer deaths (Sethi and Kang, 2011). Metastasis is a complex multi-step event and invasion of a tumour through the BM into surrounding tissue is the first crucial step of the metastasis process (Jayachandran *et al*., 2015). EMT is a biological process that causes a polarised epithelial cell which normally interacts with BM via its basal surface, to undergo changes that enable it to take on a mesenchymal cell phenotype (Kalluri and Weinberg, 2009). In the context of cancer cells, this can result in cells breaking through the BM, entering the vascular or lymphatic system and establishing secondary tumours at secondary sites (Kalluri and Weinberg, 2009). The BM provides extracellular cues for cellular adhesion, proliferation, migration and differentiation (Colon and Bhave, 2016). PXDN catalyses the sulfilimine bonds that stabilise the collagen IV network, the predominant constituent of BM. Collagen IV provides structural integrity to epithelial and vascular tissues, serves as a scaffold for macromolecular assembly and interacts with cell-surface receptors such as integrins to control cell adhesion, migration, proliferation and differentiation (Bhave *et al.*, 2012).

In this study we demonstrated that HeLa and SiHa cervical carcinoma cells undergo EMT in the presence of TGF-β1. This was concluded as a result of the changes in expression of EMT markers, Snai1, E-cadherin and vimentin when HeLa and SiHa cells were exposed to TGF-β1. Our findings agree with previous observations that TGF-β1 leads to decreased E-cadherin and promotes EMT induction in HeLa and SiHa cell lines (Yi *et al*., 2002; Kloth *et al*., 2005; Cheng and Hao, 2016). We then found that TGF-β1 downregulates PXDN expression in HeLa and SiHa cells and as far as we know this is the first time the expression pattern of PXDN has been examined in TGF-β1-induced type 3 EMT in HeLa and SiHa cells. In contrast to our results, in kidney fibrosis, PXDN shows increased deposition in the ECM in response to TGF-β1 (Péterfi *et al.*, 2009). It is possible that in this regard PXDN may play differing roles that are EMT-type specific. Next we showed that the master EMT regulator, Snai1, regulates *PXDN* expression. We

found that Snai1 binds to the *PXDN* promoter when HeLa and SiHa cells undergo TGF-β1-induced EMT. *PXDN* expression was repressed by Snai1 in the presence of TGF-β1 and when Snai1 was overexpressed in HEK293 cells. In contrast with our findings, Barnett *et al.* (2011) found that Snai1 overexpression caused significant upregulation of PXDN in human prostate cancer cells (Barnett *et al*., 2011). These opposing results may be understandable since PXDN expression patterns in cancer cells are emerging as cancer-type and probably stage specific (Castronovo *et al.*, 2006; Desmond *et al.*, 2007; Péterfi *et al.*, 2009; Liu *et al.*, 2010; Tauber *et al.*, 2010; Bai *et al.*, 2011; Barnett *et al.*, 2012; Young *et al.*, 2015; Jayachandran *et al.*, 2016). We then looked at the functional contribution of PXDN to EMT. Reducing PXDN expression in HeLa and SiHa cells had varying effects on cellular process involved in EMT, namely, cell proliferation, attachment, invasion and migration. The effect of PXDN knockdown on these cellular processes was not consistent in both cell lines, as has been shown by other studies involving PXDN knockdown (Tauber *et al.*, 2010; Young *et al.*, 2015; Jayachandran *et al.*, 2016). Our findings that Snai1 regulates *PXDN* in cervical carcinoma cell lines and that PXDN functions in EMT-related cellular such proliferation, attachment, invasion and migration in these cells, further supports a role for this ECM-modifying protein in cancer. One such example where protein expression differs according to EMT type can be seem with the ECM protein fibronectin (Zeisberg and Neilson, 2009) and PXDN may follow this pattern, since it has been shown to function in the three major processes where EMT occurs (Horikoshi *et al.*, 1999; Tindall *et al.*, 2005; Desmond *et al.*, 2007; Péterfi *et al.*, 2009; Gotenstein *et al.*, 2010; Liu *et al.*, 2010; Tauber *et al.*, 2010; Yan *et al.*, 2014; Jayachandran *et al.*, 2016). This highlights the complexity in the tissue and disease specific roles of EMT and the TGF-β1 pathways, and potentially of PXDN (Thiery *et al.*, 2009).

Future work related to PXDN in cancer cells may focus on elucidating the precise role of PXDN in cancer and metastasis by overexpressing and also knocking out PXDN and observing changes that occur when PXDN is in abundance or is absent in the tumour environment. This way we may also identify other molecules (such as downstream

targets like MMPs) linked to PXDN expression and function, as well as the signaling pathways it may affect. It may also be important to determine if other cellular processes compensate for the lack of, or abundance of, PXDN in the tumour environment.

Specific key steps following on from this work could include:

- Performing PXDN knockout studies to determine the effect of decreased PXDN expression on metastasis related cellular processes and the ECM of carcinoma cells and non-cancerous cells.
- Identifying the signaling pathways that modify PXDN expression by quantifying changes in the expression of specific signaling proteins and cellular features such as EMT.
- Identifying whether ECM modifiers including MMPs are linked to PXDN expression and determine if their function is altered based on changes levels of PXDN expression.
- Animal studies could involve injecting mice with tumour cells in which PXDN expression has been knocked out to investigate the effect of loss of PXDN on tumour growth and metastasis.

Since we have found that PXDN expression is downregulated in a TGF-β1–induced EMT environment, it is probable that PXDN may be overexpressed when secondary tumours are being established and cells undergo MET at the secondary tumour site. With the complex expression pattern of PXDN in different cancer types and stages, determining the function of PXDN in cancer cells may prove challenging, most especially because of the uniqueness of PXDN compared to its counterparts. Since PXDN consolidates collagen IV that gives structural integrity to the BM, an integral part of the metastasis process, PXDN may present a new target for cancer therapy when it comes to reducing the incidences of metastasis.

References

Akhurst, R. J. and Derynck, R. (2001) 'TGF- β signaling in cancer – a double-edged sword', *Trends in Cell Biology*, 11(11), pp. 44–51.

Arai, E., Nishida, Y., Wasa, J., Urakawa, H., Zhuo, L., Kimata, K., Kozawa, E., Futamura, N. and Ishiguro, N. (2011) 'Inhibition of hyaluronan retention by 4-methylumbelliferone suppresses osteosarcoma cells in vitro and lung metastasis in vivo', *British Journal of Cancer*. Nature Publishing Group, 105(12), pp. 1839–1849. doi: 10.1038/bjc.2011.459.

Bai, Y.-P., Hu, C.-P., Yuan, Q., Peng, J., Shi, R.-Z., Yang, T.-L., Cao, Z.-H., Li, Y.-J., Cheng, G. and Zhang, G.-G. (2011) 'Role of VPO1, a newly identified heme-containing peroxidase, in ox-LDL induced endothelial cell apoptosis.', *Free Radical Biology & Medicine*. Elsevier Inc., 51(8), pp. 1492–500. doi: 10.1016/j.freeradbiomed.2011.07.004.

Bai, Y. P., Hu, C. P., Chen, M. F., Xu, K. P., Tan, G. S., Shi, R. Z., Li, Y. J. and Zhang, G. G. (2009) 'Inhibitory effect of reinioside C on monocyte-endothelial cell adhesion induced by oxidized low-density lipoprotein via inhibiting NADPH oxidase/ROS/NF-κB pathway', *Naunyn-Schmiedeberg's Archives of Pharmacology*, 380(5), pp. 399–406. doi: 10.1007/s00210-009-0450-8.

Balasubramanian, D. and Kanwar, R. (2002) 'Molecular pathology of dityrosine cross-links in proteins : Structural and functional analysis of four proteins', *Molecular & Cellular Biochemistry*, 234–235(1), pp. 27–38.

Banerjee, P., Basu, A., Otterbein, L. E., Mizumura, K., Choi, A. M., Pal, S. and Chem, J. B. (2012) 'Signal Transduction : Heme oxygenase-1 promotes survival of renal cancer cells through modulation of molecules Martin Gasser , Ana Maria Waaga-Gasser , Supplemental material ':, *The Journal of Biological Chemistry*, 287, pp. 32113–32123. doi:

10.1074/jbc.M112.393140.

Barberà, M. J., Puig, I., Domínguez, D., Julien-Grille, S., Guaita-Esteruelas, S., Peiró, S., Baulida, J., Francí, C., Dedhar, S., Larue, L. and García de Herreros, A. (2004) 'Regulation of Snail transcription during epithelial to mesenchymal transition of tumour cells.', *Oncogene*, 23(44), pp. 7345–54. doi: 10.1038/sj.onc.1207990.

Barnett, P., Arnold, R. S., Mezencev, R., Leland, C. W. K., Zayzafoon, M. and Odero-Marah, V. (2012) 'Snail-mediated regulation of reactive oxygen species in ARCaP human prostate cancer cells', *Biochemical and Biophysical Research Communications*, 29(404), pp. 997–1003. doi: 10.1016/j.biotechadv.2011.08.021.

Barrallo-Gimeno, A. (2005) 'The Snail genes as inducers of cell movement and survival: implications in development and cancer', *Development*, 132(14), pp. 3151–3161. doi: 10.1242/dev.01907.

Batlle, E., Sancho, E., Francí, C., Domínguez, D., Monfar, M., Baulida, J. and García De Herreros, a (2000) 'The transcription factor snail is a repressor of E-cadherin gene expression in epithelial tumour cells.', *Nature Cell Biology*, 2(2), pp. 84–89. doi: 10.1038/35000034.

Beach, S., Tang, H., Park, S., Dhillon, a S., Keller, E. T., Kolch, W. and Yeung, K. C. (2008) 'Snail is a repressor of RKIP transcription in metastatic prostate cancer cells.', *Oncogene*, 27(15), pp. 2243–2248. doi: 10.1038/sj.onc.1210860.

Bensaad, K. and Vousden, K. H. (2007) 'P53: New Roles in Metabolism', *Trends in Cell Biology*, 17(6), pp. 286–291. doi: 10.1016/j.tcb.2007.04.004.

Bhave, G., Cummings, C. F., Vanacore, R. M., Kumagai-Cresse, C., Ero-Tolliver, I. a, Rafi, M., Kang, J.-S., Pedchenko, V., Fessler, L. I., Fessler, J. H. and Hudson, B. G. (2012)

'Peroxidasin forms sulfilimine chemical bonds using hypohalous acids in tissue genesis.', *Nature Chemical Biology*. Nature Publishing Group, 8(9), pp. 784–90. doi: 10.1038/nchembio.1038.

Bierie, B. and Moses, H. L. (2006) 'TGF-β and cancer.', *Cytokine & Growth Factor Reviews*, 17(1–2), pp. 29–40. doi: 10.1016/j.cytogfr.2005.09.006.

Blobe, G. C., Schiemann, W. P. and Lodish, H. F. (2000) 'Role of Transforming Growth Factor β in Human Disease', *The New England Journal of Medicine*, 342(18), pp. 1350–1358.

Busch, C., Krochmann, J. and Drews, U. (2013) 'The Chick Embryo as an Experimental System for Melanoma Cell Invasion', *PLoS ONE*, 8(1), pp. 1–9. doi:10.1371/journal.pone.0053970.

Cano, a, Pérez-Moreno, M. a, Rodrigo, I., Locascio, a, Blanco, M. J., del Barrio, M. G., Portillo, F. and Nieto, M. a (2000) 'The transcription factor snail controls epithelial-mesenchymal transitions by repressing E-cadherin expression.', *Nature Cell Biology*, 2(2), pp. 76–83. doi: 10.1038/35000025.

Castronovo, V., Waltregny, D., Kischel, P., Roesli, C., Elia, G., Rybak, J.-N. and Neri, D. (2006) 'A chemical proteomics approach for the identification of accessible antigens expressed in human kidney cancer.', *Molecular & Cellular Proteomics : MCP*, 5(11), pp. 2083–91. doi: 10.1074/mcp.M600164-MCP200.

Chelberg, M. K., Tsilibary, E. C., Hauser, A. R., Chelberg, M. K., Tsilibary, E. C., Hauser, A. R. and Mccarthy, J. B. (1989) 'Type IV Collagen-mediated Melanoma Cell Adhesion and Migration : Involvement of Multiple , Distinct Domains of the Collagen Molecule', *Cancer Research*, 49, pp. 4796–4802.

Cheng, G., Li, H., Cao, Z., Qiu, X., McCormick, S., Thannickal, V. J. and Nauseef, W. M. (2011) 'Vascular peroxidase-1 is rapidly secreted, circulates in plasma, and supports dityrosine cross-linking reactions.', *Free Radical Biology & Medicine*. Elsevier Inc., 51(7), pp. 1445–53. doi: 10.1016/j.freeradbiomed.2011.07.002.

Cheng, G., Salerno, J., Cao, Z., Pagano, P. J. and Lambeth, J. D. (2008) 'Identification and characterization of VPO1, a new animal heme- containing Peroxidase', *Free Radical Biology & Medicine*, 45(12), pp. 1682–1694. doi: 10.1016/j.freeradbiomed.2008.09.009.

Cheng, K. and Hao, M. (2016) 'Metformin Inhibits TGF-β1-Induced Epithelial-to-Mesenchymal Transition via PKM2 Relative-mTOR/p70s6k Signaling Pathway in Cervical Carcinoma Cells', *International Journal of Molecular Sciences*, 17(12), p. 2000. doi: 10.3390/ijms17122000.

Choi, A., Lao, R., Ling-Fung Tang, P., Wan, E., Mayer, W., Bardakjian, T., Shaw, G. M., Kwok, P., Schneider, A. and Slavotinek, A. (2015) 'Novel mutations in PXDN cause microphthalmia and anterior segment dysgenesis', *European Journal of Human Genetics*. Nature Publishing Group, 23(3), pp. 337–341. doi: 10.1038/ejhg.2014.119.

Christiansen, J. J. and Rajasekaran, A. K. (2006) 'Reassessing epithelial to mesenchymal transition as a prerequisite for carcinoma invasion and metastasis.', *Cancer Research*, 66(17), pp. 8319–26. doi: 10.1158/0008-5472.CAN-06-0410.

Colon, S. and Bhave, G. (2016) 'Proprotein convertase processing of peroxidasin', *Journal of Biological Chemistry*. doi: 10.1074/jbc.M116.745935.

Cortes-Reynosa, P., Robledo, T., Macias-Silva, M., Wu, S. V. and Salazar, E. P. (2008) 'Src kinase regulates metalloproteinase-9 secretion induced by type IV collagen in MCF-7 human breast cancer cells', *Matrix Biology*, 27(3), pp. 220–231. doi: 10.1016/j.matbio.2007.11.003.

De Craene, B., Gilbert, B., Stove, C., Bruyneel, E., van Roy, F. and Berx, G. (2005) 'The transcription factor snail induces tumour cell invasion through modulation of the epithelial cell differentiation program.', *Cancer research*, 65(14), pp. 6237–44. doi: 10.1158/0008-5472.CAN-04-3545.

Desmond, J. C., Raynaud, S., Tung, E., Hofmann, W.-K., Haferlach, T. and Koeffler, H. P. (2007) 'Discovery of epigenetically silenced genes in acute myeloid leukemias.', *Leukemia : Official Journal of the Leukemia Society of America, Leukemia Research Fund, U.K*, 21(5), pp. 1026–34. doi: 10.1038/sj.leu.2404611.

Egeblad, M., Rasch, M. G. and Weaver, V. M. (2010) 'Evolution', *Current Opinion in Cell Biology*, 22(5), pp. 697–706. doi: 10.1016/j.ceb.2010.08.015.

Elliott, R. L. and Blobe, G. C. (2005) 'Role of transforming growth factor β in human cancer', *Journal of Clinical Oncology*, 23(9), pp. 2078–2093. doi: 10.1200/JCO.2005.02.047.

Fang, M., Yuan, J. P., Peng, C. W., Pang, D. W. and Li, Y. (2013) 'Quantum dots-based in situ molecular imaging of dynamic changes of collagen IV during cancer invasion', *Biomaterials*. Elsevier Ltd, 34(34), pp. 8708–8717. doi: 10.1016/j.biomaterials.2013.07.069.

Fang, M., Yuan, J., Peng, C. and Li, Y. (2014) 'Collagen as a double-edged sword in tumour progression', *Tumour Biology*, 35(4), pp. 2871–2882. doi: 10.1007/s13277-013-1511-7.

Fessler, J. H. and Fessler, L. I. (1989) 'Drosophila extracellular matrix', *Annual Review Cell Biology*, 5, pp. 309–339.

Frazier, K. S. and Grotendorst, G. R. (1997) 'Expression of connective tissue growth factor mRNA in the fibrous stroma of mammary tumours', *International Journal of Biochemical Cell Biology*, 29(1), pp. 153–161.

Gotenstein, J. R., Swale, R. E., Fukuda, T., Wu, Z., Giurumescu, C. a, Goncharov, A., Jin, Y. and Chisholm, A. D. (2010) 'The C. elegans peroxidasin PXN-2 is essential for embryonic morphogenesis and inhibits adult axon regeneration.', *Development (Cambridge, England)*, 137(21), pp. 3603–13. doi: 10.1242/dev.049189.

Haraguchi, M. (2009) 'The role of the transcriptional regulator snail in cell detachment, reattachment and migration', *Cell Adhesion and Migration*, 3(3), pp. 259–263.

Haraguchi, M., Okubo, T., Miyashita, Y., Miyamoto, Y., Hayashi, M., Crotti, T. N., McHugh, K. P. and Ozawa, M. (2008) 'Snail regulates cell-matrix adhesion by regulation of the expression of integrins and basement membrane proteins', *Journal of Biological Chemistry*, 283(35), pp. 23514–23523. doi: 10.1074/jbc.M801125200.

Harris, S. L. and Levine, A. J. (2005) 'The p53 pathway: Positive and negative feedback loops', *Oncogene*, 24(17), pp. 2899–2908. doi: 10.1038/sj.onc.1208615.

Hazelbag, S., Gorter, A., Kenter, G. G., van den Broek, L. and Fleuren, G. (2002) 'Transforming Growth Factor- β1 Induces Tumour Stroma and Reduces Tumour Infiltrate in Cervical Cancer', *Human Pathology*, 33(12), pp. 1193–1199. doi: 10.1053/hupa.2002.130109.

Hemavathy, K., Ashraf, S. I. and Ip, Y. T. (2000) 'Snail/slug family of repressors: slowly going into the fast lane of development and cancer.', *Gene*, 257(1), pp. 1–12. doi: 10.1016/S0378-1119(00)00371-1.

Homma, S., Shimada, T., Hikake, T. and Yaginuma, H. (2009) 'Expression pattern of LRR and Ig domain-containing protein (LRRIG protein) in the early mouse embryo', *Gene Expression Patterns*. Elsevier B.V., 9(1), pp. 1–26. doi: 10.1016/j.gep.2008.09.004.

Horikoshi, N., Cong, J., Kley, N. and Shenk, T. (1999) 'Isolation of differentially

expressed cDNAs from p53-dependent apoptotic cells: activation of the human homologue of the Drosophila peroxidasin gene.', *Biochemical and Biophysical Research Communications*, 261(3), pp. 864–9. doi: 10.1006/bbrc.1999.1123.

Huber, M. A., Kraut, N. and Beug, H. (2005) 'Molecular requirements for epithelial – mesenchymal transition during tumour progression', *Current Opinion in Cell Biology*, 17, pp. 548–558. doi: 10.1016/j.ceb.2005.08.001.

Hutchins, J. T., Deans, R. J., Mitchell, M. S., Uchiyama, C. and Kan-Mitchell, J. (1991) 'Novel gene sequences expressed by human melanoma cells identified by molecular subtraction.', *Cancer Research*, 51(5), pp. 1418–25. Available at: http://www.ncbi.nlm.nih.gov/pubmed/1997180.

Ikeda, K., Iyama, K., Ishikawa, N., Egami, H., Nakao, M., Sado, Y., Ninomiya, Y. and Baba, H. (2006) 'Loss of Expression of Type IV Collagen α5 and α6 Chains in Colorectal Cancer Associated with the Hypermethylation of Their Promoter Region', *The American Journal of Pathology*, 168(3), pp. 856–865. doi: 10.2353/ajpath.2006.050384.

Ingber, D. E. (2002) 'Cancer as a disease of epithelial-mesenchymal interactions and extracellular matrix regulation.', *Differentiation; Research in Biological Diversity*, 70(9–10), pp. 547–60. doi: 10.1046/j.1432-0436.2002.700908.x.

Ioachim, E., Charchanti, A., Briasoulis, E., Karavasilis, V. and Tsanou, H. (2002) 'Immunohistochemical expression of extracellular matrix components tenascin , fibronectin , collagen type IV and laminin in breast cancer : their prognostic value and role in tumour invasion and progression', *European Journal of Cancer*, 38, pp. 2362–2370.

Ivanov, S. V, Ivanova, A. V, Salnikow, K., Timofeeva, O., Subramaniam, M. and Lerman, M. I. (2008) 'Two novel VHL targets, TGFBI (BIGH3) and its transactivator KLF10, are up-regulated in renal clear cell carcinoma and other tumours', *Biochemical*

and Biophysical Research Communications, 370(4), pp. 536–540. doi: 10.1109/TMI.2012.2196707.Separate.

Jakowlew, S. B. (2006) 'Transforming growth factor-β in cancer and metastasis.', *Cancer Metastasis Reviews*, 25(3), pp. 435–57. doi: 10.1007/s10555-006-9006-2.

Jayachandran, A., McKeown, S. J., Woods, B. L., Prithviraj, P. and Cebon, J. (2015) 'Embryonic Chicken Transplantation is a Promising Model for Studying the Invasive Behavior of Melanoma Cells', *Frontiers in Oncology*, 5(February), pp. 1–7. doi: 10.3389/fonc.2015.00036.

Jayachandran, A., Prithviraj, P., Lo, P.-H., Walkiewicz, M., Anaka, M., Woods, B. L., Tan, B., Behren, A., Cebon, J., McKeown, S. J. (2016) 'Identifying and targeting determinants of melanoma cellular invasion', *Oncotarget*, 7(27), pp. 41186–41202. doi: 10.18632/oncotarget.9227.

Jiang, J., Tang, Y. and Liang, X. (2011) 'A new vision of hypoxia promoting cancer progression', *Cancer Biology & Therapy*, 11(8), pp. 714–723. doi: 10.4161/cbt.11.8.15274.

Jozkowicz, A., Was, H. and Dulak, J. (2007) 'Oxygenase-1 in Tumours : Is It a False Friend?', *Antioxid Redox Signal.*, 9(12), pp. 2099–2117. doi: 10.1089/ars.2007.1659.

Justus, C. R., Leffler, N., Ruiz-Echevarria, M. and Yang, L. V. (2014) 'In vitro Cell Migration and Invasion Assays', *Journal of Visualized Experiments*, (88), pp. 1–8. doi: 10.3791/51046.

Kalluri, R. and Weinberg, R. A. (2009) 'The basics of epithelial-mesenchymal transition', *The Journal of Clinical Investigation*, 119(6), pp. 1420–1428. doi: 10.1172/JCI39104.1420.

Kaminski, K. a, Bonda, T. a, Korecki, J. and Musial, W. J. (2002) 'Oxidative stress and

neutrophil activation--the two keystones of ischemia/reperfusion injury.', *International j Journal of Cardiology*, 86(1), pp. 41–59. doi: 10.1016/S0167-5273(02)00189-4.

Kang, S. H., Won, K., Chung, H. W., Jong, H. S., Song, Y. S., Kim, S. J., Bang, Y. J. and Kim, N. K. (1998) 'Genetic integrity of transforming growth factor beta (TGF-β) receptors in cervical carcinoma cell lines: loss of growth sensitivity but conserved transcriptional response to TGF-beta.', *International Journal of Cancer. Journal International du Cancer*, 77(4), pp. 620–5. Available at: http://www.ncbi.nlm.nih.gov/pubmed/9679767.

Kataoka, H., Murayama, T., Yokode, M., Mori, S., Sano, H., Ozaki, H., Yokota, Y., Nishikawa, S. and Kita, T. (2000) 'A novel snail-related transcription factor Smuc regulates basic helix-loop-helix transcription factor activities via specific E-box motifs.', *Nucleic Acids Research*, 28(2), pp. 626–33. doi: 10.1093/nar/28.2.626.

Khan, K., Rudkin, A., Parry, D. a, Burdon, K. P., McKibbin, M., Logan, C. V, Abdelhamed, Z. I. a, Muecke, J. S., Fernandez-Fuentes, N., Laurie, K. J., Shires, M., Fogarty, R., Carr, I. M., Poulter, J. a, Morgan, J. E., Mohamed, M. D., Jafri, H., Raashid, Y., Meng, N., Piseth, H., Toomes, C., Casson, R. J., Taylor, G. R., Hammerton, M., Sheridan, E., Johnson, C. a, Inglehearn, C. F., Craig, J. E. and Ali, M. (2011) 'Homozygous mutations in PXDN cause congenital cataract, corneal opacity, and developmental glaucoma.', *American Journal of Human Genetics*. The American Society of Human Genetics, 89(3), pp. 464–73. doi: 10.1016/j.ajhg.2011.08.005.

Khoshnoodi, J., Pedchenko, V. and Hudson, B. G. (2008) 'Mammalian Collagen IV', *Microscopy Research and Technique*, 71, pp. 357–370. doi: 10.1002/jemt.20564.

Kim, J. A., Tan, Y., Wang, X., Cao, X., Veeraraghavan, J., Liang, Y., Edwards, D. P., Huang, S., Pan, X., Li, K., Schiff, R. and Wang, X. S. (2016) 'Comprehensive functional analysis of the tousled-like kinase 2 frequently amplified in aggressive luminal breast

cancers', *Nature Communications*. Nature Publishing Group, 7, pp. 1–17. doi: 10.1038/ncomms12991.

Kloth, J. N., Fleuren, G. J., Oosting, J., de Menezes, R. X., Eilers, P. H. C., Kenter, G. G. and Gorter, A. (2005) 'Substantial changes in gene expression of Wnt, MAPK and TNFalpha pathways induced by TGF-beta1 in cervical cancer cell lines.', *Carcinogenesis*, 26(9), pp. 1493–502. doi: 10.1093/carcin/bgi110.

Kudo-Saito, C., Shirako, H., Takeuchi, T. and Kawakami, Y. (2009) 'Cancer Metastasis Is Accelerated through Immunosuppression during Snail-Induced EMT of Cancer Cells', *Cancer Cell*. Elsevier Ltd, 15(3), pp. 195–206. doi: 10.1016/j.ccr.2009.01.023.

Lamouille, S., Xu, J. and Derynck, R. (2014) 'Molecular mechanisms of epithelial-mesenchymal transition.', *National Review Molecular Cell Biology*, 15(3), pp. 178–196. doi: 10.1038/nrm3758.

Lázár, E., Péterfi, Z., Sirokmány, G., Kovács, H. A., Klement, E., Medzihradszky, K. F. and Geiszt, M. (2015) 'Structure-function analysis of peroxidasin provides insight into the mechanism of collagen IV cross-linking', *Free Radical Biology and Medicine*, 83, pp. 273–282. doi: 10.1016/j.freeradbiomed.2015.02.015.

Lee, K. and Nelson, C. M. (2012) *New Insights into the Regulation of Epithelial – Mesenchymal Transition and Tissue Fibrosis*. 1st edn, *International Review Of Cell and Molecular Biology*. 1st edn. Elsevier Inc. doi: 10.1016/B978-0-12-394305-7.00004-5.

Lee, M.-Y. and Shen, M.-R. (2012) 'Epithelial-mesenchymal transition in cervical carcinoma.', *American Journal of Translational Research*, 4(1), pp. 1–13. Available at: http://www.ncbi.nlm.nih.gov/pubmed/23190089.

Li, H., Cao, Z., Moore, D. R., Jackson, P. L., Barnes, S., Lambeth, J. D. and Thannickal, V.

J. (2012) 'Microbicidal Activity of Vascular Peroxidase 1 in Human Plasma via Generation of Hypochlorous Acid', *Infection and Immunity*, 80(7), pp. 2528–2537. doi: 10.1128/IAI.06337-11.

Li, H., Cao, Z., Zhang, G., Thannickal, V. J. and Cheng, G. (2012) 'Vascular peroxidase 1 catalyzes the formation of hypohalous acids: characterization of its substrate specificity and enzymatic properties.', *Free Radical Biology & Medicine*. Elsevier, 53(10), pp. 1954–9. doi: 10.1016/j.freeradbiomed.2012.08.597.

Liu, Y., Carson-Walter, E. B., Cooper, A., Winans, B. N., Johnson, M. D. and Walter, K. a (2010) 'Vascular gene expression patterns are conserved in primary and metastatic brain tumours.', *Journal of Neuro-Oncology*, 99(1), pp. 13–24. doi: 10.1007/s11060-009-0105-0.

Lohr, M., Schmidt, C., Kluth, M., Mu, P., Nizze, H. and Jesnowski, R. (2001) 'Transforming Growth Factor- β1 Induces Desmoplasia in an Experimental Model of Human Pancreatic Carcinoma 1', *Cancer Research*, pp. 550–555.

Ma, C., Rong, Y., Radiloff, D. R., Datto, M. B., Centeno, B., Bao, S., Cheng, A. W. M., Lin, F., Jiang, S., Yeatman, T. J. and Wang, X. F. (2008) 'Extracellular matrix protein betaig-h3/TGFBI promotes metastasis of colon cancer by enhancing cell extravasation', *Genes and Development*, 22(3), pp. 308–321. doi: 10.1101/gad.1632008.

Ma, Q., Zhang, G. and Peng, J. (2013) 'Review article Vascular Peroxidase 1 : a Novel Enzyme in Promoting Oxidative Stress in Cardiovascular System', *Trends in Cardiovascular Medicine*. Elsevier, 23(5), pp. 179–183. doi: 10.1016/j.tcm.2012.11.002.

Maliekal, T. T., Anto, R. J. and Karunagaran, D. (2004) 'Differential activation of Smads in HeLa and SiHa cells that differ in their response to transforming growth factor-β', *Journal of Biological Chemistry*, 279(35), pp. 36287–36292. doi: 10.1074/jbc.M404568200.

Maragoudakis, M. E., Missirlis, E., Karakiulakis, G. D., Sarmonica, M., Bastakis, M. and Tsopanoglou, N. (1993) 'Basement membrane biosynthesis as a target for developing inhibitors of angiogenesis with anti-tumour properties', *Kidney International*. Elsevier Masson SAS, 43(1), pp. 147–150. doi: 10.1038/ki.1993.24.

Meyer, K. J., Axelsen, M., Sheffield, V. C., Patil, S. R. and Wassink, T. H. (2012) 'Germline mosaic transmission of a novel duplication of PXDN and MYT1L to two male half-siblings with autism Kacie', *Psychiatric Genetics*, 22(3), pp. 137–140. doi: 10.1097/YPG.0b013e32834dc3f5.Germline.

Miles, A. J., Skubitz, A. P. N., Furcht, L. T. and Fields, G. B. (1994) 'Promotion of cell adhesion by single-stranded and triple-helical peptide models of basement memby dependent and conformationally independent type IV collagen cell adhesionrane collagen α1(IV)531-543.', *Journal of Biological Chemistry*, 269(49), pp. 30939–30945.

Mitchell, M. S., Kan-mitchell, J., Minev, B., Edman, C. and Deans, R. J. (2000) 'A Novel Melanoma Gene (MG50) A Novel Melanoma Gene (MG50) Encoding the Interleukin 1 Receptor Antagonist and Six Epitopes Recognized by Human Cytolytic T Lymphocytes', *Cancer Research*, 60, pp. 6448–6456.

Miyoshi, A., Kitajima, Y., Kido, S., Shimonishi, T., Matsuyama, S., Kitahara, K. and Miyazaki, K. (2005) 'Snail accelerates cancer invasion by upregulating MMP expression and is associated with poor prognosis of hepatocellular carcinoma.', *British Journal of Cancer*, 92(2), pp. 252–8. doi: 10.1038/sj.bjc.6602266.

Moustakas, A. and Heldin, C. H. (2007) 'Signaling networks guiding epithelial-mesenchymal transitions during embryogenesis and cancer progression', *Cancer Science*, 98(10), pp. 1512–1520. doi: 10.1111/j.1349-7006.2007.00550.x.

Naber, H. P. H., Drabsch, Y., Snaar-Jagalska, B. E., ten Dijke, P. and van Laar, T. (2013)

'Snail and Slug, key regulators of TGF-??-induced EMT, are sufficient for the induction of single-cell invasion', *Biochemical and Biophysical Research Communications*. Elsevier Inc., 435(1), pp. 58–63. doi: 10.1016/j.bbrc.2013.04.037.

Nelson, R. E., Fessler, L. I., Takagi, Y., Blumberg, B., Keene, D. R., Olson, P. F., Parker, C. G. and Fessler, J. H. (1994) 'Peroxidasin: a novel enzyme-matrix protein of Drosophila development.', *The EMBO journal*, 13(15), pp. 3438–47. Available at: http://www.pubmedcentral.nih.gov/articlerender.fcgi?artid=395246&tool=pmcentrez&rendertype=abstract.

Nieto, M. A. (2002) 'The snail superfamily of zinc-finger transcription factors.', *Nature Reviews. Molecular Cell Biology*, 3(March), pp. 155–166. doi: 10.1038/nrm757.

Nihei, S. I., Yamashita, K., Tasaki, H., Ozumi, K. and Nakashima, Y. (2005) 'Oxidized low-density lipoprotein-induced apoptosis is attenuated by insulin-activated phosphatidylinositol 3-kinase/Akt through p38 mitogen-activated protein kinase', *Clinical and Experimental Pharmacology and Physiology*, 32(3), pp. 224–229. doi: 10.1111/j.1440-1681.2005.04177.x.

O'Brien, P. J. (2000) 'Peroxidases.', *Chemico-biological interactions*, 129(1–2), pp. 113–139. doi: 10.1016/S0009-2797(00)00201-5.

Öhlund, D., Franklin, O., Lundberg, E., Lundin, C. and Sund, M. (2013) 'Type IV collagen stimulates pancreatic cancer cell proliferation, migration, and inhibits apoptosis through an autocrine loop', *BMC Cancer*, 13. doi: 10.1186/1471-2407-13-154.

Park, S.-W., Bae, J.-S., Kim, K.-S., Park, S.-H., Lee, B.-H., Choi, J.-Y., Park, J.-Y., Ha, S.-W., Kim, Y.-L., Kwon, T.-H., Kim, I.-S. and Park, R.-W. (2004) 'Beta ig-h3 promotes renal proximal tubular epithelial cell adhesion, migration and proliferation through the interaction with alpha3beta1 integrin.', *Experimental & Molecular Medicine*, 36(3), pp.

211–9. doi: 10.1038/emm.2004.29.

Peinado, H., Ballestar, E., Esteller, M. and Cano, A. (2004) 'Snail mediates E-cadherin repression by the recruitment of the Sin3A/histone deacetylase 1 (HDAC1)/HDAC2 complex.', *Molecular and Cellular Biology*, 24(1), pp. 306–19. doi: 10.1128/MCB.24.1.306.

Peinado, H., Olmeda, D. and Cano, A. (2007) 'Snail, Zeb and bHLH factors in tumour progression: an alliance against the epithelial phenotype?', *Nature Reviews Cancer*, 7(6), pp. 415–428. doi: 10.1038/nrc2131.

Peinado, H., Quintanilla, M. and Cano, A. (2003) 'Transforming growth factor beta-1 induces Snail transcription factor in epithelial cell lines', *Journal of Biological Chemistry*, 278(23), pp. 21113–21123. doi: 10.1074/jbc.M211304200.

Persengiev, S. P., Zhu, X. and Green, M. R. (2004) 'Nonspecific, concentration-dependent stimulation and repression of mammalian gene expression by small interfering RNAs (siRNAs)', *Rna*, 10(1), pp. 12–8. doi: 10.1261/rna5160904.RNAi.

Péterfi, Z., Donkó, A., Orient, A., Sum, A., Prókai, A., Molnár, B., Veréb, Z., Rajnavölgyi, E., Kovács, K. J., Müller, V., Szabó, A. J. and Geiszt, M. (2009) 'Peroxidasin is secreted and incorporated into the extracellular matrix of myofibroblasts and fibrotic kidney.', *The American Journal of Pathology*, 175(2), pp. 725–35. doi: 10.2353/ajpath.2009.080693.

Péterfi, Z. and Geiszt, M. (2014) 'Peroxidasins: Novel players in tissue genesis', *Trends in Biochemical Sciences*, 39(7), pp. 305–307. doi: 10.1016/j.tibs.2014.05.005.

Petitclerc, E., Boutaud, A., Prestayko, A., Xu, J., Sado, Y., Ninomiya, Y., Sarras, M. P., Hudson, B. G. and Brooks, P. C. (2000) 'New Functions for Non-collagenous Domains of Human Collagen Type IV', *The Journal of Biological Chemistry*, 275(11), pp. 8051–8061.

Poser, I. and Bosserhoff, A. (2004) 'Transcription factors involved in', *Histology and Histopathology*, 19, pp. 173–188.

Radisky, D. C. (2005) 'Epithelial-mesenchymal transition.', *Journal of Cell Science*, 118(Pt 19), pp. 4325–6. doi: 10.1242/jcs.02552.

Safina, A., Vandette, E. and Bakin, A. V. (2007) 'ALK5 promotes tumour angiogenesis by upregulating matrix metalloproteinase-9 in tumour cells', *Oncogene*, 26(17), pp. 2407–2422. doi: 10.1038/sj.onc.1210046.

Scanlon, C. S., Van Tubergen, E. A., Inglehart, R. C. and D'Silva, N. J. (2013) 'Biomarkers of epithelial-mesenchymal transition in squamous cell carcinoma', *Journal of Dental Research*, 92(2), pp. 114–121. doi: 10.1177/0022034512467352.

Schwab, M. (2011) *Encyclopedia of Cancer*, *Encyclopedia of Cancer*. doi: 10.1016/B0-12-227555-1/00151-9.

Shang, D., Liu, Y., Yang, P., Chen, Y. and Tian, Y. (2012) 'TGFBI-promoted adhesion, migration and invasion of human renal cell carcinoma depends on inactivation of von hippel-lindau tumour suppressor', *Urology*. Elsevier Inc., 79(4), p. 966.e1-966.e7. doi: 10.1016/j.urology.2011.12.011.

Soini, Y., Tuhkanen, H., Sironen, R., Virtanen, I., Kataja, V., Auvinen, P., Mannermaa, A. and Kosma, V.-M. (2011) 'Transcription factors zeb1, twist and snai1 in breast carcinoma', *BMC Cancer*, 11(1), p. 73. doi: 10.1186/1471-2407-11-73.

Soulitzis, N., Karyotis, I., Delakas, D. and Spandidos, D. A. (2006) 'Expression analysis of peptide growth factors VEGF, FGF2, TGFB1, EGF and IGF1 in prostate cancer and benign prostatic hyperplasia', *International Journal of Oncology*, 29(2), pp. 305–314.

Stahl, P. J. and Felsen, D. (2001) 'Transforming Growth Factor-β, Basement Membrane, and Epithelial-Mesenchymal Transdifferentiation', *The American Journal of Pathology*, 159(4), pp. 1187–1192. doi: 10.1016/S0002-9440(10)62503-5.

Tanjore, H. and Kalluri, R. (2006) 'The role of type IV collagen and basement membranes in cancer progression and metastasis', *American Journal of Pathology*, 168(3), pp. 715–717. doi: 10.2353/ajpath.2006.051321.

Tauber, S., Jais, A., Jeitler, M., Haider, S., Husa, J., Lindroos, J., Knöfler, M., Mayerhofer, M., Pehamberger, H., Wagner, O. and Bilban, M. (2010) 'Transcriptome analysis of human cancer reveals a functional role of heme oxygenase-1 in tumour cell adhesion.', *Molecular Cancer*, 9, p. 200. doi: 10.1186/1476-4598-9-200.

Thacker, P. C. and Karunagaran, D. (2015) 'Curcumin and emodin down-regulate TGF-β signaling pathway in human cervical cancer cells', *PLoS ONE*, 10(3), pp. 1–27. doi: 10.1371/journal.pone.0120045.

Theis, M. and Buchholz, F. (2011) 'High-throughput RNAi screening in mammalian cells with esiRNAs', *Methods*. Elsevier Inc., 53(4), pp. 424–429. doi: 10.1016/j.ymeth.2010.12.021.

Thiery, J. P., Acloque, H., Huang, R. Y. J. and Nieto, M. A. (2009) 'Epithelial-Mesenchymal Transitions in Development and Disease', *Cell*, 139(5), pp. 871–890. doi: 10.1016/j.cell.2009.11.007.

Tindall, A. J., Pownall, M. E., Morris, I. D. and Isaacs, H. V. (2005) 'Xenopus tropicalis peroxidasin gene is expressed within the developing neural tube and pronephric kidney', *Developmental Dynamics*, 232(2), pp. 377–384. doi: 10.1002/dvdy.20226.

Tschuch, C., Schulz, A., Pscherer, A., Werft, W., Benner, A., Hotz-Wagenblatt, A.,

Barrionuevo, L. S., Lichter, P. and Mertens, D. (2008) 'Off-target effects of siRNA specific for GFP', *BMC Molecular Biology*, 9, pp. 1–14. doi: 10.1186/1471-2199-9-60.

Vanacore, R. (2009) 'A Sulfilimine Bond Identified in collagen IV', *Science*, 325, pp. 1230–1233. doi: 10.1126/science.1176811.

Vandewalle, C., Comijn, J., De Craene, B., Vermassen, P., Bruyneel, E., Andersen, H., Tulchinsky, E., Van Roy, F. and Berx, G. (2005) 'SIP1/ZEB2 induces EMT by repressing genes of different epithelial cell-cell junctions', *Nucleic Acids Research*, 33(20), pp. 6566–6578. doi: 10.1093/nar/gki965.

Vetter, G., Béchec, A. Le, Muller, J., Muller, A., Moes, M., Yatskou, M., Tanoury, Z. Al, Poch, O., Vallar, L. and Friederich, E. (2009) 'Time-resolved analysis of transcriptional events during SNAI1-triggered epithelial to mesenchymal transition', *Biochemical and Biophysical Research Communications*. Elsevier Inc., 385(4), pp. 485–491. doi: 10.1016/j.bbrc.2009.05.025.

Wang, H., Radjendirane, V., Wary, K. K. and Chakrabarty, S. (2004) 'Transforming growth factor β regulates cell-cell adhesion through extracellular matrix remodeling and activation of focal adhesion kinase in human colon carcinoma Moser cells', *Oncogene*, 23(32), pp. 5558–5561. doi: 10.1038/sj.onc.1207701.

Wang, Y., Shi, J., Chai, K., Ying, X. and Zhou, B. P. (2013) 'The Role of Snail in EMT and Tumourigenesis.', *Current Cancer Drug Targets*, 13(9), pp. 963–72. doi: CCDT-EPUB-57089 [pii].

Ween, M. P., Oehler, M. K. and Ricciardelli, C. (2012) 'Transforming growth factor-beta-induced protein (TGFBI)/(βig-H3): A matrix protein with dual functions in ovarian cancer', *International Journal of Molecular Sciences*, 13(8), pp. 10461–10477. doi: 10.3390/ijms130810461.

Weiler, S. R., Taylor, S. M., Deans, R. J., Kan-Mitchell, J., Mitchell, M. S. and Trent, J. M. (1994) 'Assignment of a Human Melanoma Associated Gene MG50 (D2S448) to Chromosome 2p25.3 by Fluorescence in Situ Hybridization', *Genomics*, 22(1), pp. 243–244.

Weiss, A. and Attisano, L. (2013) 'The TGFβ superfamily signaling pathway', *Wiley Interdisciplinary Reviews: Developmental Biology*, 2(1), pp. 47–63. doi: 10.1002/wdev.86.

Weiss, S. J. (2012) 'Peroxidasin: tying the collagen-sulfilimine knot.', *Nature Chemical Biology*. Nature Publishing Group, 8(9), pp. 740–1. doi: 10.1038/nchembio.1050.

Wells, R. G. (2002) 'Collagen and other extracellular matrix proteins ECM proteins in the fibrotic liver: Structure and key features of specific ECM proteins', 100, pp. 264–273.

Wen, G., Partridge, M. A., Li, B., Hong, M., Liao, W., Cheng, S. K., Calaf, G. M., Zhou, J., Zhang, Z., Shah, A. and Hei, T. K. (2011) 'TGFBI Expression Reduces In Vitro and In Vivo Metastatic Potential of Lung and Breast Tumour Cells', *Cancer Letters*, 308(1), pp. 23–32. doi: 10.1016/j.canlet.2011.04.010.TGFBI.

Whiteman, E. L., Liu, C.-J., Fearon, E. R. and Margolis, B. (2008) 'The transcription factor snail represses Crumbs3 expression and disrupts apico-basal polarity complexes.', *Oncogene*, 27(27), pp. 3875–9. doi: 10.1038/onc.2008.9.

Xu, F., Sun, Y., Chen, Y., Sun, Y., Li, R., Liu, C., Zhang, C., Wang, R. and Zhang, Y. (2009) 'Endothelial cell apoptosis is responsible for the formation of coronary thrombotic atherosclerotic plaques.', *Tohoku J Exp Med*, 218(1), pp. 25–33. doi: 10.1620/tjem.218.25.

Xu, Y., Zhao, Y., Su, B., Chen, Y. and Zhou, C. (2006) 'Expression of Collagen IV, Fibronectin, Laminin in non-small cell lung cancer and its correlation with

chemosensitivities and apoptosis', *Chinese-German Journal of Clinical Oncology*, 5(1), pp. 58–62. doi: 10.1007/s10330-005-0440-3.

Yan, X., Sabrautzki, S., Horsch, M., Fuchs, H., Gailus-Durner, V., Beckers, J., de Angelis, M. H. and Graw, J. (2014) 'Peroxidasin is essential for eye development in the mouse', *Human Molecular Genetics*, 23(21), pp. 5597–5614. doi: 10.1093/hmg/ddu274.

Yang, J. and Weinberg, R. A. (2008) 'Epithelial-Mesenchymal Transition: At the Crossroads of Development and Tumour Metastasis', *Developmental Cell*, 14(6), pp. 818–829. doi: 10.1016/j.devcel.2008.05.009.

Yang, Y., Cao, Z., Tian, L., Garvey, W. T. and Cheng, G. (2013) 'VPO1 mediates ApoE oxidation and impairs the clearance of plasma lipids.', *PloS one*, 8(2), p. e57571. doi: 10.1371/journal.pone.0057571.

Yang, Y., Xing, Y., Liang, C., Hu, L., Xu, F. and Mei, Q. (2016) 'An examination of the regulatory mechanism of Pxdn mutation-induced eye disorders using microarray analysis', *International Journal of Molecular Medicine*, 37(6), pp. 1449–1456. doi: 10.3892/ijmm.2016.2572.

Yi, J. Y., Hur, K. C., Lee, E., Jin, Y. J., Arteaga, C. L. and Son, Y. S. (2002) 'TGFbeta1 - mediated epithelial to mesenchymal transition is accompanied by invasion in the SiHa cell line.', *European Journal of Cell Biology*, 81(8), pp. 457–68. Available at: http://www.ncbi.nlm.nih.gov/pubmed/12234017.

Young, C. D., Zimmerman, L. J., Hoshino, D., Formisano, L., Hanker, A. B., Gatza, M. L., Morrison, M. M., Moore, P. D., Whitwell, C. A., Dave, B., Stricker, T., Bhola, N. E., Silva, G. O., Patel, P., Brantley-Sieders, D. M., Levin, M., Horiates, M., Palma, N. A., Wang, K., Stephens, P. J., Perou, C. M., Weaver, A. M., O'Shaughnessy, J. A., Chang, J. C., Park, B. H., Liebler, D. C., Cook, R. S. and Arteaga, C. L. (2015) 'Activating *PIK3CA*

Mutations Induce an Epidermal Growth Factor Receptor (EGFR)/Extracellular Signal-regulated Kinase (ERK) Paracrine Signaling Axis in Basal-like Breast Cancer', *Molecular & Cellular Proteomics*, 14(7), pp. 1959–1976. doi: 10.1074/mcp.M115.049783.

Zamocky, M., Jakopitsch, C., Furtmüller, P. G., Dunand, C. and Obinger, C. (2008) 'The peroxidase-cyclooxygenase superfamily: Reconstructed evolution of critical enzymes of the innate immune system.', *Proteins*, 72(2), pp. 589–605. doi: 10.1002/prot.21950.

Zavadil, J. and Böttinger, E. P. (2005) 'TGF-β and epithelial-to-mesenchymal transitions', *Oncogene*, 24(37), pp. 5764–5774. doi: 10.1038/sj.onc.1208927.

Zavadil, J., Haley, J., Kalluri, R., Muthuswamy, S. K. and Thompson, E. (2008) 'Epithelial-mesenchymal transition', *Cancer Research*, 68(23), pp. 9574–9577. doi: 10.1158/0008-5472.CAN-08-2316.

Zeisberg, M., Bonner, G., Maeshima, Y., Colorado, P., Muöller, G. A., Strutz, F. and Kalluri, R. (2001) 'Collagen composition and assembly regulates epithelial-mesenchymal transdifferentiation', *American Journal of Pathology*, 159(4), pp. 1313–1321. doi: 10.1016/S0002-9440(10)62518-7.

Zeisberg, M. and Neilson, E. G. (2009) 'Biomarkers for epithelial-mesenchymal transitions.', *The Journal of Clinical Investigation*. American Society for Clinical Investigation, 119(6), pp. 1429–37. doi: 10.1172/JCI36183.

Zhang, Y.-S., He, L., Liu, B., Li, N.-S., Luo, X.-J., Hu, C.-P., Ma, Q.-L., Zhang, G.-G., Li, Y.-J. and Peng, J. (2012) 'A novel pathway of NADPH oxidase/vascular peroxidase 1 in mediating oxidative injury following ischemia-reperfusion.', *Basic Research in Cardiology*, 107, p. 266. doi: 10.1007/s00395-012-0266-4.

Zhao, Y. L., Piao, C. Q. and Hei, T. K. (2002) 'Overexpression of βig-h3 gene

downregulates integrin α5β1 and suppresses tumourigenicity in radiation-induced tumourigenic human bronchial epithelial cells', *British Journal of Cancer*, 86(12), pp. 1923–1928. doi: 10.1038/sj.bjc.6600304.

Zhen, X. (2003) 'TGF- β 1 -promoted epithelial-to-mesenchymal transformation and cell ad- hesion contribute to TGF- β 1 -enhanced cell migration in SMMC-7721 cells' *Cell Research*, 13(5), pp. 343–350.

Appendix A

Original publication:

Peroxidasin is regulated by the epithelial-mesenchymal transition master transcription factor Snai1

Boitumelo Nonhlanhla Sitole (nee Moleya), Demetra Mavri-Damelin

The School of Molecular and Cell Biology, University of the Witwatersrand, Johannesburg, South Africa

Gene 646 (2018) 195–202

Contents lists available at ScienceDirect

Gene

journal homepage: www.elsevier.com/locate/gene

Research paper

Peroxidasin is regulated by the epithelial-mesenchymal transition master transcription factor Snai1

Boitumelo Nonhlanhla Sitole, Demetra Mavri-Damelin*

The School of Molecular and Cell Biology, University of the Witwatersrand, Johannesburg, South Africa

ARTICLE INFO

Keywords:
Snai1
Peroxidasin
Epithelial-mesenchymal transition
VPO1
Cancer
Fibrosis

ABSTRACT

Peroxidasin (PXDN), an ECM protein with peroxidase activity, is integral to basement membrane consolidation through catalysis of sulfilimine bonds in collagen IV. PXDN is also involved in processes where epithelial-mesenchymal transition (EMT) takes place, namely fibrosis, development and cancer. We therefore investigated whether PXDN is regulated by the EMT-master-regulator, Snai1. During TGF-β1-induced EMT, PXDN expression decreased by up to 47% in two cervical-carcinoma cell lines, with concomitant increases in Snai1 and vimentin, and decrease in E-cadherin. TGF-β1 induced Snai1 binding to the *PXDN* promoter (as assessed by chromatin immunoprecipitation-PCR) and significantly repressed luciferase reporter gene expression, as did Snai1 overexpression. In summary, our findings show that Snai1 mediates repression of *PXDN* and consolidate a role for this ECM-modifier during EMT.

1. Introduction

Peroxidasin (PXDN) was first identified in *Drosophila melanogaster* as an extracellular matrix (ECM)-associated peroxidase expressed by head mesoderm-derived haemocytes, where it was suggested to play a role in several important biological processes including apoptosis and consolidation of the ECM through dityrosine bridge formation (Nelson et al., 1994). Since then PXDN has been classified as a member of the haem peroxidase-cyclooxygenase superfamily and is predominantly expressed in the vascular system (O'Brien, 2000; Cheng et al., 2008; Shi et al., 2011). Similar to other family members, such as myeloperoxidase, PXDN carries out the enzymatic oxidation of substrates in the presence of hydrogen peroxide and, through the generation of hypohalous acids, PXDN is thought to be involved in host defence mechanisms (Davies et al., 2008; Zamocky et al., 2008; Chandler and Day, 2012; Gaut et al., 2001; Cheng et al., 2011; Li et al., 2012; Paumann-Page et al., 2017). One example of this function is in the vascular system where PXDN is secreted into the plasma and has been found to contribute to peroxidative reactions by using hydrogen peroxide generated through NADPH-oxidases (Cheng et al., 2011; Zhang et al., 2012). However, PXDN differs from its peroxidase family counterparts in that in addition to the enzymatic peroxidase domain, it has domains typical of proteins found in the ECM (Cheng et al., 2008; Byron et al., 2013). In an ECM context, PXDN has been shown to form dityrosine crosslinks and also catalyses sulfilimine bonds, in the presence of hypohalous acids, to connect collagen IV protomers, which are an integral component of the basement membrane (Cheng et al., 2011; Bhave et al., 2012; McCall et al., 2014; Cummings et al., 2016).

Dysregulated PXDN expression and mutations in *PXDN* have been associated with various pathologies that involve epithelial-mesenchymal transition (EMT), namely development, fibrosis and cancer (Khan et al., 2011; Yan et al., 2014; Micheal et al., 2016; Tindall et al., 2005; Gotenstein et al., 2010; Péterfi et al., 2009; Horikoshi et al., 1999; Desmond et al., 2007; Liu et al., 2010; Tauber et al., 2010; Jayachandran et al., 2016). EMT is the process whereby cells lose the epithelial phenotype and transition to a mesenchymal phenotype, which allows for cell movement. (Thiery et al., 2009). In developmental processes, mutations in *PXDN* have been associated with failure of normal eye development resulting in microphthalmia, congenital cataracts, corneal opacity and developmental glaucoma (Khan et al., 2011; Yan et al., 2014; Micheal et al., 2016). Further, the human PXDN equivalent in *Xenopus tropicalis* is expressed during early development in the neural tube and tail and may modify ECM components necessary for morphogenesis (Tindall et al., 2005). In *C. elegans*, the PXDN ortholog PXN-2 is involved in embryonic morphogenesis, basement membrane integrity post-embryonically and attachment of muscle to the epidermis (Gotenstein et al., 2010). In fibrosis, PXDN expression is elevated in human pulmonary and dermal fibroblasts, and in kidney

Abbreviations: DAPI, 4′,6-diamidino-2-phenylindole dihydrochloride; ECM, extracellular matrix; EMT, epithelial-mesenchymal transition; FBS, Fetal Bovine Serum; MET, mesenchymal-epithelial transition; PXDN, Peroxidasin; SFM, serum-free medium; TGF-β1, transforming growth factor-β1

* Corresponding author at: The School of Molecular and Cell Biology, University of the Witwatersrand, Johannesburg, Private Bag X3, WITS 2050, South Africa.
E-mail addresses: boitumelo.moleya@students.wits.ac.za (B.N. Sitole), Demetra.Mavri-Damelin@wits.ac.za (D. Mavri-Damelin).

https://doi.org/10.1016/j.gene.2018.01.011
Received 4 October 2017; Received in revised form 1 December 2017; Accepted 2 January 2018
Available online 03 January 2018
0378-1119/

fibrosis TGF-β1 treated myofibroblasts excessively deposit PXDN into the ECM (Péterfi et al., 2009). PXDN also displays aberrant expression patterns in various cancers (Horikoshi et al., 1999; Desmond et al., 2007; Liu et al., 2010; Tauber et al., 2010; Jayachandran et al., 2016). Exactly how PXDN is involved in the cancer process has yet to be fully elucidated and may be cancer-type specific, with knockdown of PXDN expression causing cell detachment in choriocarcinoma, whilst in melanoma, reduced PXDN correlated with less cell invasion (Tauber et al., 2010; Jayachandran et al., 2016).

Despite these overall relatively few studies, PXDN is clearly involved in processes that feature EMT in their progression. Since there is currently no information on the transcriptional regulators of PXDN, we considered whether the EMT master transcription factor Snai1 may be involved in regulating PXDN gene expression during TGF-β1 induced EMT, using cervical carcinoma cell lines HeLa and SiHa. SiHa cells display more features of EMT upon TGF-β1 induction and is more metastatic in nature than the HeLa cell line (Kloth et al., 2005).

2. Materials and methods

2.1. Reagents

General reagents were from Sigma Aldrich (St Louis, Missouri, USA), unless otherwise stated. Antibodies used were as follows: goat anti-PXDN; rabbit anti-Snai1; rabbit anti-β-actin; donkey anti-goat IgG-FITC; goat anti-rabbit IgG-FITC; donkey anti-goat IgG-HRP; and goat anti-rabbit IgG-HRP (Santa Cruz Biotechnology, Dallas, Texas, USA), rabbit anti-E-cadherin and rabbit anti-vimentin (Cell Signaling Technology, Danvers, Massachusetts, USA).

2.2. Cell culture

SiHa and HeLa human, epithelial, cervical carcinoma cell lines were purchased from ATCC (Manassas, Virginia, USA) and Cellonex (Johannesburg, South Africa), respectively. HEK293 cells were a kind gift from Dr Clement Penny (Faculty of Health Sciences, University of the Witwatersrand, Johannesburg). Cells were cultured in Dulbecco's Modified Eagle's Medium (DMEM)-F12 (3:1) supplemented with 10% Fetal Bovine Serum (FBS) (Lonza Group, Basel, Switzerland), 100 U/ml penicillin/0.1 mg/ml streptomycin and incubated at 37 °C in a humidified 5% CO_2 atmosphere. For TGF-β1 treatments, cells were cultured in low serum (1% FBS) overnight followed by the addition of 5 ng/ml TGF-β1 (recombinant human expressed in CHO cells) for 24 or 48 h.

2.3. Immunofluorescence confocal microscopy

To observe the cellular localization of proteins upon treatment with TGF-β1, confocal immunofluorescence microscopy was performed. Cells were seeded equally on 22 mm glass coverslips and treated as described, after which time cells were fixed with 4% formaldehyde (v/v) in 1 × PBS, for 15 min at room temperature. Cells were then permeabilised with 0.25% Triton X-100 in 1 × PBS and blocked with 0.5% BSA in 1 × PBS for 30 min at room temperature. Following overnight incubation at 4 °C in primary antibody, slides were washed (0.5% BSA in 1 × PBS) and incubated with the corresponding FITC-conjugated secondary antibodies for 1 h. Antibody dilutions were as follows anti-PXDN (1:200), anti-Snai1 (1:200), anti-E-cadherin (1:200), anti-vimentin (1:100), donkey anti-goat IgG-FITC (1:400) and goat anti-rabbit IgG-FITC (1:200). Nuclei were counterstained with (DAPI). Cells were mounted with Fluoromount and slides sealed with clear nail polish. Cells were visualized with a Zeiss LSM 780 confocal microscope at 630 × magnification with Zen 2010 software. Fluorophores were detected at the following wavelengths: FITC-$488_{ex}/525_{em}$ and DAPI-$405_{ex}/454_{em}$. For differential interference contrast (DIC) images to look at cell morphology, cells were grown on coverslips, treated and fixed, as described. Cells were overlaid with 1 × PBS for viewing under bright field using an Olympus BX63 microscope at 10 × magnification.

2.4. Western blot, immunoprecipitation and protein quantification

To quantify protein expression, cells were cultured as described, harvested by washing in cold 1 × PBS and lysed *in situ* using triple detergent lysis buffer (25 mM Tris-HCl, 150 mM NaCl, 0.1% SDS, 1% Triton X-100, 0.5% sodium deoxycholate) with protease inhibitors (1 mM PMSF, 10 μM leupeptin, 10 mM sodium fluoride, 1 mM sodium orthovanadate). Following centrifugation, total protein concentration in the supernatant was determined by the Bramhall assay (Bramhall et al., 1969). Protein (25–40 μg) was resolved on 4–8% SDS polyacrylamide gels for 60 min at 200 V and then electroblotted onto nitrocellulose membrane. Membranes were blocked in 5% fat-free milk powder in TBS-T (Tris-Buffered Saline with 0.1% Tween-20) prior to overnight incubation at 4 °C in primary antibodies as previously mentioned. Following washes in 1 × TBS-T, membranes were incubated for 1 h in the corresponding horseradish peroxidase-linked secondary antibody. Antibody dilutions used were as follows: anti-PXDN (1:200), anti-β-actin (1:1000), anti-Snai1 (1:1000), anti-Vimentin (1:1500), anti-E-cadherin (1:1000), donkey anti-goat IgG (1:5000) and goat anti-rabbit IgG (1:1000). Proteins were detected using chemiluminescence substrate SuperSignal West Pico (Thermo Fisher Scientific, Waltham, Massachusetts, USA) and visualized on X-ray film. Densitometry was performed using Image Studio Lite Software (version 5.2.5).

In order to improve yield of PXDN from total cell protein, PXDN was first immunoprecipitated from cell lysate prior to Western blotting. Cells were lysed in native lysis buffer (25 mM Tris pH 8, 75 mM NaCl, 0.5% Triton X-100) with protease inhibitors, as previously described. Protein was quantified as above and 1 μg anti-PXDN antibody added to 150 μg total protein in order to precipitate PXDN overnight at 4 °C. Samples were then rotated for 4 h at 4 °C with protein A/G-plus agarose beads (Santa Cruz Biotechnology, Dallas, Texas, USA) to bind the immunocomplexes. Pelleted beads were washed with IP buffer (native lysis buffer with 150 mM NaCl) and boiled for 10 min in 4 × denaturing protein-loading buffer, then electrophoresed on a 4–8% SDS polyacrylamide gel, electroblotted onto nitrocellulose and chemiluminescence detected, as described above.

2.5. Chromatin immunoprecipitation

To determine Snai1 interaction with the PXDN gene promoter, chromatin immunoprecipitation (ChIP) followed by PCR was performed. The E-cadherin promoter region served as a positive control as this gene is an established target of Snai1 (Cano et al., 2000; Batlle et al., 2000). Cells were seeded equally in 100 mm dishes and either untreated or treated with TGF-β1 for 24 h. Protein-DNA interactions were cross-linked with 1% formaldehyde for 10 min at room temperature and formaldehyde quenched with 0.12 M glycine. Cells were sonicated to shear chromatin using a Misonix Ultrasonic Liquid Processor XL-2000, 15 pulses for 15 s each, with cooling on ice in between pulses. Following assessment of DNA fragment sizes through agarose gel electrophoresis and quantification using a NanoDrop 1000, DNA (15 μg) was diluted in dilution buffer (1% Triton-X 100, 2 mM EDTA, 20 mM Tris, 150 mM NaCl) with protease inhibitors (1 mM PMSF, 10 μM leupeptin, 10 mM sodium fluoride, 1 mM sodium orthovanadate), and pre-cleared with 20 μl protein A/G plus agarose beads for 1 h. This was then followed by incubation with anti-Snai1 antibody overnight at 4 °C. Protein A/G plus agarose beads were then added to the immunocomplexes with rotation for 1 h at 4 °C and were subsequently pelleted at 1600 × *g*. Pellets were washed three times with wash buffer (0.1% SDS, 1% Triton-X 100, 2 mM EDTA, 20 mM Tris, 150 mM NaCl), once with final wash buffer (0.1% SDS, 1% Triton-X 100, 2 mM EDTA, 20 mM Tris, 500 mM NaCl) and twice with TE buffer (pH 8). Pre-warmed elution buffer (1% SDS, 100 mM $NaHCO_3$) was added to the beads and incubated at 65 °C for 6 h to reverse crosslinks.

Table 1
Primer sets for Snai1 vector, ChIP and luciferase reporter assay constructs.

Region	Primer sequences
pcDNA-Snai1	Forward: 5′ ATCGCTAGCATGCCGCGCTCTTTCCTCG 3′ Reverse: 5′ ATCTGATATCTCAGCGGGGACATCCTGAGCA 3′
ChIP PXDN^{Snai1+}	Forward: 5′ GAACGTTAAATAATTTCCTACGT 3′ Reverse: 5′ GGCGCAGAACAGCACGAGCG 3′
ChIP PXDN^{Snai1-}	Forward: 5′ GTTTGCGACGGGAACACGCC 3′ Reverse: 5′ AAAGCCCCTCATTCCTTTTGAGGA 3′
ChIP[a] E-cadherin^{Snai1+}	Forward: 5′ GGCCGGCAGGTGAAC 3′ Reverse: 5′ GGGCTGGAGTCTGAACTGAC 3′
ChIP E-cadherin^{Snai1-}	Forward: 5′ GCTGGTCAGTGTCAAATGCT 3′ Reverse: 5′ CCTCAGTTTCTCCACCCTCC 3′
Luciferase PXDN^{Snai1+}	Forward: 5′ ATAGCTAGCGAACGTTAAATAATTTCCTACGTGGT 3′ Reverse: 5′ ATTAGATATCGGCGCAGAACAGC ACGAGCG 3′
Luciferase PXDN^{Snai1-}	Forward: 5′ ATAGCTAGCGTTTGCGACGGGAACACGCC 3′ Reverse: 5′ AAAGATATCAAAGCCCCTCATTCCTTTTGAGGA 3′
Luciferase E-cadherin^{Snai1+}	Forward: 5′ ATTTAGCTAGCGGCCGGCAGGTGAAC 3′ Reverse: 5′ TCGTAGATATCGGGCTGGAGTCTGAACTGAC 3′
Luciferase E-cadherin^{Snai1-}	Forward: 5′ ATTTAGCTAGCGCTGGTCAGTGTCAAATGCT 3′ Reverse: 5′ TCGTAGATATCCCTCAGTTTCTCCACCCTCC 3′

[a] Primers from Vandewalle et al. span across three E-boxes in the *E-cadherin* promoter (Vandewalle et al., 2005).

Following protein digestion with 0.1 mg/ml Proteinase K (Thermo Fisher Scientific, Waltham, Massachusetts, USA) for 2 h at 50 °C, DNA was purified using the GeneJet PCR Purification kit (Thermo Fisher Scientific, Waltham, Massachusetts, USA) and analysed by PCR. Two sets of primers were used for each gene promoter (Table 1): one set that amplified across the putative and known Snai1 binding sites (Snai1 +) in the *PXDN* and *E-cadherin* gene promoters, respectively and one set that served as a non-Snai1-containing region (Snai1-) (Vandewalle et al., 2005).

2.6. Snai1 overexpression

A full-length Snai1 expressing pcDNA3.1 vector was constructed by firstly isolating total RNA from HeLa cells using TriZol and a standard phenol-chloroform RNA extraction method. Then mRNA was converted to cDNA using the RevertAid First Strand cDNA synthesis kit (Thermo Fisher Scientific, Waltham, Massachusetts, USA) with the Oligo dT primer, according to the manufacturer's instruction. The full-length Snai1 coding region was amplified by PCR (Table 1) with HiFi high-fidelity DNA polymerase (Kapa Biosystems Inc., Wilmington, Massachusetts, USA) and cloned into a pcDNA3.1 vector (Invitrogen, Carlsbad, California, USA) through the *Nhe*I and *Eco*RV (New England Biosciences, Ipswich, Massachusetts, USA) restriction sites engineered into the primers (underlined in the primer sequences in Table 1) using T4 DNA ligase (Thermo Fisher Scientific, Waltham, Massachusetts, USA). Recombinant DNA was transformed into *Escherichia coli* JM109 cells and selected on ampicillin-containing (100 μg/ml) LB agar plates. Recombinant vectors were confirmed by Sanger sequencing (Inqaba Biotec, South Africa) using the T7 primer, prior to vector amplification and isolation through a standard alkaline lysis protocol. HeLa and SiHa cells were transfected with the pcDNA3.1-Snai1 construct using TurboFect (Thermo Fisher Scientific, Waltham, Massachusetts, USA) according to manufacturer's instructions. Transient transfections were performed over 24–48 h then protein expression and localization determined, as previously described.

2.7. Luciferase reporter assay

In order to assess the ability of Snai1 to repress *PXDN* gene expression from the *PXDN* promoter, we performed luciferase reporter assays using the two regions of the *PXDN* promoter, one with (PXDN^{Snai1+}) and one without (PXDN^{Snai1-}) the identified putative Snai1 *E*-boxes. The two regions were amplified by high fidelity PCR and cloned (Biomatik, Ontario, Canada) into the pGL4.10 vector (Promega, Madison, Wisconsin, USA) using T4 DNA ligase, through the NheI and EcoRV restriction sites engineered into the primers, as underlined in the primer sequences (Table 1). Sanger sequencing was used to confirm the recombinant vector sequences prior to transfections. The vectors pGL4.10-PXDN^{SnaiI+} and pGL4.10-PXDN^{SnaiI-} were co-transfected with pcDNA-Snai1 into HEK293 cells using TurboFect transfection reagent (Thermo Fisher Scientific, Waltham, Massachusetts, USA). After 24 h, the luciferase assay was performed using the Steady-Glo Luciferase assay system (Promega, Madison, Wisconsin, USA) and a GloMax-96 Microplate Luminometer (Promega, Madison, Wisconsin, USA), according to manufacturer's instructions. The E-cadherin promoter served as the control, whereby the Snai1-binding and Snai1 non-binding sites were cloned into pGL4.10, using primers listed in Table 1, to generate pGL4.10-E-cadherin^{SnaiI+} and pGL4.10-E-cadherin^{SnaiI-}, respectively.

2.8. Statistical analysis

All results are representative of three independent experiments. Data were analysed and comparisons made using paired Student's *t*-test where relevant; a P value of < 0.05 was considered significant.

3. Results

3.1. PXDN expression decreases in response to TGF-β1

In order to establish whether Snai1 regulates *PXDN*, we first considered whether PXDN expression is modified by TGF-β1, a classic inducer of EMT and Snai1 expression (Peinado et al., 2003). First we looked at the effect of TGF-β1 treatment on EMT induction in HeLa and SiHa cells by examining morphological changes in cell shape, since cells undergoing EMT take on fibroblast-like features (Zavadil and Böttinger, 2005). Indeed, the morphology of both HeLa (Fig. 1A) and SiHa (Fig. 1B) cells changed as expected in that cells took on a mesenchymal phenotype with a spindle-like shape and loss of cell-to-cell contacts. Next, we assessed expression levels of PXDN along with the EMT markers Snai1, E-cadherin and vimentin in response to TGF-β1 (5 ng/ml) treatment over 48 h. In HeLa cells (Fig. 1A) PXDN expression decreased significantly in by 26% after 24 h and 29% after 48 h and in SiHa cells (Fig. 1B) by 25% at 24 h and 47% at 48 h, as compared to untreated cells. Snai1 expression increased by 38% at 24 h then decreased to untreated levels by 48 h in HeLa cells (Fig. 1A) whilst SiHa cells exhibited 46% and 9% increases at 24 and 48 h, respectively, as compared to untreated controls (Fig. 1B). As expected, we found that E-cadherin expression decreased in response to TGF-β1, by 43% and 67% over 24 and 48 h, respectively in HeLa cells (Fig. 1A), whilst in SiHa cells the decrease over the same time periods were 29% and 46% (Fig. 1B). Vimentin, a marker for the mesenchymal phenotype, showed increased protein expression with ~22% over 48 h in HeLa (Fig. 1A) and ~35% in SiHa cells (Fig. 1B). Immunofluorescence confocal microscopy showed the distinctive patterns of protein localisation as well as supporting the degree of expression seen in the Western blotting for both HeLa (Fig. 2A) and SiHa (Fig. 2B). Expression levels and extracellular localisation of PXDN and E-cadherin diminished over 24 h with TGF-β1 (5 ng/ml) treatment, and foci of vimentin increased, in particular in the SiHa cell. As expected, Snai1 exhibited an accumulation in the nuclei upon TGF-β1 treatment.

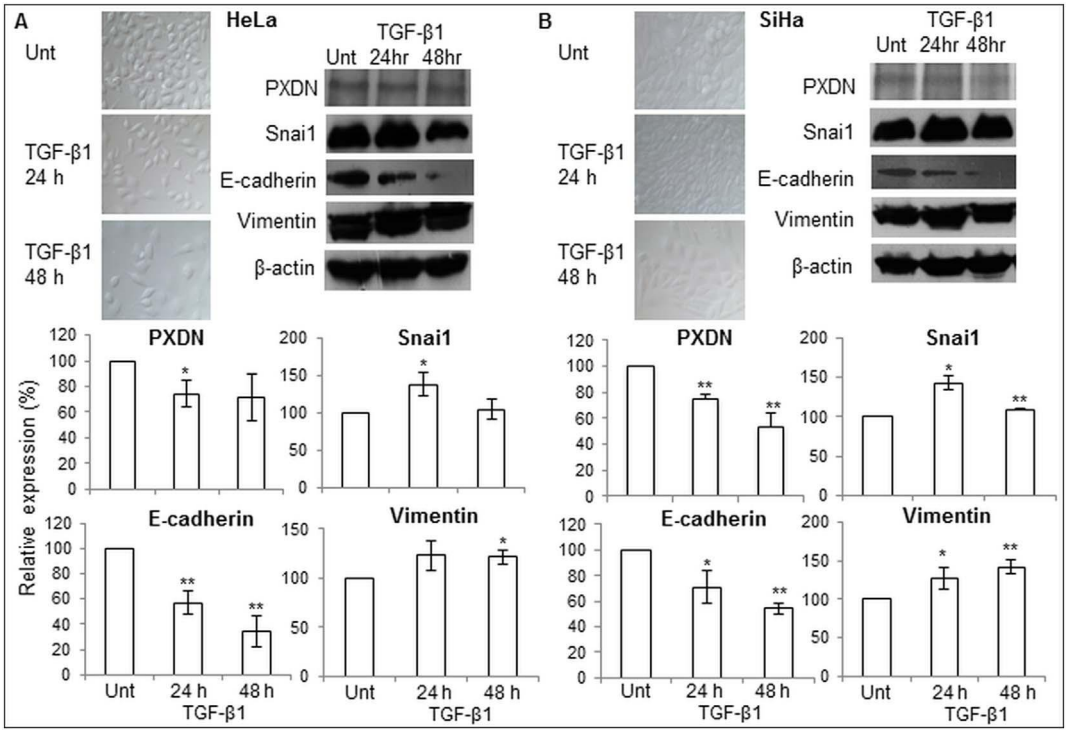

Fig. 1. PXDN and EMT marker expression in response to TGF-β1. A) HeLa and B) SiHa show morphological changes following treatment of cells with TGF-β1 (5 ng/ml) for 48 h depict long fibroblast-like features and loss of cell-cell contacts. Western blot analysis of the effect of TGF-β1 (5 ng/ml) for 24 and 48 h on protein expression of PXDN and EMT markers Snai1, E-cadherin, vimentin. PXDN expression decreased over 24 and 48 h. As expected, Snai1 expression increased at 24 h then decreased by 48 h of TGF-β1 treatment; with a concomitant decrease in E-cadherin and increase in vimentin expression (β-actin was used as a loading control; n = 3 ± SD; *p ≤ 0.05, **p ≤ 0.01).

3.2. Snai1 binds to the PXDN promoter in response to TGF-β1

To determine whether Snai1 interacts with *PXDN* promoter region we performed ChIP-PCR. We identified three E-boxes close to the transcription start site in the *PXDN* promoter and designed one set of primers that amplified across the putative Snai1 binding sites ($PXDN^{Snai1+}$) and one that amplified a region with no E-boxes ($PXDN^{Snai1-}$) (Fig. 3A and Table 1). In both cell lines, amplification of the $PXDN^{Snai1+}$ region of the promoter occurred in TGF-β1 treated cells only (Fig. 3B). This was also the case with the positive control; the E-

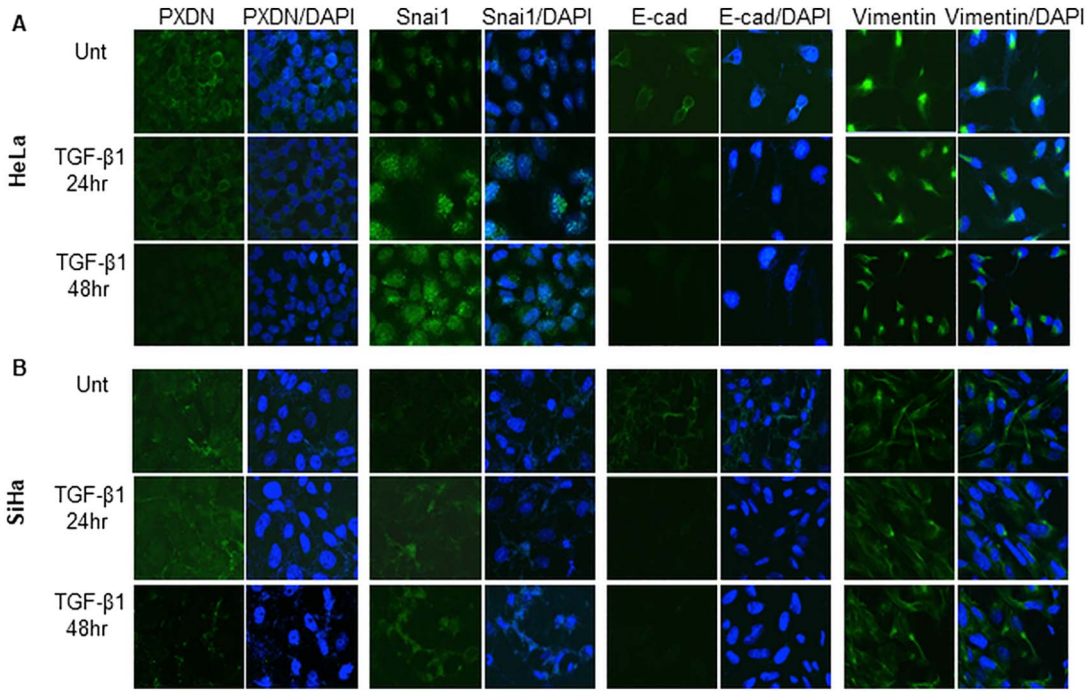

Fig. 2. Protein localisation in response to TGF-β1-induced EMT. Immunofluorescence confocal microscopy of A) HeLa and B) SiHa cells treated with 5 ng/ml TGF-β1 for 24 and 48 h showed PXDN expression was reduced with a disruption in organization of PXDN in the extracellular environment. In both cell lines, there was increased nuclear translocation of Snai1 with reduced E-cadherin and increased vimentin, over 24 and 48 h. Nuclei were counterstained with DAPI.

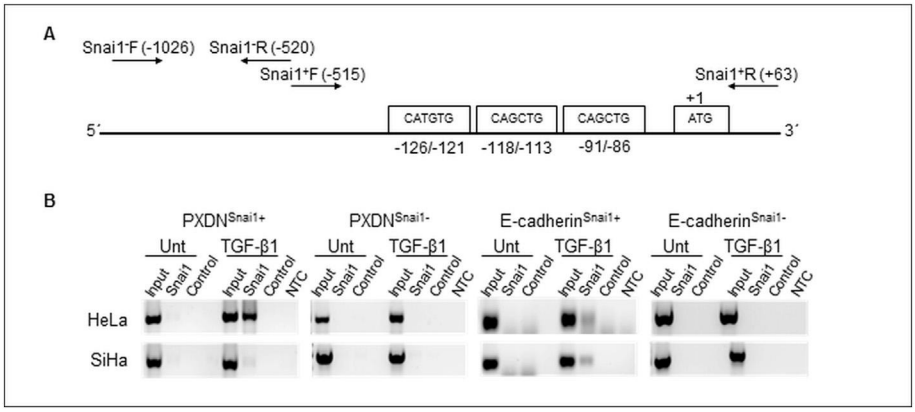

Fig. 3. ChIP-PCR analysis of the *PXDN* promoter following TGF-β1 treatment. A) *PXDN* promoter region depicting the three E-boxes as putative Snai1 binding sites. One set of primers was designed to span across these three sites (Snai1^{+}F and Snai1^{+}R) and one set of primers was designed to amplify across a region with no identified E-boxes (Snai1^{-}F and Snai1^{-}R). B) ChIP-PCR on cells treated with TGF-β1 (5 ng/ml) for 24 h. Snai1-immunoprecipitated DNA was amplified by PCR with products generated for the PXDN^{Snai1+} region when cells were exposed to TGF-β1 treatment only. The E-cadherin promoter, which served as the positive control for Snai1 binding, showed PCR products for the E-cadherin^{Snai1+} region only, as expected. Both the PXDN^{Snai1-} and E-cadherin^{Snai1-} without Snai1 binding sites were negative by PCR. The ChIP control (Control) was negative by PCR as expected, input DNA served as a positive control and gave PCR bands of the expected sizes as expected, and no amplification was found in the no template control (NTC) samples, which served as the negative control for the PCR. Results represent three independent experiments.

cadherin^{Snai1+} promoter region was positive for PCR products with TGF-β1 treatment (Fig. 3B). This indicates that Snai1 binds to the *PXDN* promoter region in the presence of TGF-β1. Primer sets designed to flank regions without Snai1-binding sites in both *PXDN* (PXDN^{Snai1-}) and *E-cadherin* (E-cadherin^{Snai1-}) promoter regions were negative by PCR, indicating that Snai1 was not bound to these DNA regions and therefore did not immunoprecipitate during ChIP, as expected (Fig. 3B). PCR on input DNA, which had not been processed by immunoprecipitation, confirmed the presence of the target DNA sequences in the genomic DNA and the successful PCR for each primer set. The negative control containing only the protein A/G agarose beads gave no PCR products indicating that there was no non-specific binding of DNA to the beads.

3.3. Snai1 represses PXDN gene expression

To further investigate the involvement of Snai1 in repressing *PXDN* expression, we conducted luciferase reporter assays. To this end, we cloned two regions of the *PXDN* promoter either with (PXDN $^{Snai1+}$) or without (PXDN $^{Snai1-}$) the E-boxes into the luciferase gene reporter vector pGL4.10. Similarly, luciferase reporter gene constructs were generated for E-cadherin^{Snai1+} and E-cadherin^{Snai1-} regions, to serve as positive controls. HEK293 cells were transiently transfected with each of the luciferase reporter vectors (pGL4.10-PXDN^{Snai1+}, pGL4.10-PXDN^{Snai1-}, pGL4.10-E-cadherin^{Snai1+}, and pGL4.10-E-cadherin^{Snai1-}) and treated with TGF-β1. In addition, we also performed these assays with Snai1 overexpression, by creating a pcDNA-Snai1 over-expression vector. First we assessed the effect of the pcDNA-Snai1 vector on to show that with Snai1 overexpression PXDN expression decreases, as does E-cadherin and with increased vimentin as expected (Fig. 4A and B). In the transfected TGF-β1 treated cells, luciferase expression from the PXDN^{Snai1+} promoter region was reduced significantly by 67% compared to untreated cells transfected with the pGL4.10-PXDN^{Snai1+} vector alone (Fig. 4C). Similarly, co-transfection of HEK293 cells with pcDNA-Snai1 and pGL4.10-PXDN^{Snai1+} resulted in a 71% decrease in luciferase reporter gene expression, compared to untreated cells (Fig. 4C). Similar results were obtained for the E-cadherin control, where pGL4.10-E-cadherin^{Snai1+} with TGF-β1 gave a 79% reduction and the pGL4.10-E-cadherin^{Snai1+}/pcDNA-Snai1 co-transfected cells showed a 94% decrease in luciferase reporter gene expression (Fig. 4D). The pGL4.10-PXDN^{Snai1-} and pGL4.10-E-cadherin^{Snai1-} vectors did not show any significant changes in luciferase reporter activity with TGF-β1 treatment (Fig. 4C and D). However, we saw some decrease with pcDNA-Snail co-transfection for the PXDN^{Snail-} region, which may indicate that Snai1 might be interacting with this region. This would not be completely unsurprising considering the small and somewhat non-specific nature of the Snai1 binding site. The empty-vector control for Snai1 overexpression gave no significant change in luciferase activity as compared to untreated cells (data not shown).

4. Discussion

Whilst the various physiological and pathophysiological roles of PXDN have yet to be fully elucidated, several studies have found that PXDN is involved in the three major processes where EMT occurs. Firstly, during development in the model organisms *X. tropicalis* and *C. elegans*, PXDN orthologues were found to be integral to embryonic development, and in humans, mutations in *PXDN* have been associated with congenital abnormalities of the eye (Yan et al., 2014; Micheal et al., 2016; Tindall et al., 2005; Gotenstein et al., 2010; Péterfi et al., 2009). Secondly, in fibrosis, myofibroblasts excessively deposit PXDN into the ECM in response to TGF-β1 in the kidney (Horikoshi et al., 1999). Thirdly, altered expression of PXDN is found in various cancers with PXDN implicated in cell attachment and invasion, although the full extent of the role of PXDN in cancer has yet to be determined (Desmond et al., 2007; Liu et al., 2010; Tauber et al., 2010; Jayachandran et al., 2016; Thiery et al., 2009). The EMT process results in the loss of cell polarity and cell-cell adhesion, which can lead to a more motile cellular phenotype. This requires the repression of the epithelial phenotype, as reflected by markers such as E-cadherin, and the acquisition of the mesenchymal phenotype, whereby markers such as vimentin becomes apparent (Khan et al., 2011). Multiple factors, including TGF-β1, can trigger EMT in these aforementioned contexts, but interestingly one of the common denominators is the activation of the transcription factor Snai1, which is considered a master-regulator of the EMT process (Lamouille et al., 2014; Barrallo-Gimeno and Nieto, 2005). Considering the involvement of PXDN in EMT, we investigated whether PXDN is regulated by Snai1, and is the first such study looking at the transcriptional regulators of PXDN.

We first assessed PXDN expression in HeLa and SiHa cells in response to TGF-β1, and found that this decreases over 48 h, a pattern also seen with one of the classic markers of the epithelial phenotype, E-cadherin (Cano et al., 2000; Batlle et al., 2000). There was a concomitant increase in Snai1 at 24 h then a drop in expression at 48 h. This pattern is not surprising since Snai1 expression has more recently been determined to act over a shorter time period than previously thought, although the downstream effects of Snai1 on its target genes are longer lasting (Vetter et al., 2009). Our findings agree with previous observations that TGF-β1 leads to decreased E-cadherin and promotes EMT induction in HeLa and SiHa cell lines (Yi et al., 2002; Kloth et al., 2005; Cheng and Hao, 2016).

Whilst in our study we found that TGF-β1 causes decreased PXDN expression, in kidney fibrosis, PXDN shows increased deposition in the ECM (Horikoshi et al., 1999). On the surface, this seems in conflict with our results, however, the difference in PXDN expression in these two processes makes this entirely understandable as whilst similar pathways

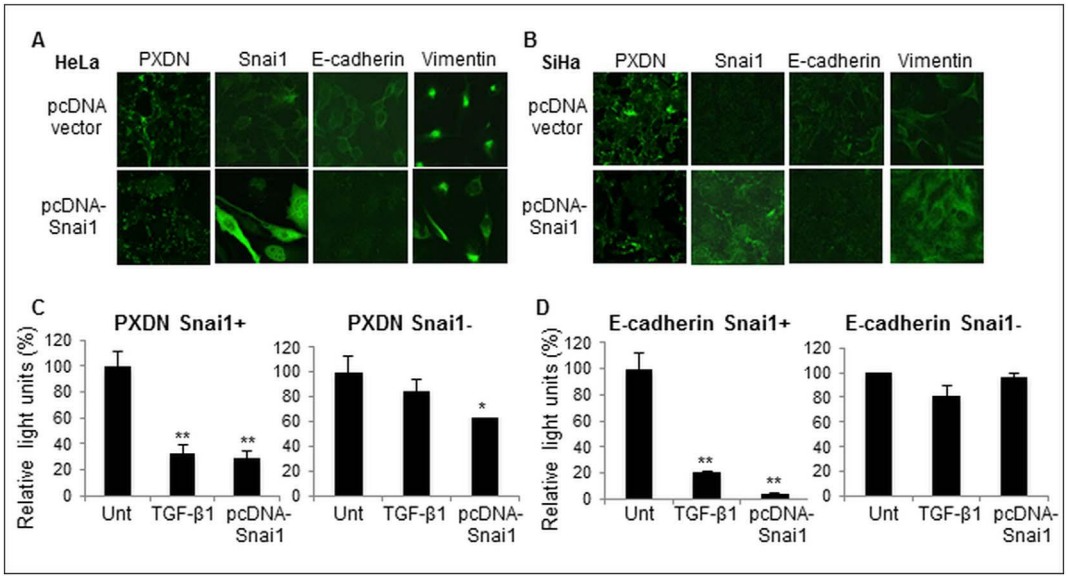

Fig. 4. Luciferase reporter assay for regulation of PXDN expression by TGF-β1 and Snai1 overexpression. A) HeLa and B) SiHa cells were grown on coverslips then transfected for 24 h with Snai1 expression vector, pcDNA-Snai1. Immunofluorescence confocal microscopy indicated that transiently transfected cells exhibited an increase in Snai1 and vimentin expression and a decrease in E-cadherin, as expected. Both cell lines showed a decrease in PXDN with Snai1 overexpression. Luciferase vector constructs for C) PXDN (pGL4.10-PXDN^{Snai1+} and pGL4.10-PXDN^{Snai1-}) and D) E-cadherin (pGL4.10-E-cadherin^{Snai1+} and pGL4.10-E-cadherin^{Snai1-}) were transfected into HEK293 cells, either in the presence of TGF-β1 or co-transfected with the pcDNA-Snai1 overexpression vector. Luciferase reporter gene expression was significantly lower with both TGF-β1 treatment and with Snai1 overexpression, from the region of the *PXDN* promoter containing the putative Snai1 binding sites (Snai1$^+$). The Snai1$^-$ region of the promoter showed no significant decrease with TGF-β1 but there was some decrease with Snai1 overexpression. The E-cadherin promoter regions with Snai1 E-boxes (Snai1$^+$) gave significantly reduced luciferase reporter gene expression with TGF-β1 and Snai1 overexpression, but not for the E-cadherin Snai1$^-$ region, relative to untreated, as expected. ($n = 3 \pm SD$; $p < 0.05$.)

are triggered, outcomes can differ between cancer and fibrosis (Liu, 2011). From a cancer perspective, Barnett et al. found that Snai1 overexpression caused significant up-regulation of PXDN in human prostate cancer cells, which differs from our findings (Barnett et al., 2011). However, as with many other proteins, PXDN expression patterns are emerging as cancer-type and probably stage specific; one recent comprehensive study looking at PXDN in breast cancer cell lines, found that even within the basal or luminal subtypes, expression differed significantly from highly expressed to not at all (Young et al., 2015). Certainly, the triggers of PXDN expression in cancer will also undoubtedly prove to be context-specific, with TGF-β1, for example, known to play opposing roles in cancer progression (Roberts and Wakefield, 2003; Heerboth et al., 2015).

Once we had established that, in our model, TGF-β1 causes EMT and this involved a decrease in PXDN expression, we looked at whether Snai1 binds to the *PXDN* promoter. Snai1 is known to interact with E-boxes in target gene promoters, which have the consensus sequence CANNTG (Nieto, 2002). Considering the rather degenerate nature of this sequence, we identified multiple putative Snai1 binding sites within the PXDN promoter, through a manual search. As we found a cluster of three such E-boxes in the *PXDN* promoter proximal to the transcription start site (Fig. 2A), we hypothesized that this would be the likely region of Snai1 binding. Through ChIP-PCR, we observed that in the presence of TGF- β1, Snai1 binds to this particular region of the promoter only. To then look at whether Snai1 can direct gene repression from this E-box containing region of the *PXDN* promoter, we used luciferase reporter assays, and found reduced gene expression with the addition of TGF- β1. Since this potent growth factor can activate a host of transcription factors that may potentially interact with the PXDN promoter to modify expression, we also co-transfected cells with a Snai1 overexpression vector. We found that this specifically causes *PXDN* gene repression from the E-box containing region to levels similar to those caused by TGF- β1. Indeed, Snai1-regulated genes usually contain clusters of more than one Snai1 E-box, as in the PXDN promoter, but the reason for multiple Snai1 binding has not yet been clarified (Batlle et al., 2000; Beach et al., 2008; Whiteman et al., 2008). Mutation studies have shown that destroying one or more of these sites still confers the ability to repress gene expression *via* Snai1; only when all sites were mutated was there no regulation by Snai1 of the target genes (Batlle et al., 2000). Therefore, the importance of each individual E-box and the level to which each is responsible for regulating target gene expression, including for *PXDN*, remains to be seen. Furthermore, Snai1 has been conventionally understood as a transcriptional repressor, through the recruitment of histone deacetylases to gene promoters (Peinado et al., 2004). However, recent evidence suggests that Snai1 is also involved in the activation of gene expression and therefore it may be plausible that different Snai1sites direct these opposing roles under different cellular situations (Rembold et al., 2014).

5. Conclusion

In summary, the process of EMT is integral to a number of physiological and disease states. TGF-β1 is a major effector of this process that activates various key transcription factors such as Snai1. Regardless of the type of EMT, this process leads to modifications in the ECM and Snai1 has been identified as a biomarker for disease progression (Heerboth et al., 2015). Our findings that Snai1 regulates PXDN in cervical carcinoma cell lines, further supports a role for this ECM modifying protein in cancer. Delineating the details of PXDN expression in cancer, will require careful consideration of the various triggers and stage of cancer progression. Furthermore, considering the breadth of processes that Snai1 is involved in, such as EMT, our work highlights the significance of considering PXDN when studying these processes, which will be critical to deciphering the role of PXDN in normal physiology and disease processes.

Conflicts of interest

All authors have no conflicts of interest to disclose.

Acknowledgements

We thank Dr Clement Penny and Dr Aurelie Deroubaix for assistance with confocal microscopy at the NRF-funded Life Sciences Imaging Facility, Faculty of Health Sciences, University of the Witwatersrand, Johannesburg. We acknowledge the Microscopy and Microanalysis Unit, University of the Witwatersrand, Johannesburg for use of the Olympus BX63 microscopy.

Funding

This work was supported by the University of the Witwatersrand, Johannesburg. BNS is supported by an Innovations PhD bursary from the National Research Foundation and a University of the Witwatersrand Postgraduate Merit Award. Funders were not involved in any decisions pertaining to experimental design or manuscript content.

Author's contribution

BNS performed all experiments, conducted data analysis and interpretation, and assisted in drafting the manuscript. DMD conceived and designed the study, conducted data analysis and interpretation, drafted and approved the final manuscript.

References

Barnett, P., Arnold, R.S., Mezencev, R., Chung, L.W., Zayzafoon, M., Odero-Marah, V., 2011. Snail-mediated regulation of reactive oxygen species in ARCaP human prostate cancer cells. Biochem. Biophys. Res. Commun. 404, 34–39.

Barrallo-Gimeno, A., Nieto, M.A., 2005. The Snail genes as inducers of cell movement and survival: implications in development and cancer. Development 132, 3151–3161.

Batlle, E., Sancho, E., Francí, C., Domínguez, D., Monfar, M., Baulida, J., García De Herreros, A., 2000. The transcription factor snail is a repressor of E-cadherin gene expression in epithelial tumour cells. Nat. Cell Biol. 2, 84–89.

Beach, S., Tang, H., Park, S., Dhillon, A.S., Keller, E.T., Kolch, W., Yeung, K.C., 2008. Snail is a repressor of *RKIP* transcription in metastatic prostate cancer cells. Oncogene 27, 2243–2248.

Bhave, G., Cummings, C.F., Vanacore, R.M., Kumagai-Cresse, C., Ero-Tolliver, I.A., Rafi, M., Kang, J.S., Pedchenko, V., Fessler, L.I., Fessler, J.H., Hudson, B.G., 2012. Peroxidasin forms sulfilimine chemical bonds using hypohalous acids in tissue genesis. Nat. Chem. Biol. 8, 784–790.

Bramhall, S., Noack, N., Wu, M., Loewenberg, J.R., 1969. A simple colorimetric method for determination of protein. Anal. Biochem. 31, 146–148.

Byron, A., Humphries, J.D., Humphries, M.J., 2013. Defining the extracellular matrix using proteomics. Int. J. Exp. Pathol. 94, 75–92.

Cano, A., Pérez-Moreno, M.A., Rodrigo, I., Locascio, A., Blanco, M.J., del Barrio, M.G., Portillo, F., Nieto, M.A., 2000. The transcription factor snail controls epithelial-mesenchymal transitions by repressing E-cadherin expression. Nat. Cell Biol. 2, 76–83.

Chandler, J.D., Day, B.J., 2012. Thiocyanate: a potentially useful therapeutic agent with host defense and antioxidant properties. Biochem. Pharmacol. 84, 1381–1387.

Cheng, K., Hao, M., 2016. Metformin inhibits TGF-β1-induced epithelial-to-mesenchymal transition via PKM2 relative-mTOR/p70s6k signaling pathway in cervical carcinoma cells. Int. J. Mol. Sci. 17, 2000.

Cheng, G., Salerno, J.C., Cao, Z., Pagano, P.J., Lambeth, J.D., 2008. Identification and characterization of VPO1, a new animal heme-containing peroxidase. Free Radic. Biol. Med. 45, 1682–1694.

Cheng, G., Li, H., Cao, Z., Qiu, X., McCormick, S., Thannickal, V.J., Nauseef, W.M., 2011. Vascular peroxidase-1 is rapidly secreted, circulates in plasma, and supports dityrosine cross-linking reactions. Free Radic. Biol. Med. 51, 1445–1453.

Cummings, C.F., Pedchenko, V., Brown, K.L., Colon, S., Rafi, M., Jones-Paris, C., Pokydeshava, E., Liu, M., Pastor-Pareja, J.C., Stothers, C., Ero-Tolliver, I.A., McCall, A.S., Vanacore, R., Bhave, G., Santoro, S., Blackwell, T.S., Zent, R., Pozzi, A., Hudson, B.G., 2016. Extracellular chloride signals collagen IV network assembly during basement membrane formation. J. Cell Biol. 213, 479–494.

Davies, M.J., Hawkins, C.L., Pattison, D.I., Rees, M.D., 2008. Mammalian heme peroxidases: from molecular mechanisms to health implications. Antioxid. Redox Signal. 10, 1199–1234.

Desmond, J.C., Raynaud, S., Tung, E., Hofmann, W.K., Haferlach, T., Koeffler, H.P., 2007. Discovery of epigenetically silenced genes in acute myeloid leukemias. Leukemia 21, 1026–1034.

Gaut, J.P., Yeh, G.C., Tran, H.D., Byun, J., Henderson, J.P., Richter, G.M., Brennan, M.L., Lusis, A.J., Belaaouaj, A., Hotchkiss, R.S., Heinecke, J.W., 2001. Neutrophils employ the myeloperoxidase system to generate antimicrobial brominating and chlorinating oxidants during sepsis. Proc. Natl. Acad. Sci. U. S. A. 98, 11961–11966.

Gotenstein, J.R., Swale, R.E., Fukuda, T., Wu, Z., Giurumescu, C.A., Goncharov, A., Jin, Y., Chisholm, A.D., 2010. The *C. elegans* peroxidasin PXN-2 is essential for embryonic morphogenesis and inhibits adult axon regeneration. Development 137, 3603–3613.

Heerboth, S., Housman, G., Leary, M., Longacre, M., Byler, S., Lapinska, K., Willbanks, A., Sarkar, S., 2015. EMT and tumor metastasis. Clin. Transl. Med. 4, 6.

Horikoshi, N., Cong, J., Kley, N., Shenk, T., 1999. Isolation of differentially expressed cDNAs from p53-dependent apoptotic cells: activation of the human homologue of the *Drosophila* peroxidasin gene. Biochem. Biophys. Res. Commun. 261, 864–869.

Jayachandran, A., Prithviraj, P., Lo, P.-H., Walkiewicz, M., Anaka, M., Woods, B.L., Tan, B.S., Behren, A., Cebon, J., McKeown, S.J., 2016. Identifying and targeting determinants of melanoma cellular invasion. Oncotarget 7, 41186–41202.

Khan, K., Rudkin, A., Parry, D.A., Burdon, K.P., McKibbin, M., Logan, C.V., Abdelhamed, Z.I.A., Muecke, J.S., Fernandez-Fuentes, N., Laurie, K.J., Shires, M., Fogarty, R., Carr, I.M., Poulter, J.A., Morgan, J.E., Mohamed, M.D., Jafri, H., Rasshid, Y., Meng, N., Piseth, H., Toomes, C., Casson, R.J., Taylor, G.R., Hammerton, M., Sheridan, E., Johnson, C.A., Inglehearn, C.F., Craig, J.E., Ali, M., 2011. Homozygous mutations in *PXDN* cause congenital cataract, corneal opacity, and developmental glaucoma. Am. J. Hum. Genet. 89, 464–473.

Kloth, J.N., Fleuren, G.J., Oosting, J., de Menezes, R.X., Eilers, P.H., Kenter, G.G., Gorter, A., 2005. Substantial changes in gene expression of Wnt, MAPK and TNFalpha pathways induced by TGF-beta1 in cervical cancer cell lines. Carcinogenesis 26, 1493–1502.

Lamouille, S., Xu, J., Derynck, R., 2014. Molecular mechanisms of epithelial–mesenchymal transition. Nat. Rev. Mol. Cell Biol. 15, 178–196.

Li, H., Cao, Z., Moore, D.R., Jackson, P.L., Barnes, S., Lambeth, J.D., Thannickal, V.J., Cheng, G., 2012. Microbial activity of vascular peroxidase 1 in human plasma via generation of hypochlorous acid. Infect. Immun. 80, 2528–2537.

Liu, Y., 2011. Cellular and molecular mechanisms of renal fibrosis. Nat. Rev. Nephrol. 7, 684–696.

Liu, Y., Carson-Walter, E.B., Cooper, A., Winans, B.N., Johnson, M.D., Walter, K.A., 2010. Vascular gene expression patterns are conserved in primary and metastatic brain tumours. J. Neuro-Oncol. 99, 13–24.

McCall, A.S., Cummings, C.F., Bhave, G., Vanacore, R., Page-McCaw, A., Hudson, B.G., 2014. Bromine is an essential trace element for assembly of collagen IV scaffolds in tissue development and architecture. Cell 157, 1380–1392.

Micheal, S., Siddiqui, S.N., Zafar, S.N., Iqbal, A., Khan, M.I., den Hollander, A.I., 2016. Identification of novel variants in LTBP2 and PXDN using whole-exome sequencing in developmental and congenital glaucoma. PLoS ONE 11, e0159259.

Nelson, R.E., Fessler, L.I., Takagi, Y., Blumberg, B., Keene, D.R., Olson, P.F., Parker, C.G., Fessler, J.H., 1994. Peroxidasin: a novel enzyme-matrix protein of *Drosophila* development. EMBO J. 13, 3438–3447.

Nieto, M.A., 2002. The Snail superfamily of zinc-finger transcription factors. Nat. Rev. Mol. Cell Biol. 3, 155–166.

O'Brien, P.J., 2000. Peroxidases. Chem. Biol. Interact. 129, 113–139.

Paumann-Page, M., Katz, R.S., Bellei, M., Schwartz, I., Edenhofer, E., Sevcnikar, B., Soudi, M., Hofbauer, S., Battistuzzi, G., Furtmüller, P.G., Obinger, C., 2017. Pre-steady-state kinetics reveal the substrate specificity and mechanism of halide oxidation of truncated human peroxidasin 1. J. Biol. Chem. 292, 4583–4592.

Peinado, H., Quintanilla, M., Cano, A., 2003. Transforming growth factor beta-1 induces snail transcription factor in epithelial cell lines: mechanisms for epithelial mesenchymal transitions. J. Biol. Chem. 278, 21113–21123.

Peinado, H., Ballestar, E., Esteller, M., Cano, A., 2004. Snail mediates E-cadherin repression by the recruitment of the Sin3A/histone deacetylase 1 (HDAC1)/HDAC2 complex. Mol. Cell Biol. 24, 306–319.

Péterfi, Z., Donkó, A., Orient, A., Sum, A., Prókai, A., Molnár, B., Veréb, Z., Rajnavölgyi, E., Kovács, K.J., Müller, V., Szabó, A.J., Geiszt, M., 2009. Peroxidasin is secreted and incorporated into the Extracellular Matrix of myofibroblasts and fibrotic kidney. Am. J. Pathol. 175, 725–735.

Rembold, M., Ciglar, L., Yáñez-Cuna, J.O., Zinzen, R.P., Girardot, C., Jain, A., Welte, M.A., Stark, A., Leptin, M., Furlong, E.M., 2014. A conserved role for Snail as a potentiator of active transcription. Genes Dev. 28, 167–181.

Roberts, A.B., Wakefield, L.M., 2003. The two faces of transforming growth factor beta in carcinogenesis. Proc. Natl. Acad. Sci. U. S. A. 100, 8621–8623.

Shi, R., Hu, C., Yuan, Q., Yang, T., Peng, J., Li, Y., Bai, Y., Cao, Z., Cheng, G., Zhang, G., 2011. Involvement of vascular peroxidase 1 in angiotensin II-induced vascular smooth muscle cell proliferation. Cardiovasc. Res. 91, 27–36.

Tauber, S., Jais, A., Jeitler, M., Haider, S., Husa, J., Lindroos, Knöfler, M., Mayerhofer, M., Pehamberger, H., Wagner, O., Bilban, M., 2010. Transcriptome analysis of human cancer reveals a functional role of Heme Oxygenase-1 in tumour cell adhesion. Mol. Cancer 9, 200–216.

Thiery, J.P., Acloque, H., Huang, R.Y., Nieto, M.A., 2009. Epithelial-mesenchymal transitions in development and disease. Cell 139, 871–890.

Tindall, A.J., Pownall, M.E., Morris, I.D., Isaacs, H.V., 2005. *Xenopus tropicalis* peroxidasin gene is expressed within the developing neural tube and pronephric kidney. Dev. Dyn. 232, 377–384.

Vandewalle, C., Comijn, J., De Craene, B., Vermassen, P., Bruyneel, E., Andersen, H., Tulchinsky, E., Van Roy, F., Berx, G., 2005. SIP1/ZEB2 induces EMT by repressing genes of different epithelial cell-cell junctions. Nucleic Acids Res. 33, 6566–6578.

Vetter, G., Le Béchec, A., Muller, J., Muller, A., Moes, M., Yatskou, M., Al Tanoury, Z., Poch, O., Vallar, L., Friederich, E., 2009. Time-resolved analysis of transcriptional events during SNAI1-triggered epithelial to mesenchymal transition. Biochem. Biophys. Res. Commun. 385, 485–491.

Whiteman, E.L., Liu, C.J., Fearon, E.R., Margolis, B., 2008. The transcription factor snail represses Crumbs3 expression and disrupts apico-basal polarity complexes. Oncogene 27, 3875–3879.

Yan, X., Sabrautzki, S., Horsch, M., Fuchs, H., Gailus-Durner, V., Beckers, J., de Angelis, Hrabě, Graw, J., 2014. Peroxidasin is essential for eye development in the mouse. Hum. Mol. Genet. 23, 5597–5614.

Yi, J.Y., Hur, K.C., Lee, E., Jin, Y.J., Arteaga, C.L., Son, Y.S., 2002. TGFbeta1-mediated epithelial to mesenchymal transition is accompanied by invasion in the SiHa cell line. Eur. J. Cell Biol. 81, 457–468.

Young, C.D., Zimmerman, L.J., Hoshino, D., Formisano, L., Hanker, A.B., Gatza, M.L., Morrison, M.M., Moore, P.D., Whitwell, C.A., Dave, B., Stricker, T., Bhola, N.E., Silva, G.O., Patel, P., Brantley-Sieders, D.M., Levin, M., et al., 2015. Activating PIK3CA mutations induce an epidermal growth factor receptor (EGFR)/extracellular signal-regulated kinase (ERK) paracrine signaling axis in basal-like breast cancer. Mol. Cell. Proteomics 14, 1959–1976.

Zamocky, M., Jakopitsch, C., Furtmüller, P.G., Dunand, C., Obinger, C., 2008. The peroxidase-cyclooxygenase superfamily: reconstructed evolution of critical enzymes of the innate immune system. Proteins 72, 589–605.

Zavadil, J., Böttinger, E.P., 2005. TGF-beta and epithelial-to-mesenchymal transitions. Oncogene 24, 5764–5774.

Zhang, Y.S., He, L., Liu, B., Li, N.S., Luo, X.J., Hu, C.P., Ma, Q.L., Zhang, G.G., Li, Y.J., Peng, J., 2012. A novel pathway of NADPH oxidase/vascular peroxidase 1 in mediating oxidative injury following ischemia-reperfusion. Basic Res. Cardiol. 107, 1–19.